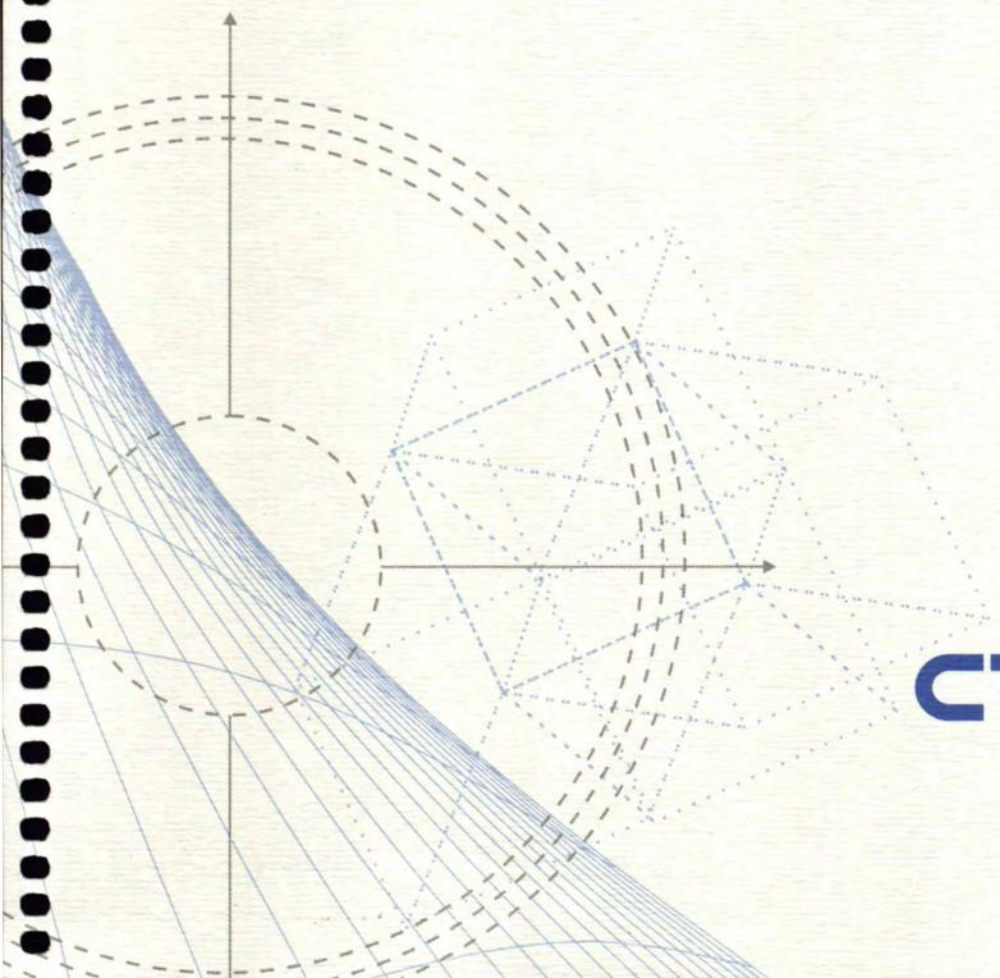

Communications
Research Centre
Centre de recherches
sur les communications

Industry Canada Industrie Canada

Canada

The Northwest Passage Propagation Experiment

Report of the 1985-1986 Measurement Program

by
Claude Bilodeau and
François Dubé

Radiocommunications and
Broadcast Research

CRC REPORT No. CRC-RP-96-001
OTTAWA, MARCH 1996

TABLE OF CONTENTS

FIGURES

THE NORTHWEST PASSAGE PROPAGATION EXPERIMENT

REPORT OF THE 1985-1986 MEASUREMENT PROGRAM

by

CLAUDE BILODEAU and FRANÇOIS DUBÉ

ABSTRACT

The signal strengths received over six VHF and four UHF links in the Lancaster Sound area were monitored for several months. Of the ten paths involved, all but one were over sea, with lengths in the range 62 to 139 km. Detailed monthly summaries of path loss and fading measurements are presented and analyzed.

RÉSUMÉ

Les ondes radio métriques et décimétriques d'une dizaine de trajets point à point situés le long des rives est du passage du Nord-Ouest ont été étudiées pendant plusieurs mois. Les trajets avaient des longueurs variant de 62 à 139 km et leurs trajectoires, à l'exception d'un parcours, s'élevaient au dessus de la mer. Ce rapport présente une analyse statistique des mesures d'évanouissement et d'affaiblissement des signaux reçus.

1.0 INTRODUCTION

1.1 BACKGROUND

The Communications Research Centre[1] (CRC) has conducted over the years several propagation experiments in the VHF and UHF bands. Most of these measurements have taken place in the sparsely populated and remote Northern areas of Canada, since little was known about propagation characteristics in these regions.

Results of early work were reported by Palmer [1979, 1980]. Work under military contracts was undertaken later at Eureka and Alert (N.W.T.), but reports were reserved for internal use only [Strickland, 1981]. In the mid 80's, publications by Butler et al. [1984, 1985] and Whitteker [1985] contain extensive information on VHF/UHF propagation characteristics for two very different climatic regions: the harsh, desert climate of the central Arctic and the more temperate, rainy climate of the Maritimes. Butler [1985] in particular, demonstrated that ship-to-shore reliable VHF communications could be provided in the Northwest Passage using a chain of UHF repeaters along the coastline. In 1985/86, another set of measurements was undertaken in the Northwest Passage, this time in the Lancaster Sound area, east of Resolute Bay. Data analysis of that experiment has been deferred for several years because of a lack of resources. It is only recently, that the analysis was initiated and the findings are now presented in this report.

Meanwhile, another experiment started in September 1986 and lasted over a year, in the Hudson Strait area [Bilodeau, 1988]. The last experiment of the series is a feasibility study of a troposcatter link between Alert and Eureka (N.W.T.) [Bilodeau and McCormick, 1994]. Altogether, data from no less than three dozen radio links have been collected during the past sixteen years or so.

1.2 PURPOSE

The initial purpose of this experiment was to extend the Northwest Passage Propagation measurement program to achieve greater confidence in specifying a VHF mobile radio system covering the entire Passage (see interim recommendations by Butler [1985]).

In the early eighties, the Telecommunications and Electronics Branch of the Canadian Coast Guard was maintaining a close interest in the Northwest Passage Experiment and had funded part of the measurement program. In 1985, the Coast Guard, like CRC, suffered important financial cuts and could not maintain its support to the program. The CRC was also undergoing important structural reorganization changes and became unable to provide resources for completing the program. After about a year of operation, the sites

1. The CRC is a research facility of the federal Department of Industry. The work described in this report was performed when the CRC was still part of the Department of Communications.

were dismantled and the data put aside. It is only recently that resources became available again to analyse the collected information. The purpose of the current report is not to complete the study undertaken by Butler and Dubinski years ago, since the possibility of increased marine traffic through the Northwest Passage because of natural resource development appears rather dim at this time, but to present a coarse analysis of the propagation characteristics observed in this eastern part of the Canadian Arctic.

1.3 SCOPE

This report describes the results of an experiment conducted within the 156-174 MHz and 450-470 MHz frequency bands on ten line of sight links, of which half exceed 100 km and only one does not involve propagation over water. Detailed monthly summaries of signal strength distribution and fade depth are presented and analysed.

The experiment was conducted during the period June 1985 to July 1986, and as such, cannot be expected to give results entirely representative of weather conditions occurring outside the test period. Ideally, one would like to conduct this type of experiment during a long enough period, say several years, so that the test-area conditions are not only representative of their global climatology but are each represented in fair proportion.

2.0 DESCRIPTION OF THE EXPERIMENT

The main goal of the experiment was to measure the signal strength received at VHF/UHF over a number of paths for at least a year in order to assess propagation conditions in the Lancaster Sound area. Except for Stanley Peak, which is located west of Resolute Bay, all sites were chosen to provide a series of clear paths extending east of Resolute Bay.

Figure 1 shows the propagation paths and sites, which were named arbitrarily according to the nearest predominant geographical landmark. The path profiles are shown in Figures 2a and 2b assuming 4/3 earth curvature. The paths are line-of-sight and are 98% or more located above sea water, except Stanley-Martyr which is entirely overland.

Site coordinates and elevation, transmitter frequency and antenna polarization are given in Table 1. The frequencies used were in the 156-174 MHz and 450-470 MHz bands, and were nearly the same as those used previously in the Northwest Passage area west of Resolute Bay [Butler, 1985]. The antenna polarizations were alternated on adjacent UHF paths to minimize signal coupling between antennas at a station.

At each remote site (see Figure 1), a transmission of constant UHF power was directed westward (except at Stanley where the transmission was eastward) toward the next receiving site, where periodic measurements were made of the field strength. Since the sites were located in unattended areas, all measurements were relayed to the next site

until they finally reached the base station in Resolute Bay, nearby Martyr Peak, where they were recorded automatically. Measurements were also taken at Martyr, Hurd and Lemieux of the field strengths received from the nearest pair of adjacent VHF transmission sites.

TABLE 1. Site coordinates and elevation (above mean sea level), frequency of transmission and antenna polarization

SITE NAME	AREA	LAT. (N)	LONG. (W)	ELEV. (m)	FREQ. (MHz)	POL.
Stanley Peak	Cornwallis Is.	75° 09.0'	96° 15.0'	193	169.6	Vert.
Cape Martyr	Cornwallis Is.	74° 41.3'	95° 03.9'	174	----	----
Irvine Peak	Somerset Is.	74° 07.5'	92° 48.8'	172	466.0	Horiz.
					169.9	Vert.
Hurd Peak	Devon Is.	74° 32.4'	89° 55.7'	335	452.5	Vert.
Sargent Peak	Brodeur Pen.	73° 51.0'	86° 08.2'	375	465.0	Horiz.
					170.2	Vert.
Lemieux Peak	Devon Is.	74° 32.5'	82° 32.1'	500	451.3	Vert.
Cape Joy	Borden Pen.	73° 39.5'	83° 12.2'	10	170.5	Vert.

The relay of the measurements was carried out at UHF by modulating the radio signal to be measured. Passing the information this way avoided the use of a parallel radio system. The measurement bandwidth was kept larger than the transmitted bandwidth so the modulation process would not affect the results. Of concern was the serial nature of the transmissions; as lights in a Christmas tree, when one goes the whole lighting set goes. First, the design left enough signal margin on each path to accommodate fairly deep fades. Secondly, the equipment was designed for high reliability of operation. Unfortunately, even though the electronics never failed, the external RF cable assemblies and antennas were damaged at one site by polar bears during the recording period. Several months of data were lost for this reason. Specific details are given in Section 4.0.

3.0 DESCRIPTION OF THE REPEATERS

The measurement system, as used in this experiment, was entirely conceived and built at CRC and did not require the development of any new technology. Every element was either bought or put together from parts readily available commercially. However, the design required a great deal of good engineering to which many have contributed in their own way over the years.

The measurement system was designed to operate for at least a year on air depolarized caustic alkaline cells AD608Z and at temperatures as low as -50°C. The primary power at each site was provided by two battery banks made out of 12 cells connected in series for a rated capacity of 2000 Ah per bank. To preserve the cell efficiency at this low temperature, the current drain had to be kept under 200 mA [Armstrong and Barnes, 1979]. This was achieved by careful design of the electronics and the power distribution system.

Both the transmitting and receiving UHF antennas consisted of a parabolic cylinder reflector of about 208 cm x 104 cm x 61 cm with a two-element yagi primary radiator, providing a gain of 17 dBi. The VHF antennas had four collinear half-wave folded dipole elements with 10.7 dBi gain, except at Stanley and Cap Joy where a shorter antenna with 5.2 dBi gain was used.

The nominal RF power of the VHF and UHF transmitters was 100 mW; the noise figure of the receivers did not exceed 4 dB. The link margins were further increased, without imposing any extra power consumption, by limiting the system intermediate frequency (IF) bandwidth to 15 kHz. Even though this was about twice the necessary bandwidth, it relaxed the necessary frequency stability of the oscillators, and allowed the use of a simple temperature compensation technique.

The UHF transmitters used FM(FSK) modulation and were essentially composed of a VHF Voltage-Controlled-Oscillator (VCO) followed by a frequency doubler and a buffer/filter amplifier. To maintain frequency stability, but nevertheless allow modulation deviation of ±3.5 kHz around the carrier, the VCO was locked to a Voltage-Controlled-Crystal-Oscillator (VCXO) through a high ratio, low-power frequency divider. Any frequency deviation imposed on the VCXO by the baseband signal was in this way multiplied 180 times before reaching the output. The VHF transmitters were not modulated and a simple crystal oscillator followed by a frequency doubler generated the required carrier.

The receiver design was based on the standard heterodyne technique, using a single frequency conversion stage to obtain an intermediate frequency of 21.4 MHz or 10.7 MHz according to the frequency band of operation. Because of the remote and isolated environment, image rejection and co-channel interference rejection were of less concern. The low noise figure was achieved by using a commercial hybrid preamplifier followed by a low-loss filter. The demodulation was done by a crystal quadrature detector.

Processing of the asynchronous data, before modulation and after demodulation, was under the control of an 8-bit CMOS microprocessor. Bit recovery was performed by comparison with a self-adjusting threshold level. Word synchronization and randomization, as well as analog-to-digital conversion, were entirely dependent on software algorithms.

The electronics were not only designed for low current consumption but low temperature operation as well. To alleviate this requirement, the transmitter, receiver and logic

circuitry were surrounded within their metallic enclosure by 5 cm of polystyrene foam of high thermal resistance. Heat released by the equipment served to raise its own operating temperature by as much as 10°C on average. The equivalent thermal resistance of a complete enclosure was measured to be about 4.5°C per watt.

A UHF antenna was mounted on a 5 metre triangular tower made of reinforced but light aluminum, with a side mast extension for supporting a VHF antenna. Four legs or braces coming from the base of the tower and extending horizontally provided vertical stability. Cables that came down from near the top to join the braces halfway were added for additional stability. The tower was secured to the ground by the use of a large wooden box placed over the foot of each those legs, filled with rocks to at least 450 kg weight. The electronics enclosure, measuring about 50 cm x 20 cm x 80 cm, was attached 2 metres above the ground on one side of the tower.

The battery of cells was kept in a wooden crate placed on the ground near the central mast and just below the enclosure containing the electronics. All of this hardware was designed compactly enough to fit on board a Twin-Otter aircraft and be ferried to the top of mountain peaks by a Bell-206 helicopter. Three persons could do a complete site installation in less than a day.

4.0 DATA MEASUREMENT, PROCESSING, AND ACCURACY

At the end of each path, power measurement of the received RF signals was done in the IF section of the receivers. Each receiver incorporated three logarithmic stages of power detection to produce a dc voltage, in the range of 0 to 5 V, proportional to the strength of the received RF signal.

Before field installation, each receiver had undergone a thorough calibration process in the laboratory. By means of an automated test setup, calibration data were gathered in 0.1 dB increments over the 75 dB dynamic range of the power detectors. Each calibration was repeated at temperatures of -40°, -20°, 0° and +20°C.

During the experiment, the output voltage of the detector was sampled once every 2.5 seconds, and the data immediately digitized and transmitted to Resolute Bay where it was recorded. Each sample so taken was eventually retrieved from the magnetic cartridges for performing the signal analysis.

During the analysis, the collected samples were converted to power values and compensated for temperature effects by using one of the four calibration curves.

The power measurement error is estimated to be less than ±1.0 dB for most of the dynamic range of the receivers. The resolution varies from 1.5 dB to 0.1 dB (0.4 dB typically) depending whether the measurement is done or not in the knees joining the logarith-

mic detection levels. At low signal-to-noise ratios the resolution gradually worsens as the receivers reach their noise floor around -128 dBm.

It must be pointed out that measurement of relative signal strength was the main concern and that the system was only loosely calibrated to make absolute field strength measurements. For the purpose of link calculation, antenna characteristics were assumed to be in accordance with manufacturer's specification, losses through transmission line, connector, and adaptors were accounted for by assuming typical values. Therefore, adding to the receiver and transmitter calibration errors are the uncertainties about antenna gain, impedance mismatch, line loss error, azimuth alignment, polarization skew, etc. These additional factors must be counted twice, once for each end of the link, to estimate the total error. The root-mean-square absolute measurement error could easily total ±3.5 dB.

Sampling of the data was done with an accuracy of 8 bits (one byte). Every 2.5 seconds, a string of 20 bytes was recorded on a magnetic cartridge. Ten bytes contained the ten samples of signal strength measured at the receivers, and four others, the relative time of sampling. Five cyclic redundancy check bytes were also embedded in the recorded string for determining if there were transmission errors in the data. Finally, the last byte was a form feed character for string synchronization. Although a cartridge could hold about 4 Mbytes of data, taking more than 5 days to be filled, these were normally changed twice a week on a regular basis and mailed to Ottawa.

Upon receipt of a cartridge from Resolute Bay, the data were transferred to 9-track magnetic tape. The 14-month recording period necessitated the use of sixteen tapes, at 800 byte-per-inch density. Since the data recording format included the necessary timing information to easily retrieve the precise sampling time, the data was grouped in daily blocks of 24 hours, Universal Time (UT). For each block, ten hourly power distribution files were generated, a file for each of the receivers.

Since each receiver was calibrated over a 75 dB power detection range, with a 0.1 dB resolution, as many as 750 different received power levels could be distinguished. Each hourly power distribution file contained the distribution of the samples over the 750 "bins" and the 24 one-hour intervals (UT) making the day. The file format was compressed so that empty bins were not stored.

Hourly distribution files were subsequently added to each other to produce the monthly distributions, the latter combined to get the seasonal distributions, and so on. Two types of corrections were made along the way:

1) the hourly distributions were examined and cleaned up from any obvious transmission errors;
2) any hour within the hourly distributions that was found short sampled by more than 10% was rejected from the data. This could occasionally happen because of a power outage at Resolute Bay or a late cartridge change.

In the course of the experiment, strong blizzards damaged the RF cable assemblies and antennas at some repeater stations. Some assemblies did not withstand the extreme temperature, icing, and wind conditions. Polar bears were also responsible for some outages caused by destruction of RF cables and power cables. Visual inspection of the recorded data by means of temporal plots quickly led to the identification and deletion of the affected data.

Another problem that led to the deletion of some data was the difficulty to read the 9-track magnetic tapes that were used for storing data. The analysis having been postponed for several years, some tapes had loss part of their magnetization retention. The periods of data availability on the various paths are summarized in Table 2.

TABLE 2. Periods of Data Availability

PATH	J '85	J	A	S	O	N	D	J '86	F	M	A	M	J	J	TOTAL (days)
VHF															
Joy-Lemieux	24	21	31	4	28	3									111
Lemieux-Sargent	24	21	31	4	28	2									110
Sargent-Hurd	24	21	31	6	31	6									119
Hurd-Irvine	29	21	31	6	31	30	29	24	28	31	27	31	30	31	379
Irvine-Martyr	27	21	31	6	31	30	29	24	28	31	27	31	30	31	377
Stanley-Martyr	25	21	31	30	31	30	29	24	28	31	27	31	30	31	399
UHF															
Lemieux-Sargent	24														24
Sargent-Hurd	24	21	31	6	31	30	25								168
Hurd-Irvine	29	21	31	6	31	30	29	24	28	31	27	31	30	31	379
Irvine-Martyr					31	30	29	24	28	31	27	31			231

5.0 CLIMATE OF THE EXPERIMENTAL REGION

Climatological data recorded at Resolute Bay over the years by the Atmospheric Environment Service [Environment Canada, 1982] indicate poor weather condition and harsh climate in this Canadian Arctic area. The experimental region (see Figure 1) lies within two of the climatic areas defined by Maxwell [1981]: the sites west of Irvine Peak belong to the *sub-region Ic* whereas the others are in *sub-region IVa*. The site on Irvine Peak itself is on the climatic contour that delimits those two regions. In many respects, climatic conditions are similar in both sub-regions. The climate is an Arctic desert type, with

less than 15 cm of annual water equivalent precipitation in the *sub-region Ic* and with twice as much water on the exposed slopes of Devon Islands in *sub-region IVa*. The mean daily temperature is +4°C in July and -20°C to -33°C from east to west in January. Fog or ice fog occur about 15%-30% of the time in the months June to August and 5%-20% in the months December to February.

In winter widespread thermal inversions occur 75%-80% of the time because of radiative cooling of the surface, and even in the period June to August the atmosphere remains largely non-convective over the nearly isothermal surface of ice and sea water, so that thermal inversions occur for 30%-40% of the time.

The seasonal behaviour of surface refractivity at selected sites in Canada was reported by Segal and Barrington [1977]. The pertinent data for Resolute Bay were adapted to the presentation made in Figure 3.

The top diagram shows the monthly mean refractivity and the double standard deviation upper and lower limits about the mean. Both the refractivity and its range are characteristically reduced during the summer period; a trend commonly observed in other Arctic regions, and opposite of what is observed in the more southern regions. Also shown on this diagram is the mean dry air component of the refractivity which depends almost uniquely on the temperature variations.

The water vapour contribution to the refractivity is shown in the middle diagram. From November to April, the mean wet air component is almost negligible.

Finally, the diagram at the bottom represents the summer and winter probability distributions of the ground-based refractivity gradient averaged over the lowest 100 metres of the atmosphere. During most of the year, the refractivity gradient medians are close to the median of the temperate region (-39 N/km) which corresponds to an effective 4/3 true earth radius. Ducting ($dN/dz < -157$ N/km) is not extremely rare, about one percent as a fraction of the year, and twice as much between July and September. Earth bulging ($dN/dz > 0$), the blocking of radio paths by the surface, could be more common with about 2% occurrence in the summer.

6.0 DATA ANALYSIS AND RESULTS

6.1 PREDICTED AND OBSERVED LONG TERM MEDIANS

The CRC propagation prediction computer program [Whitteker, 1983] was used on each path to calculate the expected long term median levels and excess loss over free space. These estimates and comparison to the measured median levels are given in Table 3. The predicted values are based on an earth-radius factor k of four-thirds.

TABLE 3. Some long term median statistics

PATH	PATH LENGH (km)	Predicted excess loss (or gain): Reflected (dB)	Diffracted (dB)	Predicted Median (dBm)	Observed Median (dBm)	Observed minus Predicted (dB)
VHF						
Joy-Lemieux	105	-	20.5	-103.0	-103.3[a]	-0.3
Lemieux-Sargent	135	(0.7)	-	-78.6	-80.7[a]	-2.1
Sargent-Hurd	139	-	7.6	-87.1	-85.5[a]	+1.6
Hurd-Irvine	98	-	1.7	-78.1	-81.7[b]	-3.6
Irvine-Martyr	95	-	10.7	-86.9	-89.7[b]	-2.8
Stanley-Martyr	62	-	13.9	-91.8	-102.1[b]	-10.3
UHF						
Lemieux-Sargent	135	(2.4)	-	-72.7	-80.0[c]	-7.3
Sargent-Hurd	139	-	2.6	-78.2	-77.6[d]	+0.6
Hurd-Irvine	98	(2.8)	-	-69.6	-71.3[b]	-1.7
Irvine-Martyr	95	-	6.3	-78.7	-79.0[e]	-0.3

a. Median for the period June 1985 to November 1985

b. Median for the period June 1985 to July 1986 (14 months)

c. Median for the month of June 1985 only

d. Median for the period June 1985 to December 1985

e. Median for the period October 1985 to May 1986

The observed median values are close to the predicted values and, except for two links, the differences are not judged very significant considering the absolute measurement accuracy of the system (see Section 4.0 on page 6). The first important discrepancy is for the UHF link Lemieux-Sargent where a difference of 10.3 dB is estimated. However, this is not really a fair comparison since only 24 days of data were available from this path; furthermore, this was for the summer period where propagation conditions are the least stable and not usually representative of the longer term fading characteristics. The other large discrepancy is for the VHF link Stanley-Martyr where a difference of 7.3 dB is found between the predicted and observed medians. This is the only link where transmission is overland. There is some doubt about the exact geographical position of the site at Stanley since the nature of the terrain in this area (Stanley Peak appears as just one more low altitude bump in a mogul-like environment) did not permit precise orientation to be

made and since poor weather conditions, during both site installation and site dismantlement, prevented definitive surveying. Whether the discrepancy of these medians is attributable to a few hundred metres of site misalignment or propagation effects related to overland transmission remains to be determined.

Lemieux-Sargent is the link that has the largest clearance height (see Figures 2a and 2b) and reflections over the sea surface are expected to provide 0.7 and 2.4 decibels of excess gain, at VHF and UHF respectively, over free space levels. The highest excess gain is expected on the UHF link Hurd-Irvine where the path is also characterized by a strong inclination angle. None of the paths are believed to have an excess loss due to reflection from the sea surface.

Losses by diffraction should occur on seven of the ten experimental links. The VHF link Joy-Lemieux has a considerable excess loss of over 20 dB, the transmitter at Cape Joy being almost at sea level. Note that on this path, as for five other VHF and UHF paths that are diffracted, the clearance height is less than 60% of the Fresnel zone radius.

6.2 MONTHLY 50, 10, AND 90 PERCENTILE LEVELS

Monthly medians are shown in Figures 4a, 4b and 4c. The monthly 10 and 90 percentiles are also shown on the same figures. Detailed monthly summaries of fade depth and distribution are provided in graphical format in Annexes A and B. Take note that the 10 and 90 percentile levels for September and November 1985 are magnified for some of the paths because of the fewer number of days available for calculating the distribution of those particular months (see Table 2). This also applies to graphs and statistics given for the same months in Annexes A and B.

Previous measurements made in the high Arctic or near the arctic circle have revealed that fading on oversea paths is most severe during the summer period [Butler, 1985; Bilodeau, 1988]. The observed fading trend, especially at the 10% probability level, is not so much the same for all nine paths being analyzed here. However, it can be seen that as a whole, the summer season remains quite active as far as propagation characteristics are concerned. The main difference, though, may be in the high occurrence of enhancement observed on almost all the paths throughout the year.

The overland path Stanley to Martyr has a fading trend that is unlike any of the other oversea paths. Most of the intense fading occurs during the winter months whereas fading occurrence is lesser in summer.

It is well known that depressions in signal strength can be characterized by changes in the refractive index of the atmosphere. Unfortunately, there is not enough tropospheric refractivity data available covering this part of the continent to be able to correlate it with the propagation characteristics observed here.

Figures 5a, 5b and 5c give more insight into what happened on each path during the observation period. The days that no data were available create the blank gaps seen between the curves. Examples of strong enhancements that lasted more than a day can be observed in February on one UHF path and three VHF paths. Examples of deeply depressed signals are seen during the summer months, June to September, of almost every path.

6.3 ANNUAL, SEASONAL, AND WORST MONTH CUMULATIVE DISTRIBUTIONS OF THE RECEIVED SIGNAL STRENGTH

Figures 6a to 6i give the relative cumulative distributions for the six VHF paths and three of the four UHF paths. The path Lemieux to Sargent is not presented here since only 24 days of valid data were collected during the whole monitoring period (see Section 6.5). Each distribution is offset by the value of the long term median observed on the corresponding path. Three distributions are given on each plot, covering the long-term, summer, and worst-month time periods. The time interval used for the long-term period is the total observation period shown for each path in Table 2.

The months chosen for the summer period are June, July, August and September, as was pointed out in Section 6.2 on page 11. The selection of the worst months within the June 1985 - July 1986 period was made by looking mainly at the low probability end or tail of the monthly cumulative distributions (Annex A). Based on different criteria, such as the level of the monthly medians or 10 percentiles, other choices might have been made.

Many of the monthly distribution curves shown in Annex A are characterized by a marked asymmetry about the median level axis. Below the median, the levels seem endlessly and monotonously decreasing in value, whereas above, they conversely flatten out almost completely. Such asymmetry is typical of long term fading in maritime arctic climates [Butler, 1985; Bilodeau, 1988]. On the annual, seasonal and worst month cumulative distribution curves of Figures 6a to 6i this characteristic is not so obvious.

Turning our attention for a moment to the field strength above the median (the least important part of the distribution), the enhancements at the 99.99% probability level are confined within a 3 to 14 dB range above the median. For about half of the paths, field strength values reach above free space levels and a good part of the increase must therefore result from superrefractive conditions or even ducting. The path Sargent to Hurd is certainly the one where this is most easily noticed (see Figure B1, July and August 1985, for examples).

For most paths, enhancements are slightly more frequent during the summer months, although the difference with the annual occurrence rate is small. The occurrence of ducts seems as prevalent on these paths as indicated by the radiosonde data (see Segal and Barrington, 1977) even though the radiosonde measurements were obtained over land and may not accurately represent the oversea conditions.

From a system design viewpoint, the field strength distribution below the median is certainly of utmost importance. It is an essential constituent in determining the required link margin and guaranteeing system reliability. That part of the distribution is best analyzed by breaking it down into three portions or regions of fade depth:

- tail region with fades having considerable depth (about 15 dB or more);
- a transition region (fade depths between about 3 and 15 dB);
- a region with fades having less than a few decibels of depth (0 to about 3 dB).

The boundary points suggested in parentheses seem to best characterize the set of data reported by Bilodeau [1988]. Under the different climatic conditions of the current geographical sub-regions, somewhat different boundaries are distinguishable, although they are less distinct. The low fade region spans 3 to 5 dB below the median on most of the long term probability curves whereas the knee delimiting the tail region and the transition region is absent on several paths. In fact, the paths Irvine-Martyr (UHF) and Joy-Lemieux, Lemieux-Sargent, Stanley-Martyr (VHF) do not show a tail region at all. The fading on those paths was much less severe than on the other paths.

These fade depth divisions correspond roughly to the regions where different mixtures of physical mechanisms cause the fading. In the large fade depth region (such as those seen in Figures 6a, 6b, 6f and 6g), Olsen et al. [1987] have pointed out the evidence that the atmospheric effects, particularly defocussing, are mainly responsible for reducing the direct signal to a level where the sea reflected signal can interfere destructively with it. Part of the deep fading would also be attributable, although likely to a much smaller degree, to the occurrence of atmospheric multipath. Conversely, from some point in the transition region up to around the median, sea surface reflection and multipath effects are believed to play a less important role in the fading mechanism. This is because the magnitude of the direct signal is relatively large and therefore little affected by the weaker interfering signals. In the small fade depth region, long-term atmospheric mechanisms such as scintillation would seem to be dominant; in the transition region, defocussing is most likely the commanding mechanism.

Large amounts of experimental data show that the cumulative amplitude distribution of fading in the deep-fade region has a prevailing slope of 10 dB per decade of probability [Lin, 1971]. Such a slope is one of the characteristics of the Rayleigh distribution, the Nakagami-Rice distribution, and other more complex distributions [Beckmann, 1967]. In Figures 6a, 6b, 6f and 6g, for the annual and summer periods, a large part of the fluctuations are contained within ±3 dB of the Rayleigh slope.

One has to note in Figures 6a, 6b and 6g, the quasi-parallelism between the large fade depth tails of the distributions for a given path: the curves for the annual, summer, and worst month distribution are almost parallel. The tails of the summer and worst month distributions seem offset from the annual distribution by near constant amounts. This is due to the bi-seasonal nature of the observed fading. Outside of the summer period, there is so

little fading that the fall-winter-spring cumulative distribution is relatively flat and almost tailless. Consequently, the tail of the annual distribution is mainly determined by the tail of the summer distribution but adjusted by its time contribution.

Looking back at the plots a and c of Figure 6, one would be tempted to conclude that the fading at UHF tends to get worse for the more eastern paths. It is to be noted however that no statistic was available for the summer period on the link Irvine-Martyr (see Table 2).

Of these paths, the one from Stanley has one of the less severe characteristics of annual fade depth. Stanley is also the only path that is overland.

6.4 SEASONAL FADE DEPTH AND ENHANCEMENT LEVEL STATISTICS

A fade is a reduction of the received signal level as measured from an arbitrary level such as the monthly or annual median, or the calculated free-space level. Conversely, an enhancement is an increase of the received signal level usually measured from the same reference level. The number and duration of fades or enhancements which occur depend on the fade-depth or enhancement thresholds set about the reference level.

The distributions of number of fades (enhancements) and average fade (enhancement) duration observed as a function of fade depth (enhancement level) are shown in Figures 7a and 7b. The fade depths and enhancement levels were measured from the monthly medians of the most active months (see Table 4). Statistics from each selected month[1] were then cumulated to produce the "seasonal" data of Figures 7a and 7b.

The number of enhancements observed follows in all cases a monotonic progression. The duration of the enhancements is also motonously decreasing, except for the VHF link Irvine-Martyr. On the latter path, enhancement levels of at least +3, +6 and +9 dB lasted on average the same time i.e. approximately 80 minutes.

The fade distributions, both in duration and in number, are not as smooth as the enhancement distributions. The statistics for the paths Sargent-Hurd-Irvine indicate that fades last longer at VHF than at UHF but occur less frequently, regardless of the fade depth (for e.g., compare the top left diagrams of Figures 7a and 7b, or the top right diagrams of the same Figures).

It is interesting to note that on the path Stanley-Martyr, the only overland path, the number of fades (or enhancements) is not maximum at the value of the seasonal median. Fades having depths of -3 and -6 dB occurred more frequently than the median level itself but lasted significantly less longer. Such characteristic is not observed in the long term statistics of any of the oversea paths.

---

1. Detailed monthly fade depth and enhancement level statistics are given in Annex C.

TABLE 4. Monitoring periods selected for cumulating the seasonal fade depth and enhancement level statistics of Figures 7a and 7b

PATH	Selected Months	
	in 1985	in 1986
UHF		
Sargent-Hurd	June, July, August, September	-
Hurd-Irvine	June, July, August, September	June, July
VHF		
Sargent-Hurd	June, July, August, September	-
Hurd-Irvine	June, July, August, September	June, July
Irvine-Martyr	June, July, August, September	June, July
Stanley-Martyr	June, July, August, September	June, July

6.5 PARTIAL STATISTICS FOR THE PATH LEMIEUX-SARGENT

The UHF link Lemieux-Sargent, one of the termination links of the repeater chain, suffered from the equipment problems discussed in Section 4.0 on page 6 and therefore could not be thoroughly analyzed.

The statistics for the Lemieux-Sargent path, which is the eastern most UHF path and second longest path of the relay system, are presented in Figure 8. Like the other UHF data, the cumulative distribution of power received shows considerable fading during the month of June 1985.

6.6 EXAMPLES OF VHF/UHF CORRELATED EVENTS

As was mentioned in Section 4.0 on page 6, temporal plots of the recorded data were generated for visual inspection of the data. Some data segments are presented in this section to exemplify cases of strong fading and enhancement correlation between the VHF and UHF signals of a same path.

The general trend of enhancements and fadings is shown on Figures 9 and 10 respectively. The plots were lightened by decimating the raw data to the median value of every 24 and 30 second interval respectively. Both enhancement and fading last for several hours at a time and usually affect the signals at VHF and UHF in similar but not identical manner. There are also times when this correlation is reversed and fading is observed at

one frequency while enhancement is occurring at the other frequency. Such an event is shown on Figure 11. By visual inspection of the raw data, it would appear that the latter, a case of negative correlation, does not occur frequently.

6.7 UHF SCINTILLATION NOISE

Amplitude scintillations are caused by scattering from tropospheric turbulence and precipitation particles. Generally wave propagation along slant paths can be affected by tropospheric turbulences, ice clouds and rain simultaneously. At UHF and below however, rain, hail, snow and fog are of no consequence. Received signal strengths vary with time mainly because of changes in the refractive index of the atmosphere [Hall, 1979]. To what extent the signal is affected by scintillation induced by tropospheric turbulence (small-scale fluctuations of the refractive index) at UHF is unknown to the author.

Figure 12 shows a rare case during the test period June 1985 to July 1986 where scintillation appears unusually intense, almost predominant over other fading mechanisms. The event occured on the slanted path Hurd-Irvine, at UHF, on October 24th 1985. From the top plot it can be seen that the scintillation is riding on top of a much slower fade probably created by a slow-moving air mass. The bottom plot shows the time series of the signal as recorded every 2.5 seconds. A Fourier transform was performed on this data segment and revealed a flat frequency spectrum, typical of any white random noise. This was to be expected because of the low sampling rate used to record the signal. Other cases of scintillation were seen on this same path, none of them reaching such magnitude.

6.8 DIURNAL VARIATION

Diurnal variations were not analyzed thoroughly. Partial results are shown in Figure 13 for the UHF path Hurd to Irvine. Very similar results were obtained for all the other paths, but because of their close similarity, are not detailed here. The main characteristic which appears in Figure 13 is the lack of any pronounced diurnal variation around the median. A diurnal amplitude of about 1 dB is observed in August and September, but without well defined temporal pattern. As for the cumulative distribution data, the variations are most important during the summer months (June to September inclusive) whereas in winter, the curves are almost perfectly flat. This latter characteristic is rather similar to that observed by Butler [1985] in *sub-region Ic* and variation, or rather lack of variation in summer, is also very similar to that observed by Bilodeau [1988] in the Hudson Strait area. Diurnal amplitude could possibly vary more if measured at either end of the distribution rather than at the median.

7.0 CONCLUSIONS

The signal strengths received across four UHF links and six VHF links in the Lancaster Sound area of the North West Passage were monitored to study the reliability of transmission. All paths but one were over sea, with lengths in the range 62 to 139 km.

As was originally observed on some paths in the central Arctic [Butler, 1985], this eastern region of the Canadian Arctic islands is an area of great variability of radio propagation conditions. In general, propagation is most stable during the period of winter darkness (although strong exceptions to this rule may occur), and is most variable during the period of continuous daylight.

On eight of the ten propagation paths analysed, there was a good agreement of observation with theoretical predictions of median signal levels.

Ducting was frequently observed on most of the paths, agreeing with the degree of occurrence predicted by radiosonde measurements. On any given path, fading events of VHF and UHF signals were usually correlated positively. Signal enhancements at VHF were at times also observed during signal fading at UHF.

There does not seem to be important geographical dependence of the fading characteristics throughout the Sound. Lack of pronounced diurnal variation around the median was observed on all paths.

8.0 ACKNOWLEDGEMENTS

The major part of the project was under the initiative of Dick Butler. Dick left CRC before having the pleasure to see any result of his experiment. To him, I wish to record my thanks for whatever measure of success has been achieved.

I am especially grateful to Keith Bedal for his meticulous and persistent efforts during laboratory preparation of the radio relay system.

Space and facilities for the digital recording system based at Resolute Bay were kindly provided by Transport Canada. The Telecommunications and Electronics Branch of the Canadian Coast Guard has maintained a close interest in the Northwest Passage Experiment, arranging for support at Resolute of the data recording system. I would like to thank A.K. Khan, Superintendent of Communications Systems, and Dick Galvin, Telecommunications Area Manager at Resolute, for their invaluable co-operation.

The experiment has been supported in its field operations by the Polar Continental Shelf Project of the Department of Energy, Mines and Resources, and by Bradley Air Services Ltd. The friendly contribution of their staff was an asset to our work.

My thanks are also due to the staff members of the Radio Propagation Laboratory who contributed in numerous ways to the realization of the experiment, analysis of the results, and preparation of this report.

9.0 REFERENCES

Armstrong W.A. and W.D. Barnes (1979), "*A Battery for Arctic Radio Repeater Systems*", DREO Technical Note No.79-27, Defence Research Establishment, Ottawa

Beckmann P. (1967), "*Probability in Communication Engineering*", Harcourt, Brace and World, Inc., New York

Bilodeau C. (1988), "*Measurements of UHF Radio Propagation on the Baffin and Labrador Coasts (U)*", CRC Report No. 1430, Communications Research Centre, Department of Communications, Ottawa

Bilodeau C. and K.S. McCormick, "*The High Arctic Troposcatter Experiment: Final Report*", CRC Report No. CRC-RP-94-002, Communications Research Centre, Department of Communications, Ottawa

Butler R.S., J.I. Strickland and C. Bilodeau, (1984), "*VHF and UHF Propagation in the Canadian High Arctic*", in AGARD Conference Proceedings, CP-346, Characteristics of the Lower Atmosphere Influencing Radio Propagation, pp. 27-1, 27-8.

Butler R.S. (1985), "*The Northwest Passage Propagation Experiment: Report of the 1983-1984 Measurement Program*", CRC Report No.1391, Communications Research Centre, Department of Communications, Ottawa

Environment Canada (1982), "*Canadian Climate Normals: Vol.2 Temperature 1951-1980*", Atmospheric Environment Service, Ottawa

Hall M.PM. (1979), "*Effects of the troposphere on radio communications*", IEE Electromagnetic Waves Series 8, Institution of Electrical Engineers, New York

Lin B.H. (1971), "*Statistical Behavior of a Fading Signal*", in The Bell System Technical Journal, pp. 3211-3270

Maxwell J.B. (1981), "*Climatic Regions of the Canadian Arctic Islands*", in Arctic, Vol.34, No.3, Toronto, pp. 225-240

Olsen R.L., L. Martin, and T. Tjelta (1987), "*A review of the role of surface reflection in multipath propagation over line-of-sight terrestrial microwave links*", in NATO/AGARD Conf. Proc., No. CP-407, National Technical Information Service, Springfield, VA, USA, Nov. 1987, pp. 2/1-23

Palmer F.H. (1979), "*VHF and UHF Propagation Studies in the Canadian Arctic*", CRC Report No.1327, Communications Research Centre, Department of Communications, Ottawa

Palmer F.H. (1980), "*Report on the Great Lakes Propagation Measurement Program: Comparisons of the Canadian Data with the Predictions of FCC R-6602*", CRC Report No.1332, Communications Research Centre, Department of Communications, Ottawa

Segal B. and R.E. Barrington (1977), "*The Radio Climatology of Canada - Tropospheric Refractivity Atlas for Canada*", CRC Report No.1315-E, Communications Research Centre, Department of Communications, Ottawa

Strickland J. (1981), Private communications

Whitteker J.H. (1983), "*Propagation Prediction from Topographic Data Base*", in Proceedings of IEEE International Conference on Communications, Boston, pp. A2.1.1 - A2.1.5

Whitteker J.H. (1985), "*Measurements of VHF/UHF Radio Propagation in a Maritime Temperate Climate*", CRC Report No.1380, Communications Research Centre, Department of Communications, Ottawa

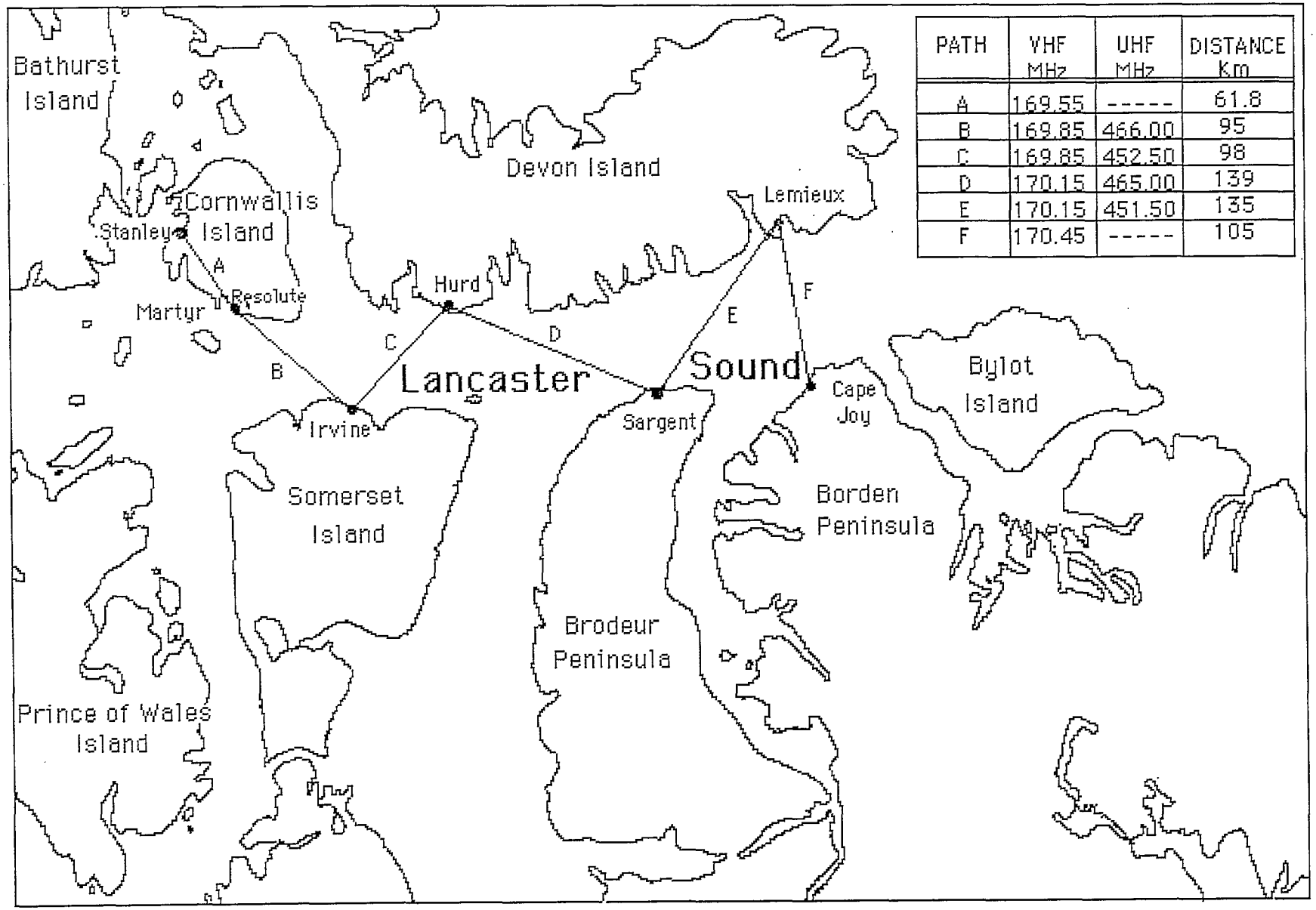

PATH	VHF MHz	UHF MHz	DISTANCE Km
A	169.55	-----	61.8
B	169.85	466.00	95
C	169.85	452.50	98
D	170.15	465.00	139
E	170.15	451.50	135
F	170.45	-----	105

Figure 1: The experimental region, showing equipment locations and propagation paths

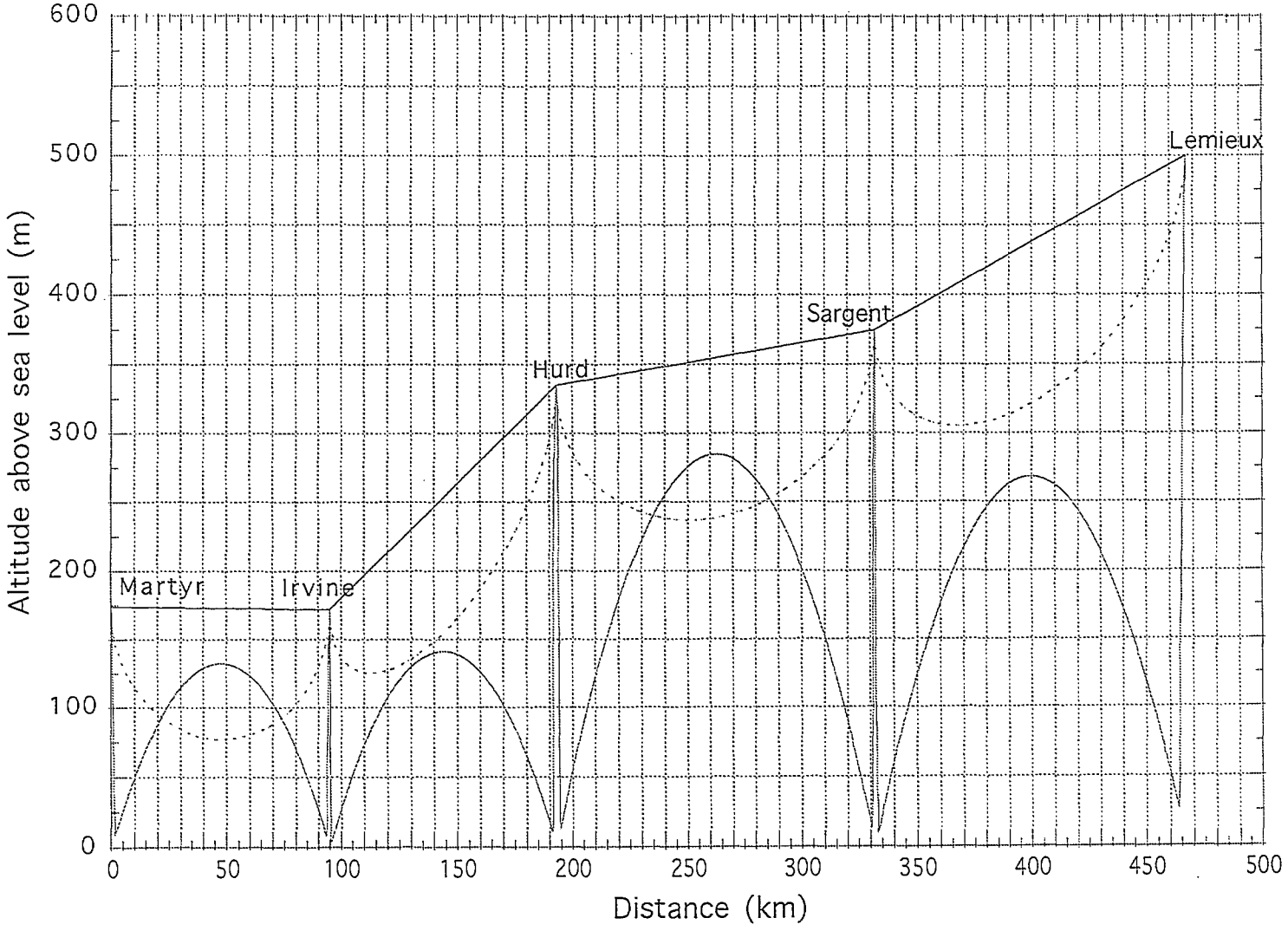

Figure 2a: Profiles of four UHF paths, including four-thirds earth curvature for refraction, with 0.6 Fresnel zone

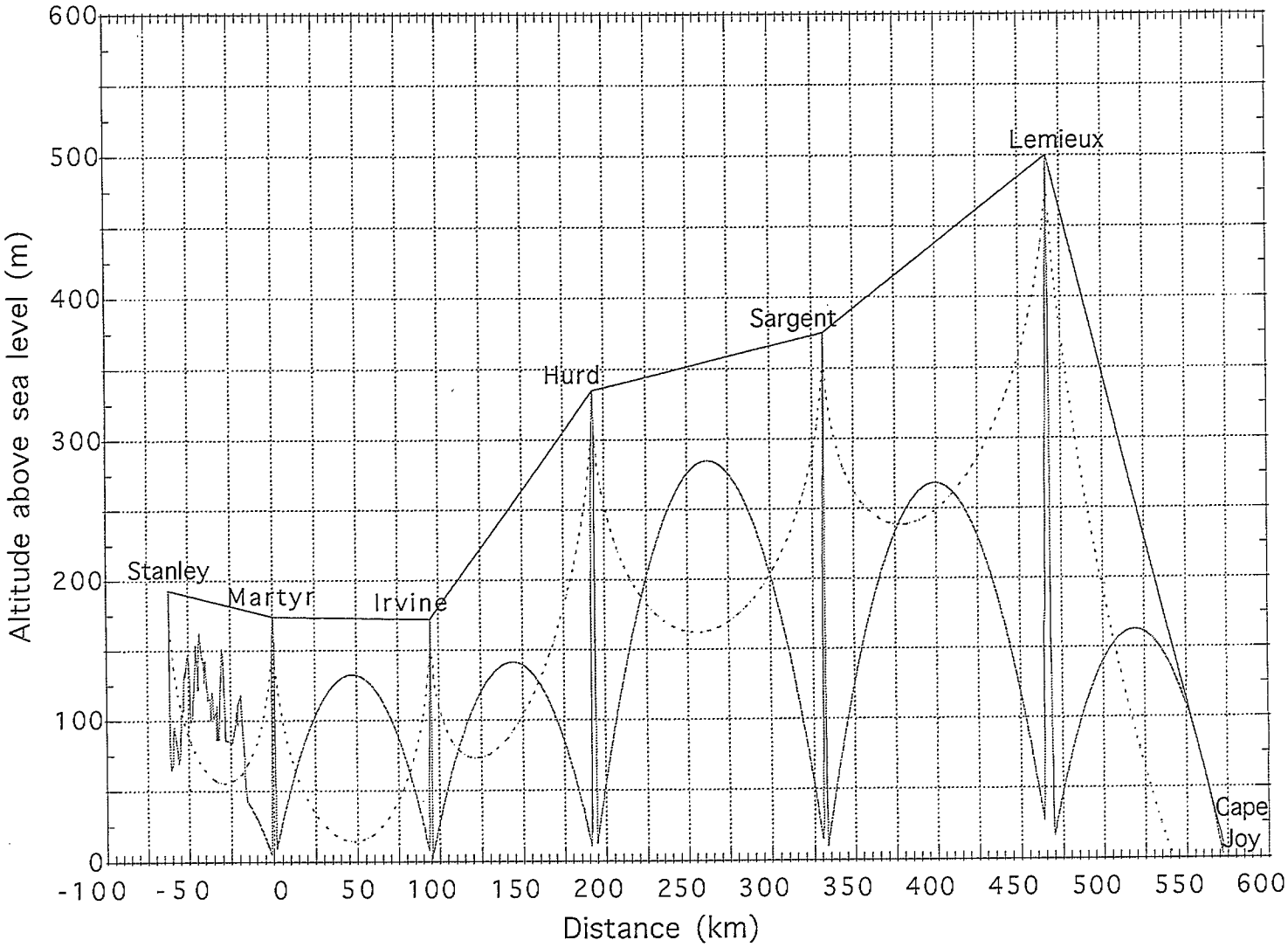

Figure 2b: Profiles of six VHF paths, including four-thirds earth curvature for refraction, with 0.6 Fresnel zone

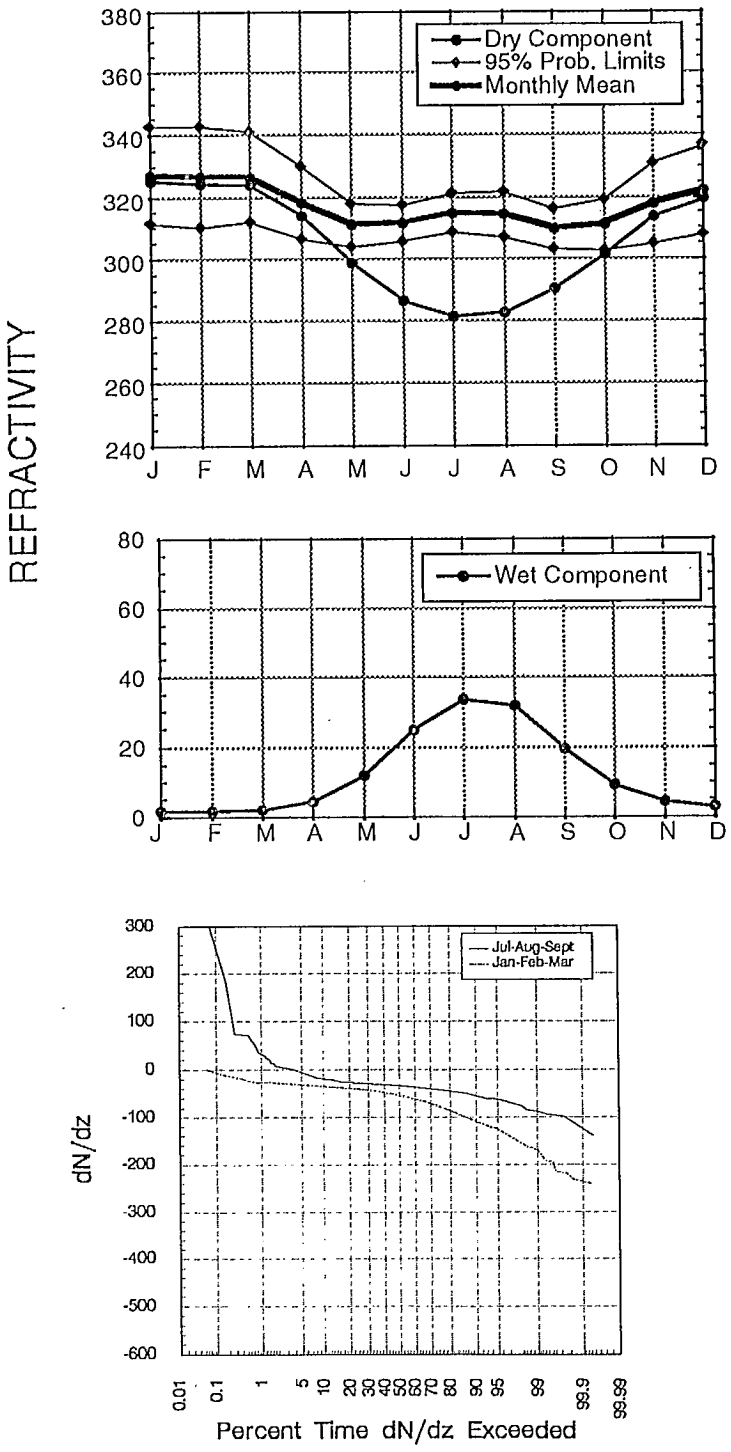

Figure 3: Refractivity data for Resolute Bay
(after Segal and Barrington, 1977)

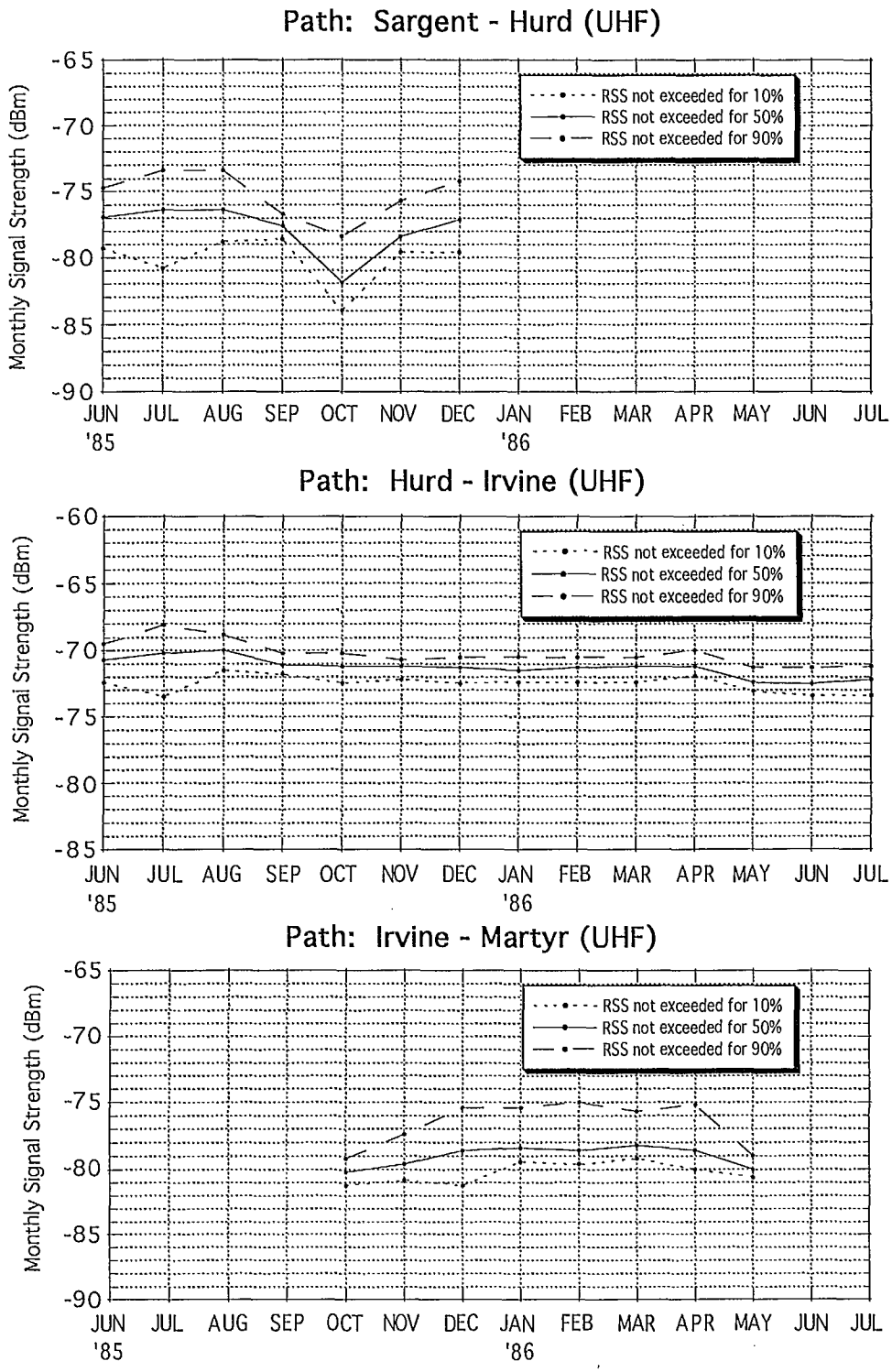

Figure 4a: Monthly 10, 50, and 90 percentiles of Received Signal Strength (RSS).

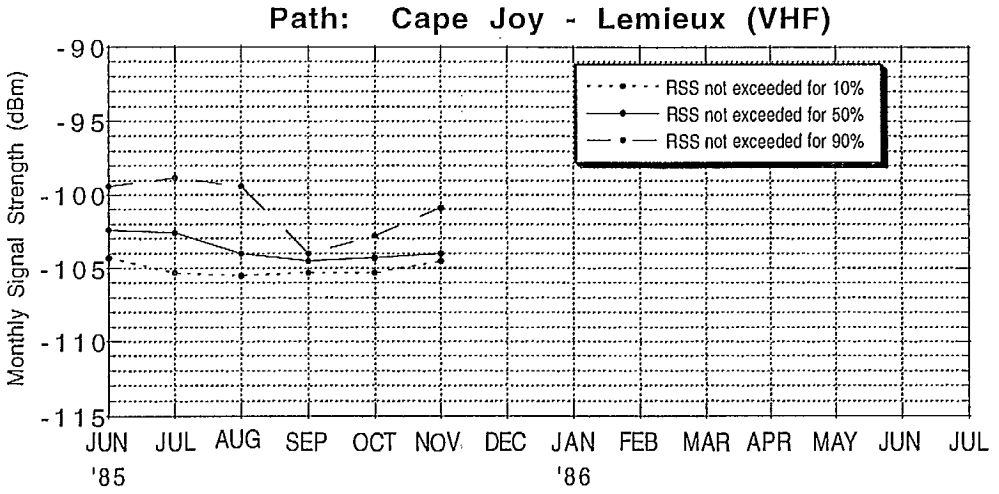

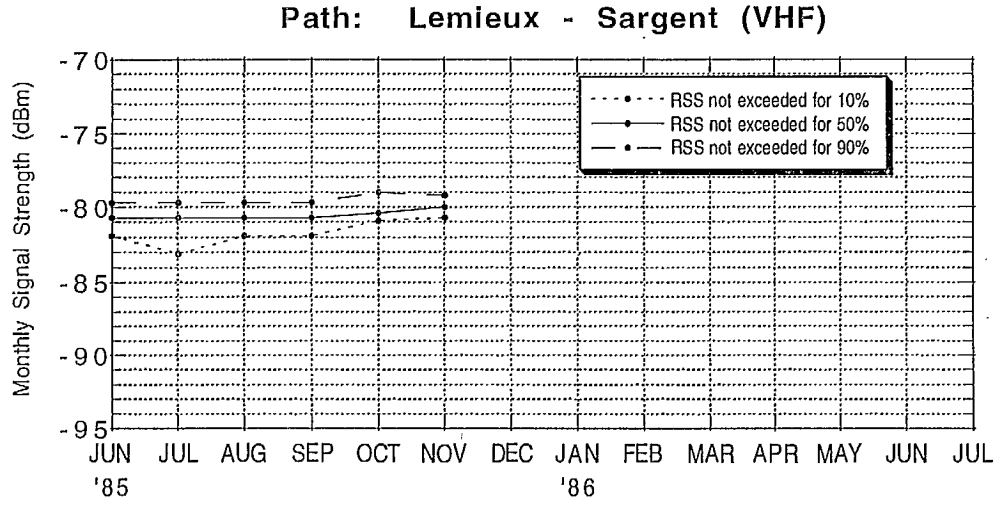

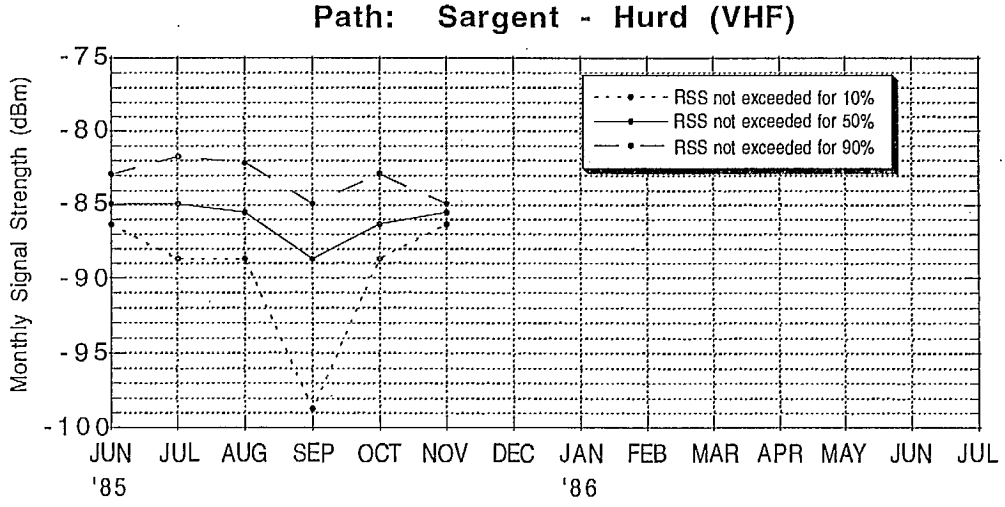

Figure 4b: Monthly 10, 50, and 90 percentiles of Received Signal Strength (RSS).

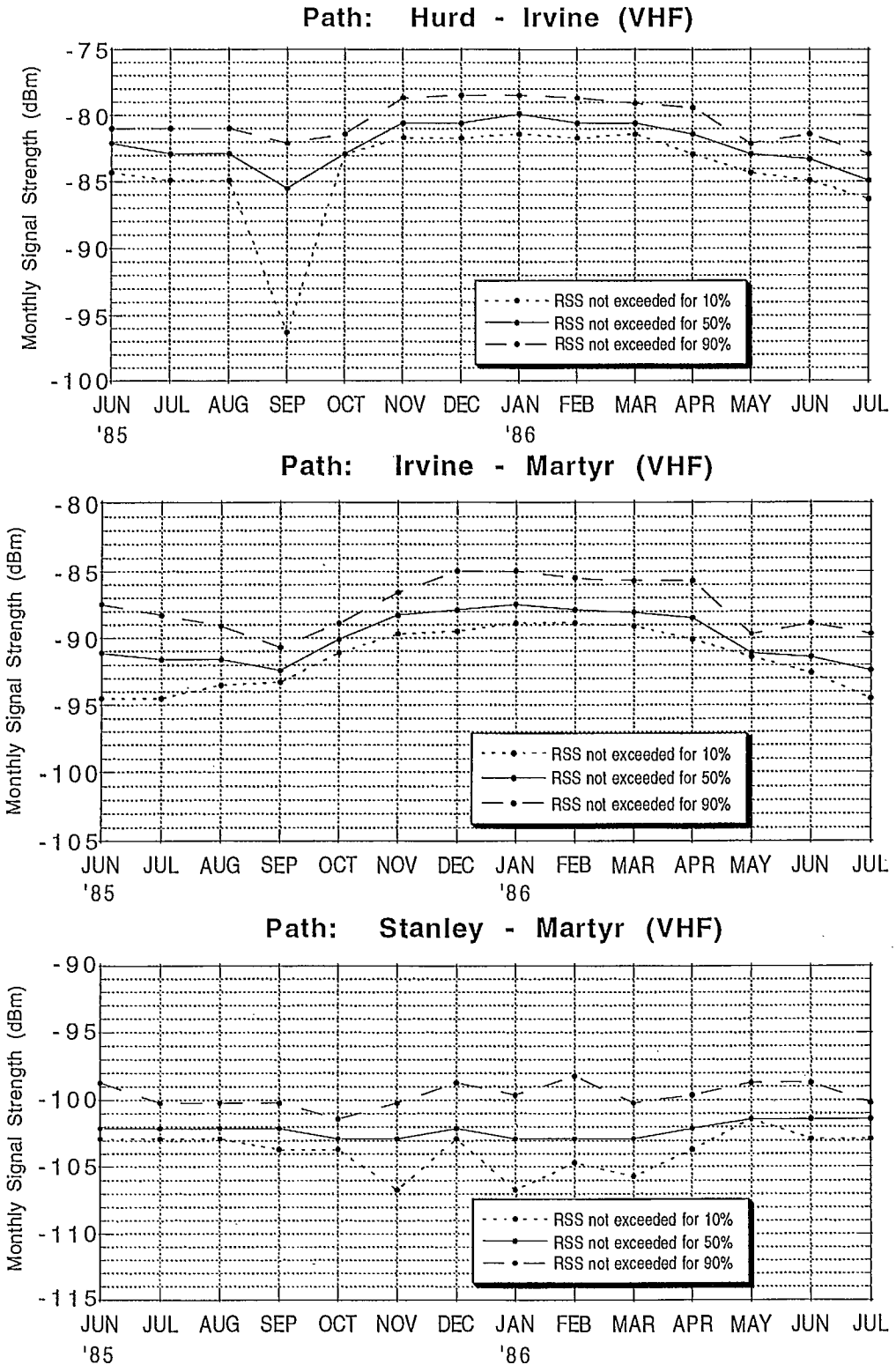

Figure 4c: Monthly 10, 50, and 90 percentiles of Received Signal Strength (RSS).

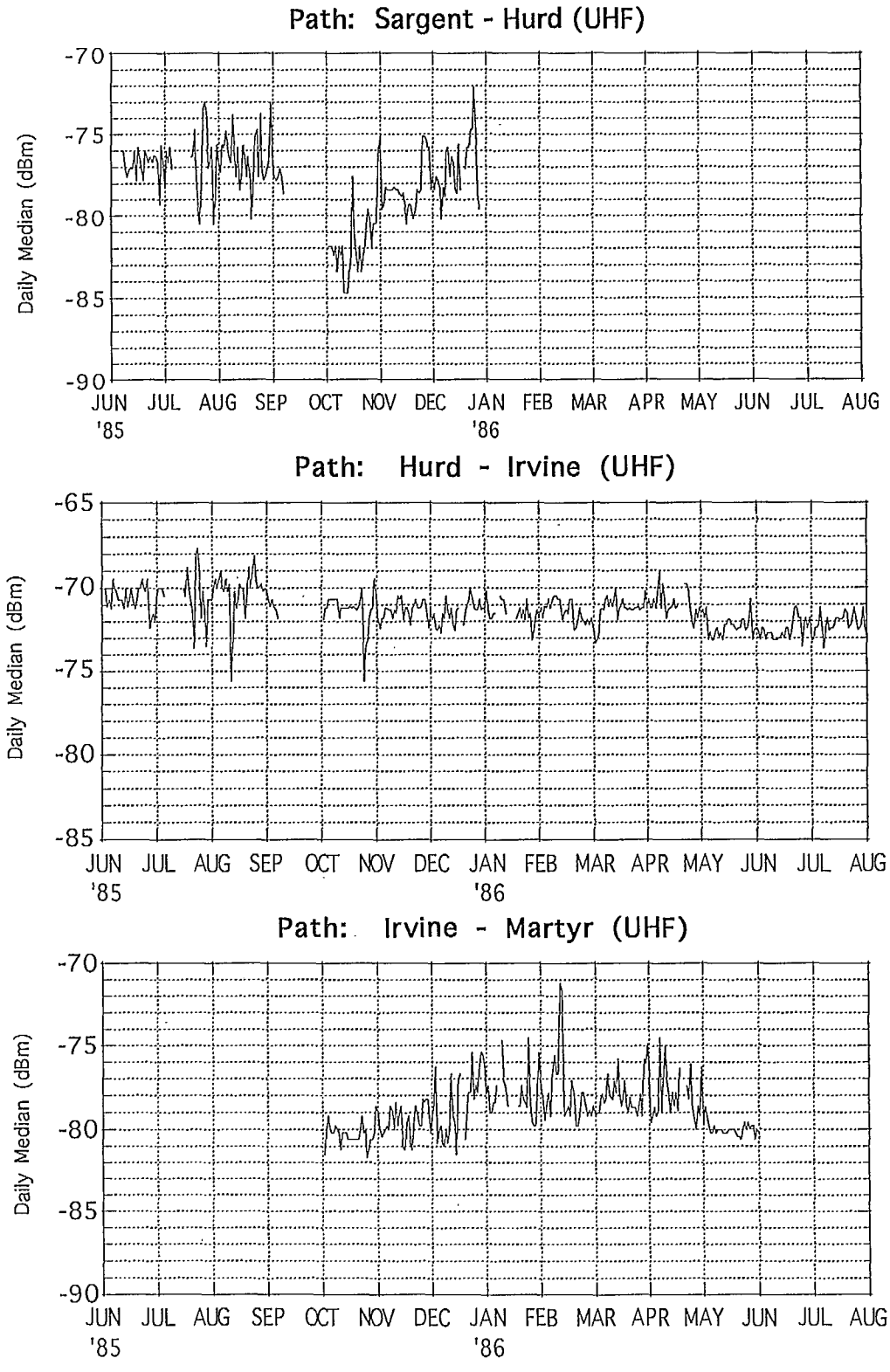

Figure 5a: Daily median values of Received Signal Strength.

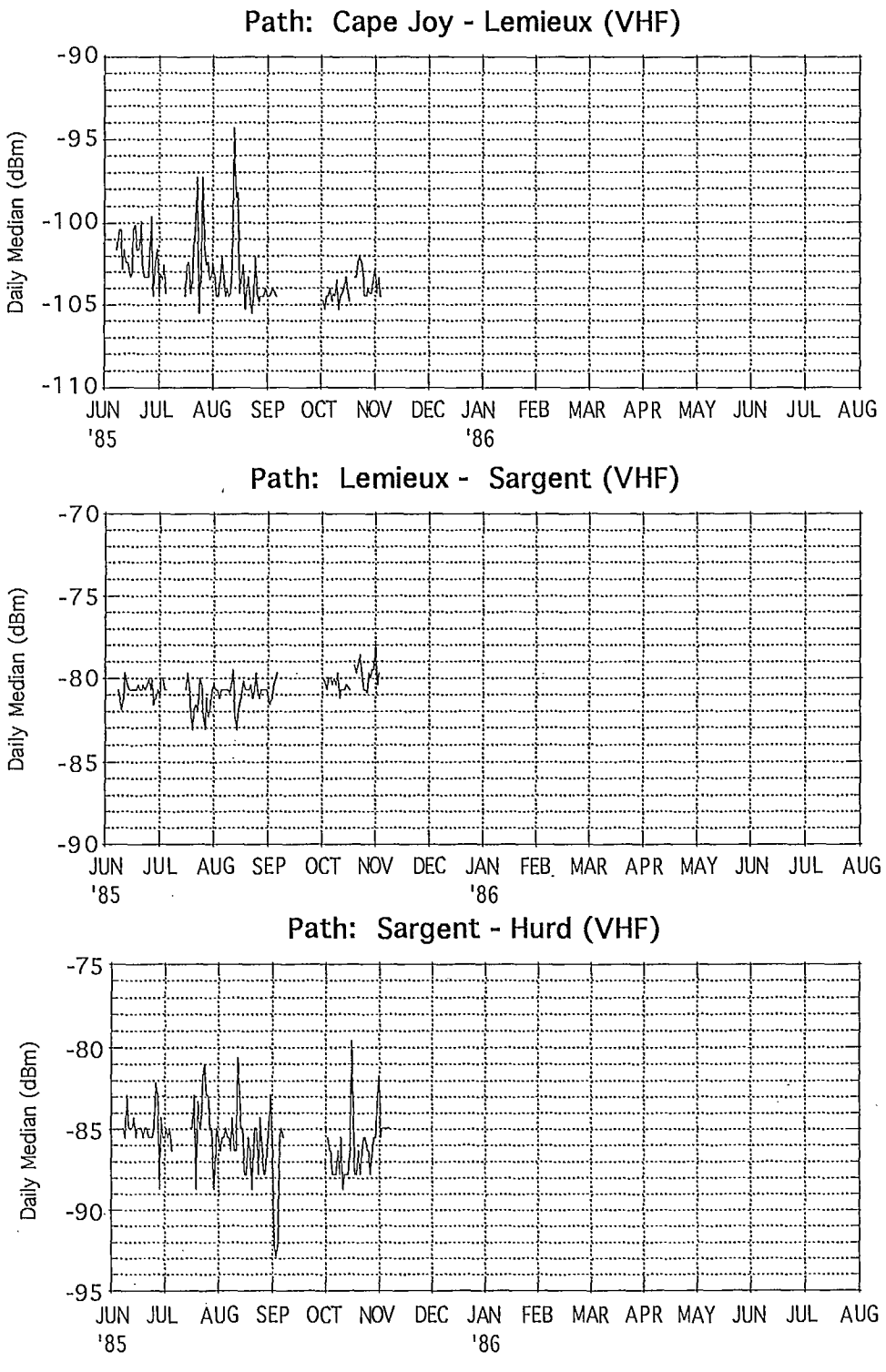

Figure 5b: Daily median values of Received Signal Strength.

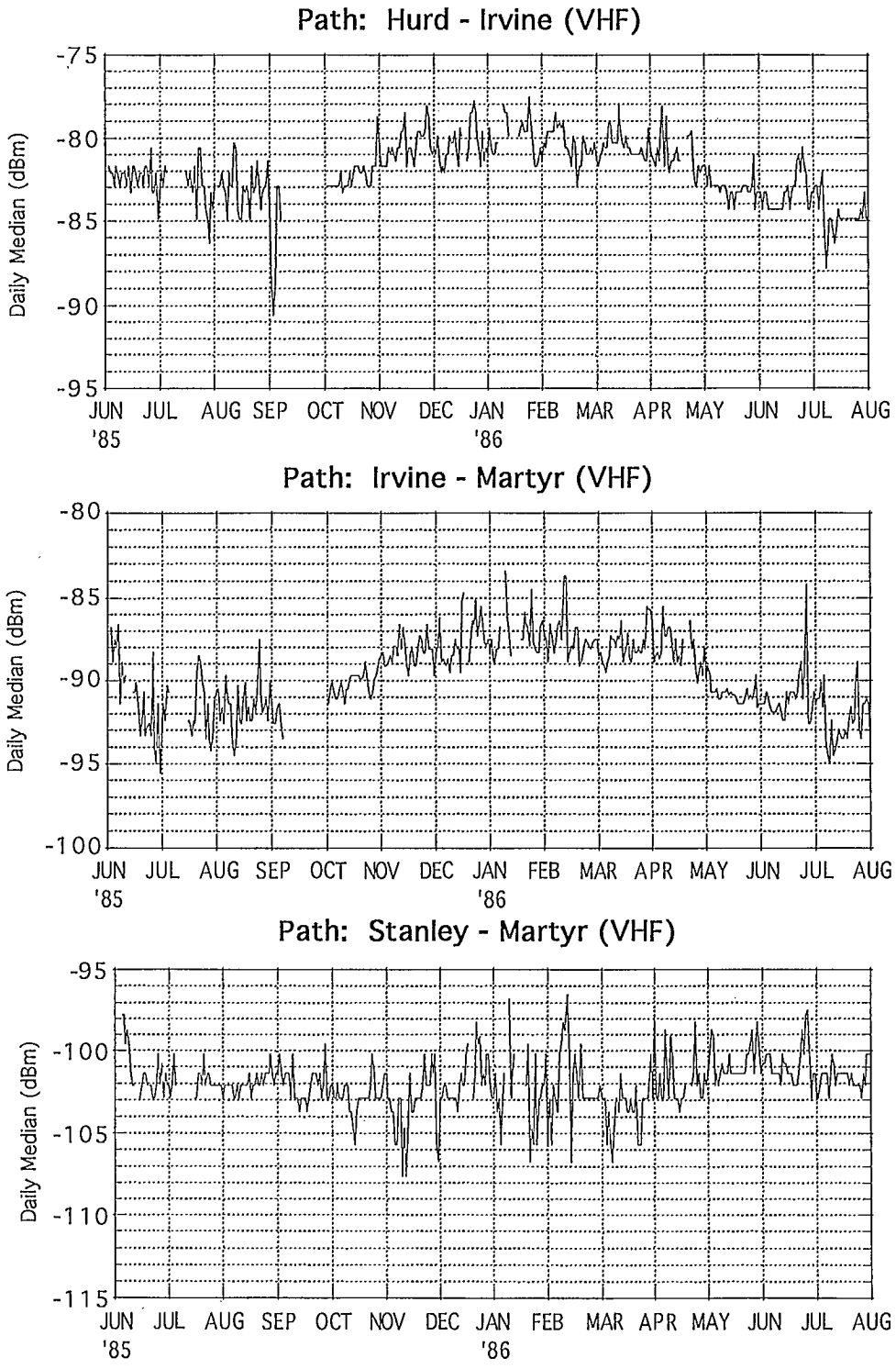

Figure 5c: Daily median values of Received Signal Strength.

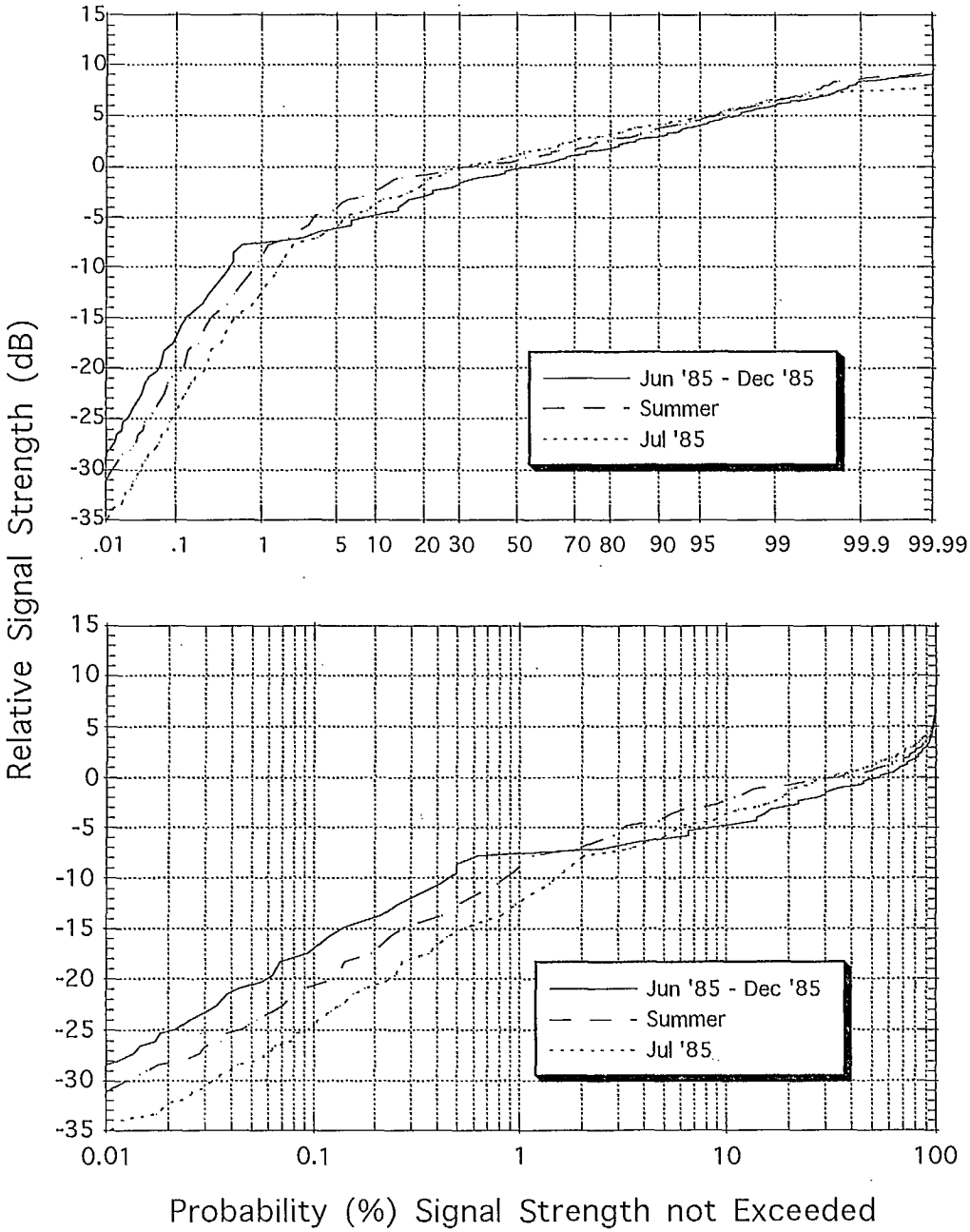

Figure 6a: Long term, seasonal, and worst month cumulative distributions of power received at HURD PEAK from SARGENT Peak (UHF), relative to the long term median (-77.6 dBm).
Upper plot: Log-Gauss, Lower plot: Log-Log.

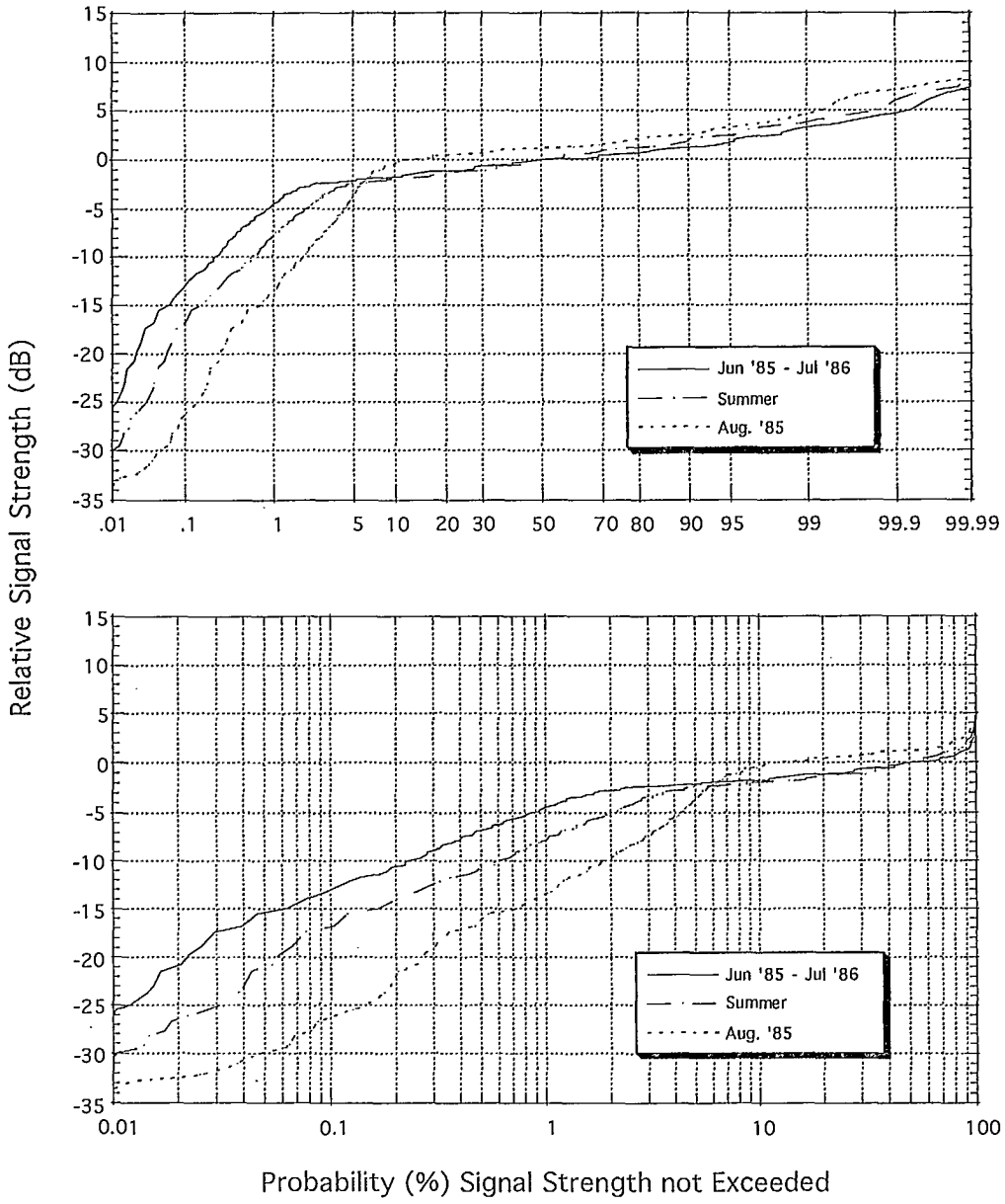

Figure 6b: Long term, seasonal, and worst month cumulative distributions of power received at IRVINE PEAK from HURD PEAK (UHF), relative to the long term median (-71.3 dBm).
Upper plot: Log-Gauss, Lower plot: Log-Log.

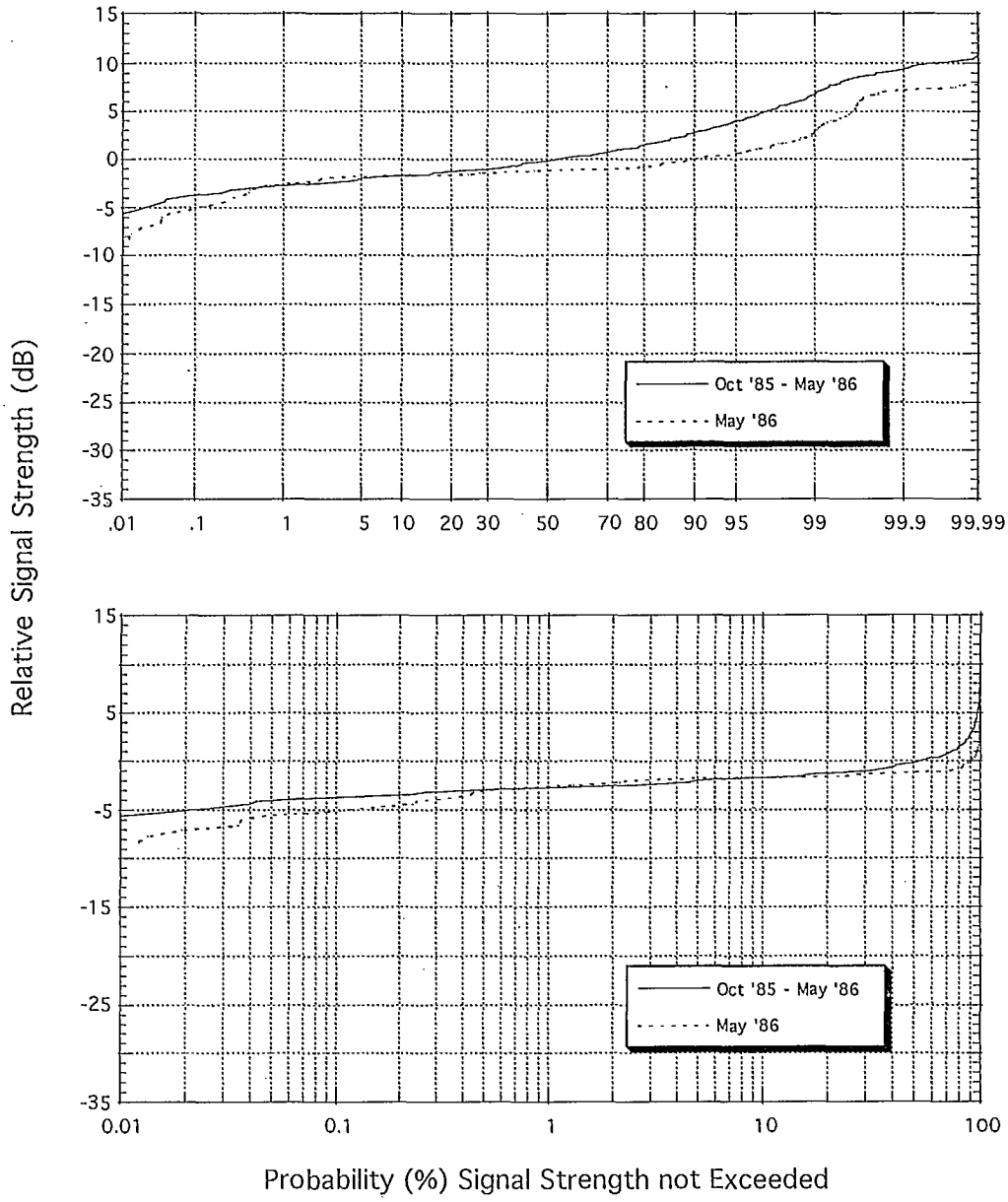

Figure 6c: Long term and worst month cumulative distributions of power received at CAPE MARTYR from IRVINE PEAK (UHF), relative to the long term median (-79.0 dBm). Upper plot: Log-Gauss, Lower plot: Log-Log.

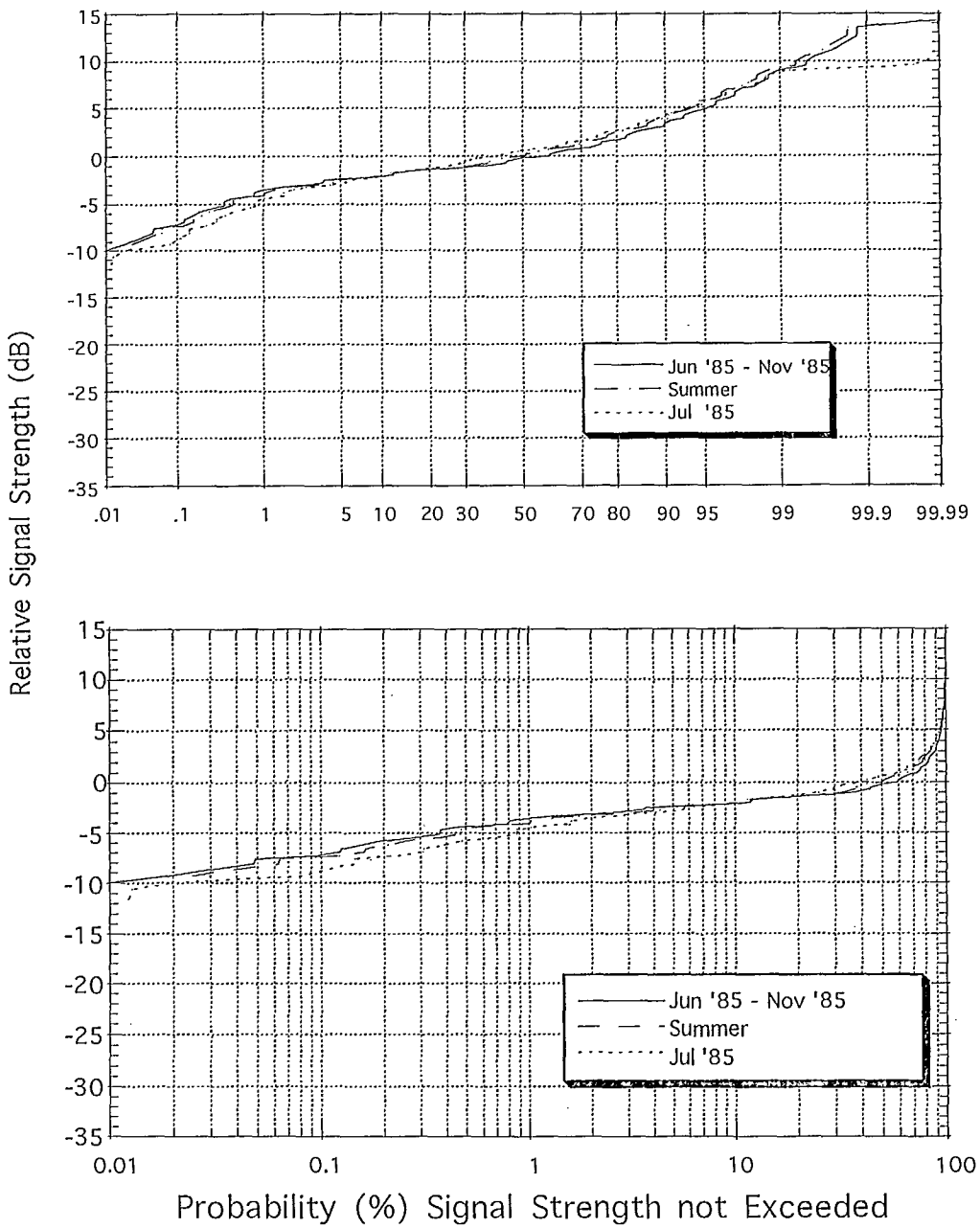

Figure 6d: Long term, seasonal, and worst month cumulative distributions of power received at LEMIEUX PEAK from CAPE JOY (VHF), relative to the long term median (-77.6 dBm).
Upper plot: Log-Guass, Lower plot: Log-Log.

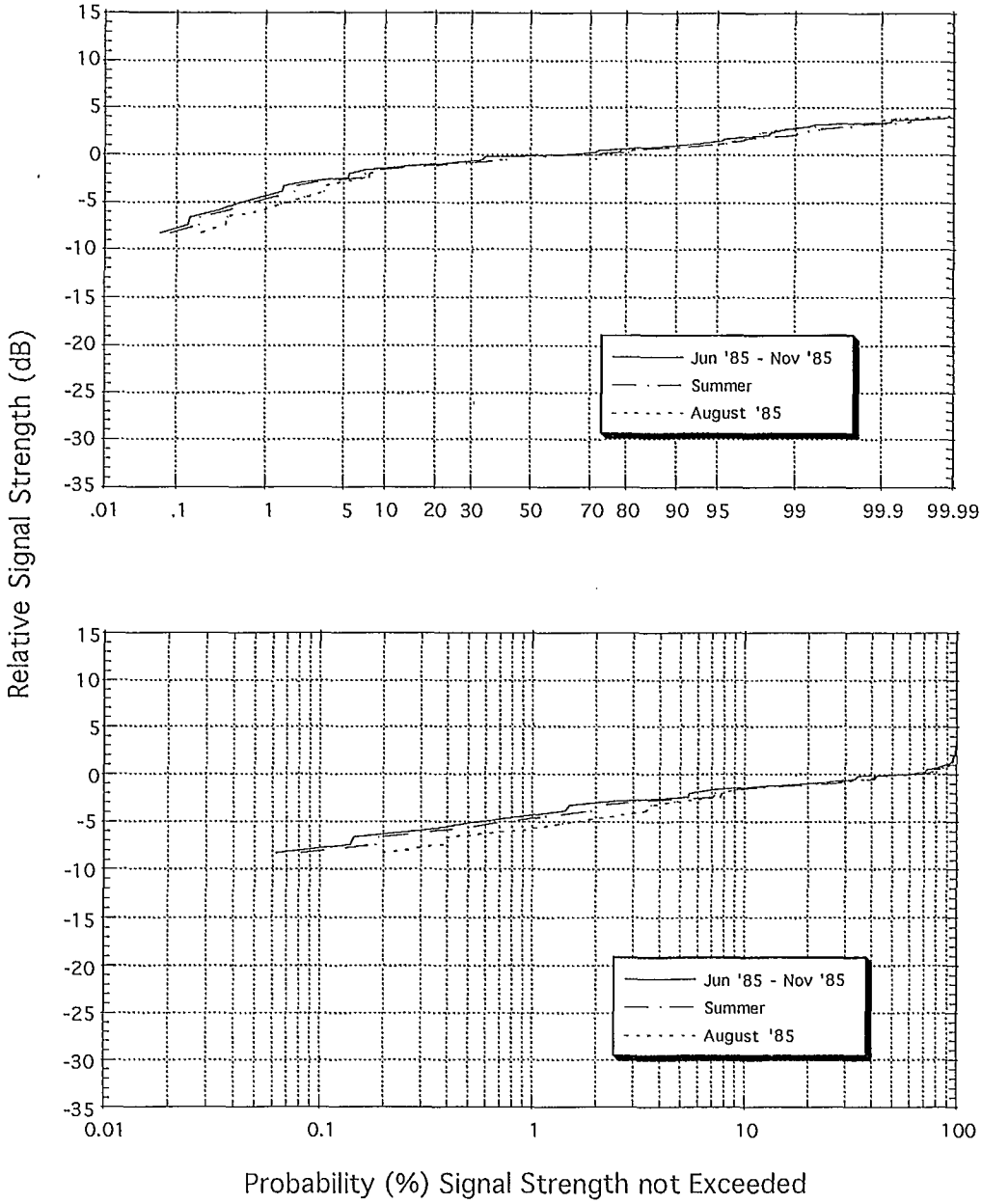

Figure 6e: Long term, seasonal, and worst month cumulative distributions of power received at LEMIEUX PEAK from SARGENT PEAK (VHF), relative to the long term median (-80.7 dBm).

Upper plot: Log-Gauss, Lower plot: Log-Log.

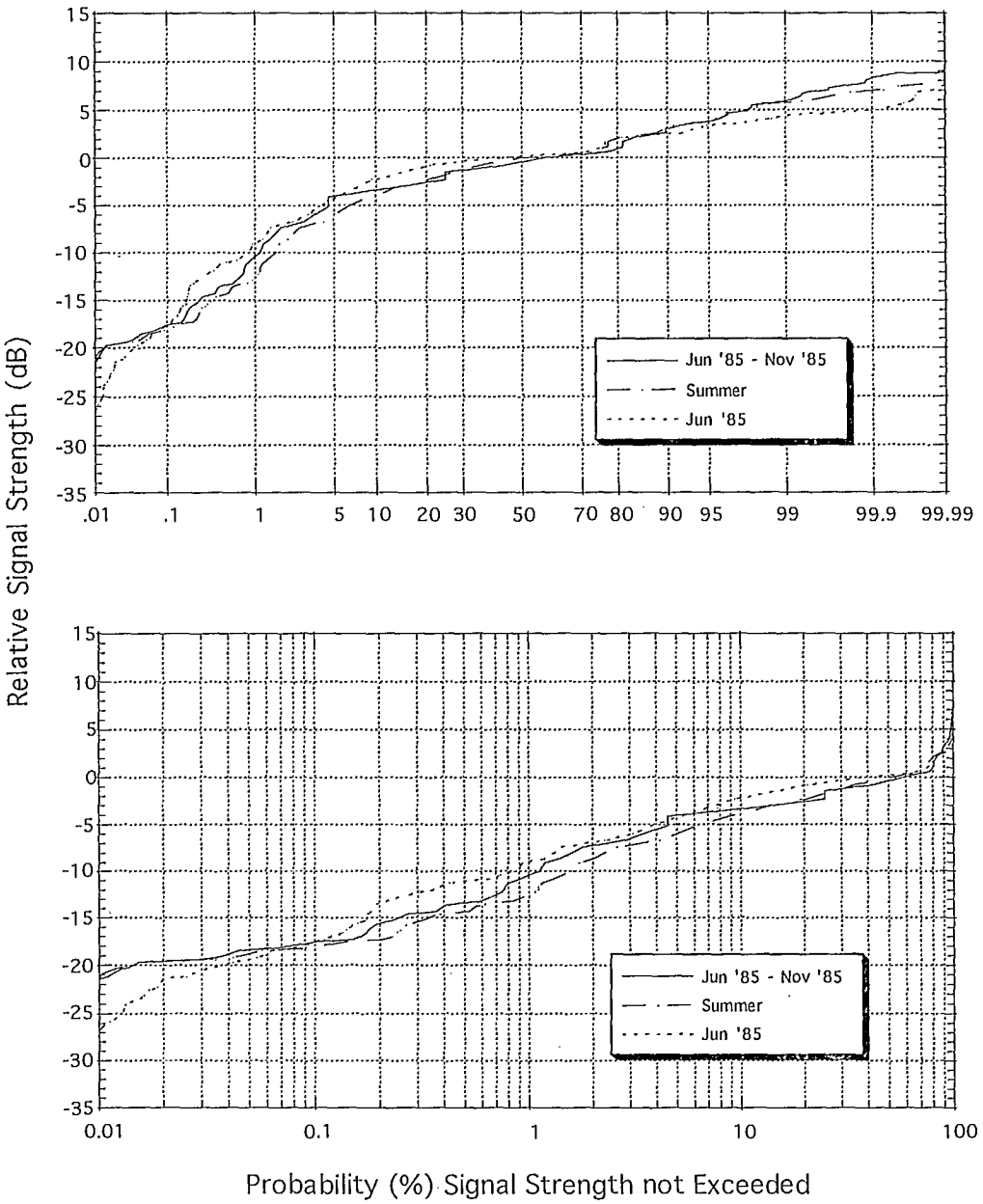

Figure 6f: Long term, seasonal, and worst month cumulative distributions of power received at HURD PEAK from SARGENT PEAK (VHF), relative to the long term median (-85.5 dBm).
Upper plot: Log-Gauss, Lower plot: Log-Log.

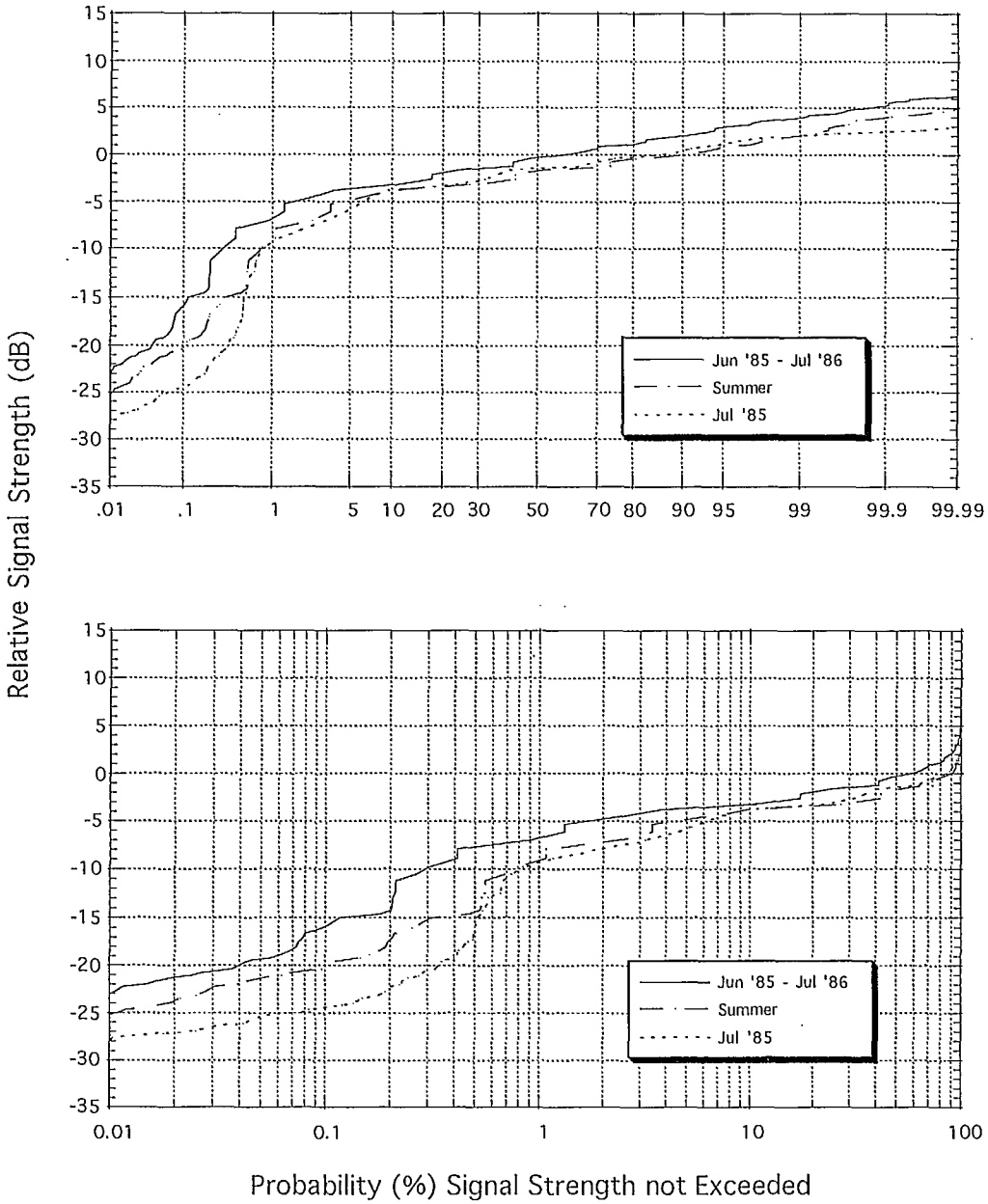

Figure 6g: Long term, seasonal, and worst month cumulative distributions of power received at HURD PEAK from IRVINE PEAK (VHF), relative to the long term median (-81.7 dBm).
Upper plot: Log-Gauss, Lower plot: Log-Log.

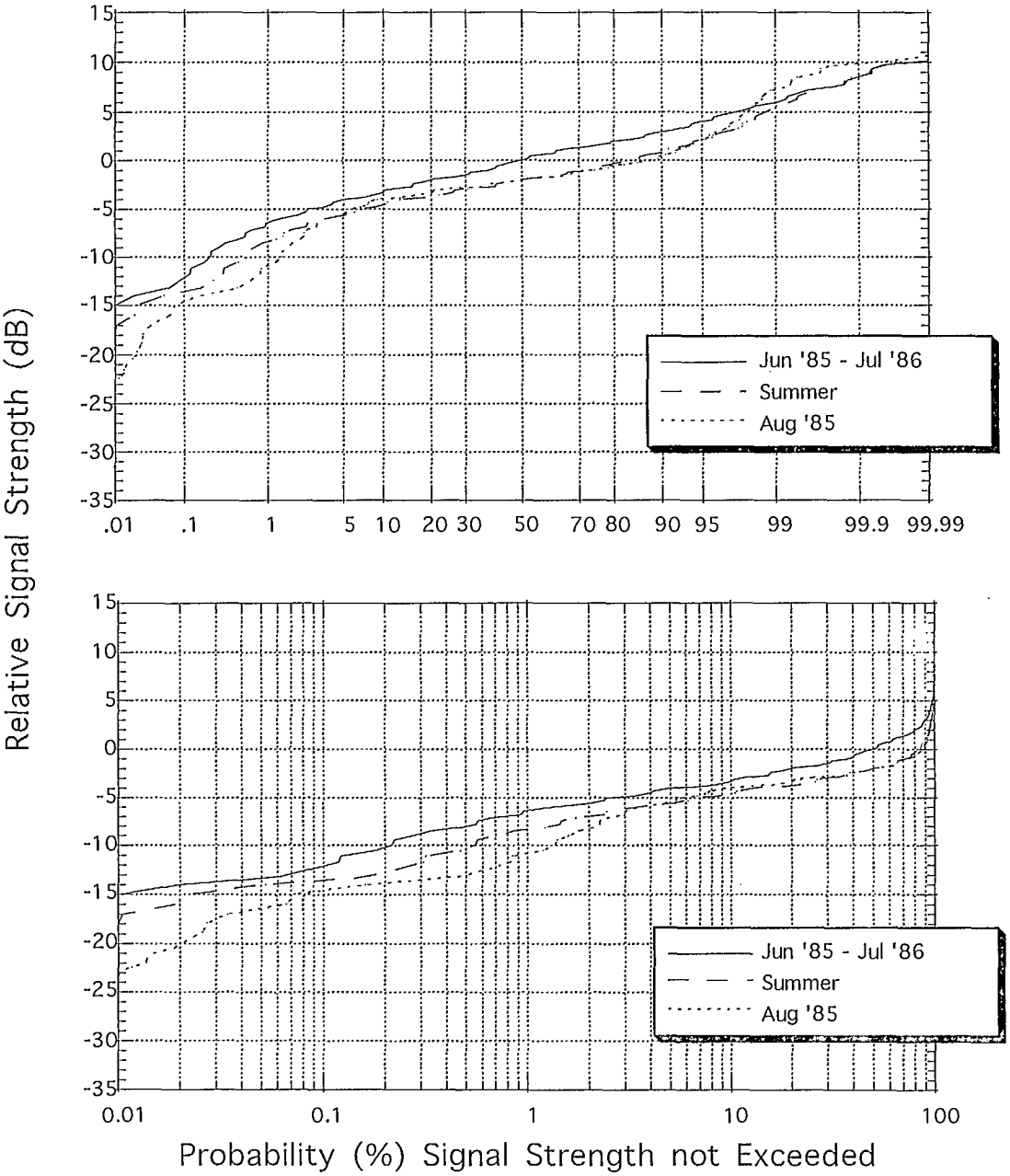

Figure 6h: Long term, seasonal, and worst month cumulative distributions of power received at CAPE MARTYR from IRVINE PEAK (VHF), relative to the long term median (-89.7 dBm).

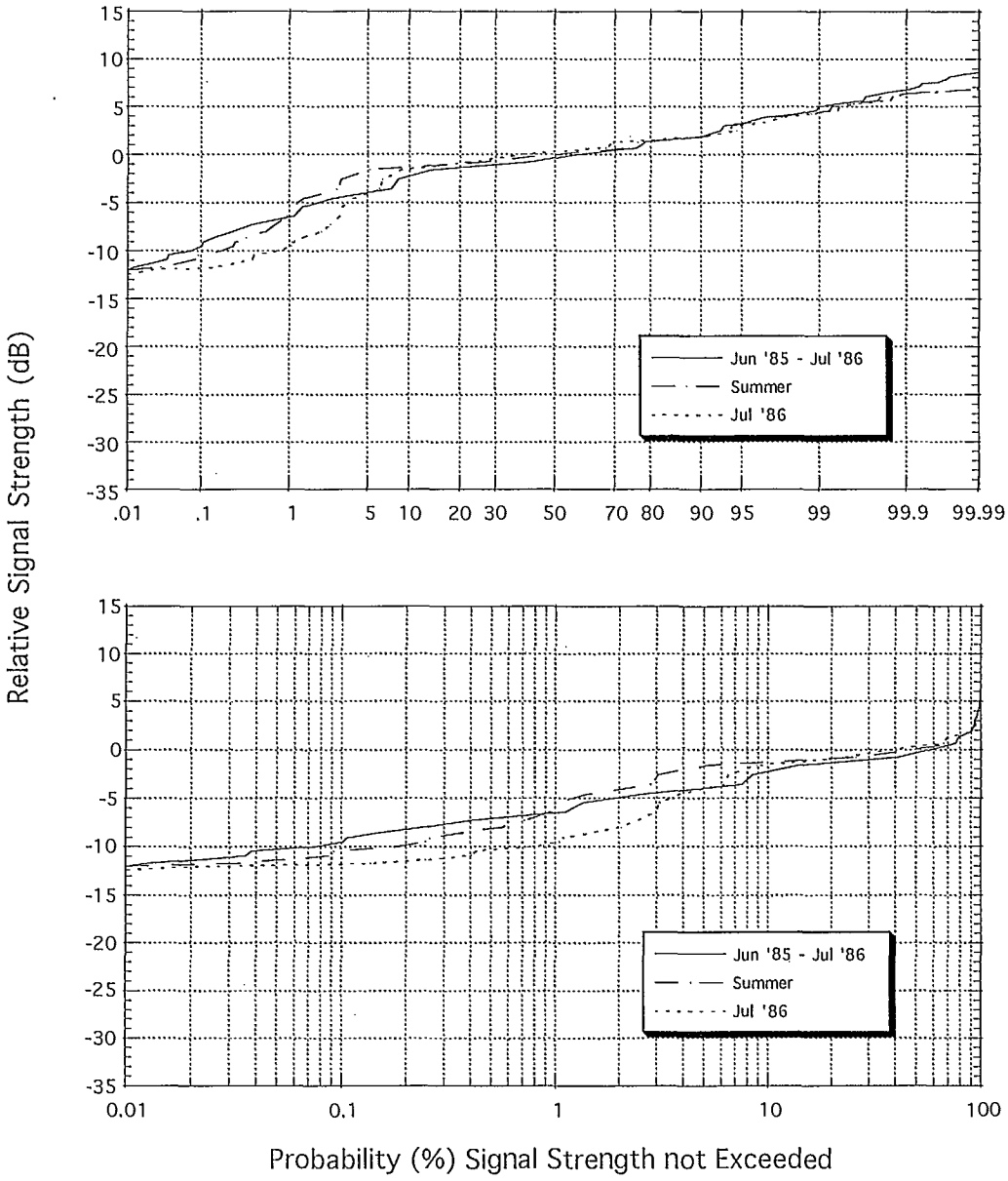

Figure 6i: Long term, seasonal, and worst month cumulative distributions of power received at CAPE MARTYR from STANLEY PEAK (UHF), relative to the long term median (-102.1 dBm).
Upper plot: Log-Gauss, Lower plot: Log-Log.

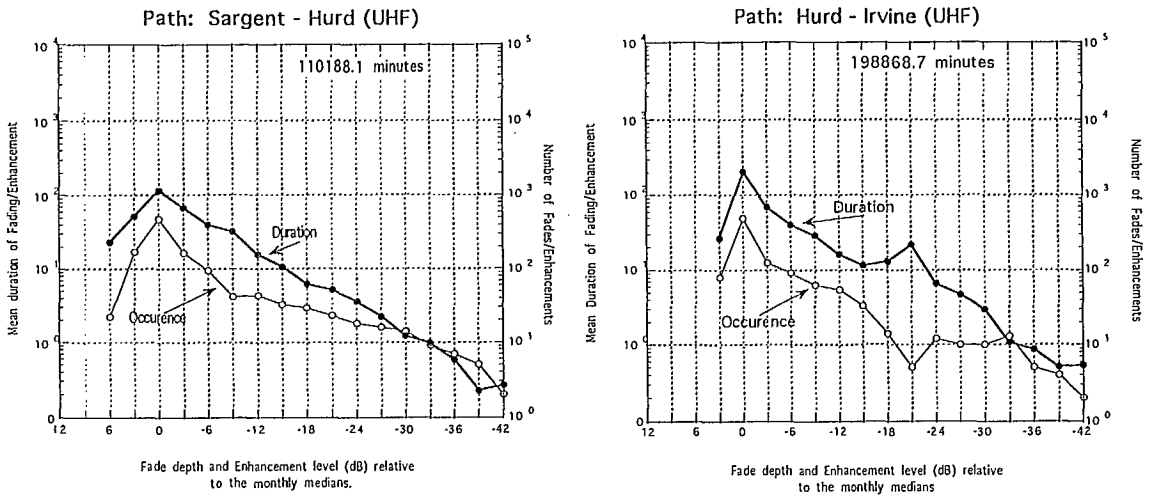

Figure 7a: Number of UHF Fades/Enhancements and their mean duration observed during the summer months.

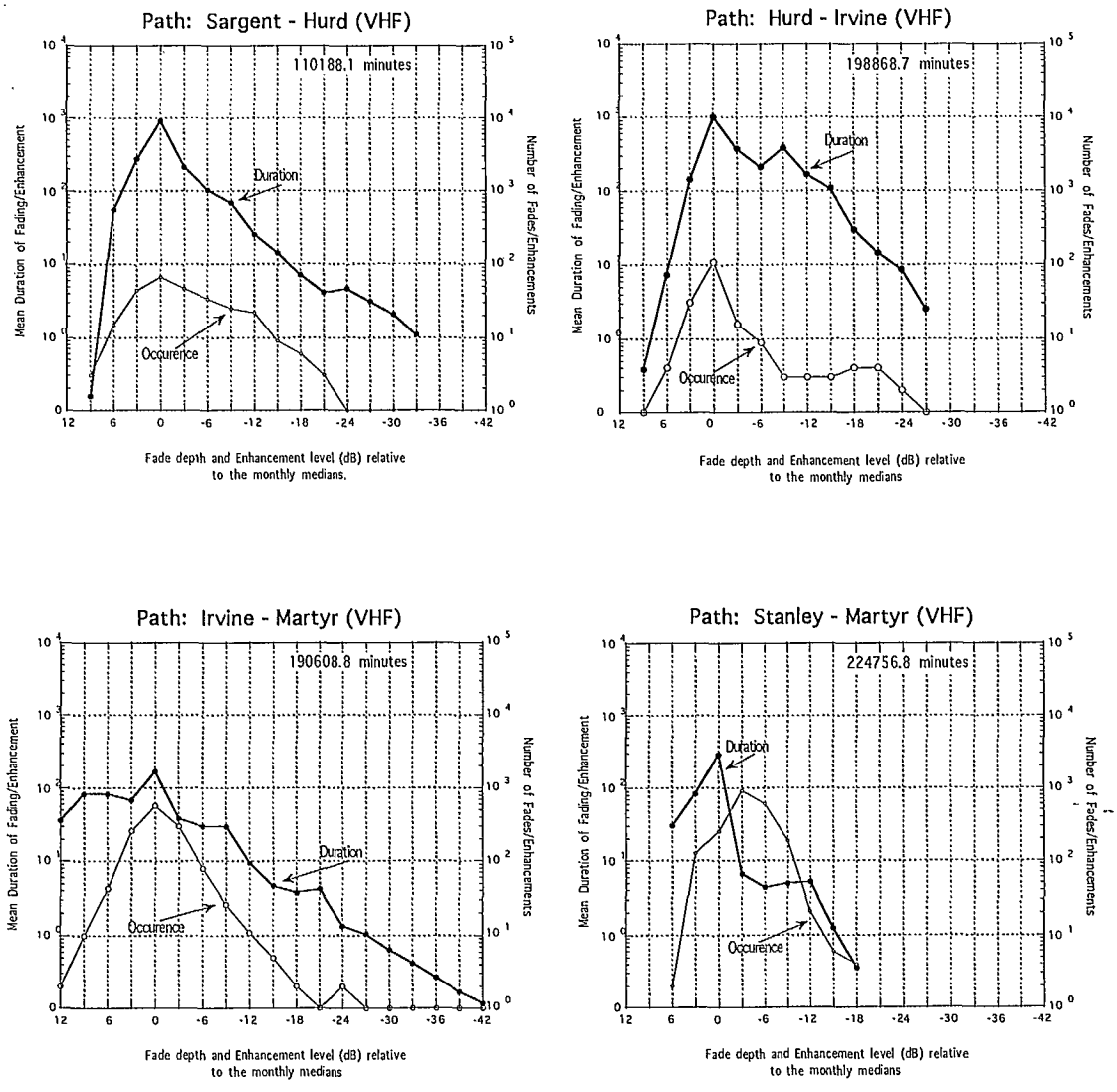

Figure 7b: Number of VHF Fades/Enhancements and their mean duration observed during the summer months.

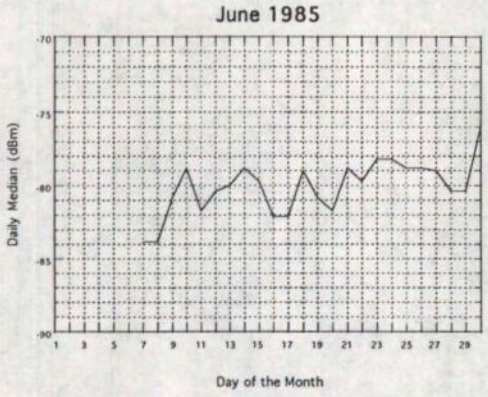

Figure 8a: Daily median values of power received at SARGENT PEAK from LEMIEUX PEAK (UHF) during June 1985.

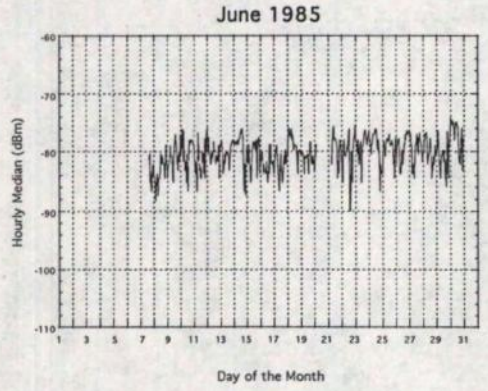

Figure 8b: Hourly median values of power received at SARGENT PEAK from LEMIEUX (UHF) during June 1985.

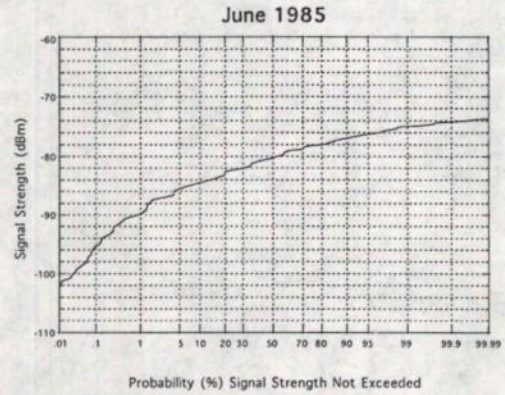

Figure 8c: Cumulative distribution of power received at SARGENT PEAK from LEMIEUX PEAK (UHF) during June 1985.

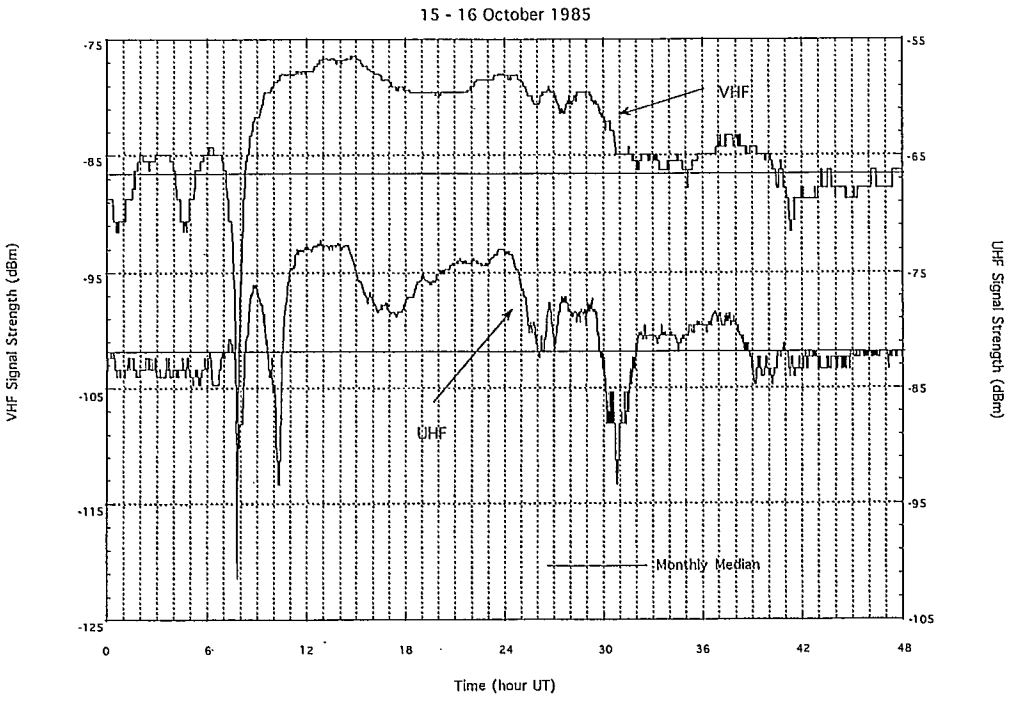

Figure 9: Comparison of median variations during a selected period on the path SARGENT-HURD.

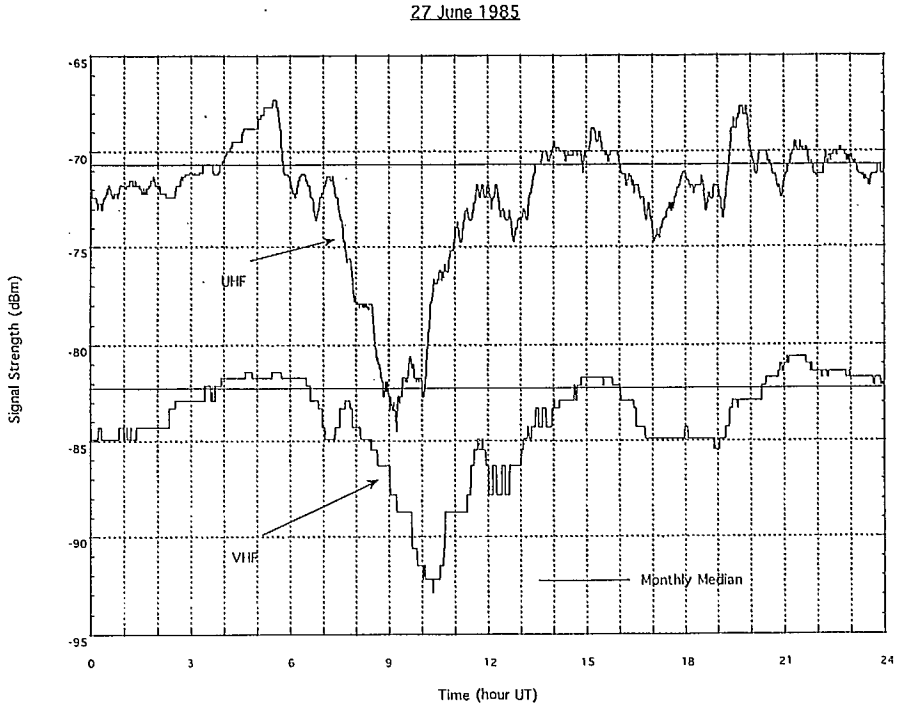

Figure 10: Comparison of median variations during a selected period on the path HURD-IRVINE.

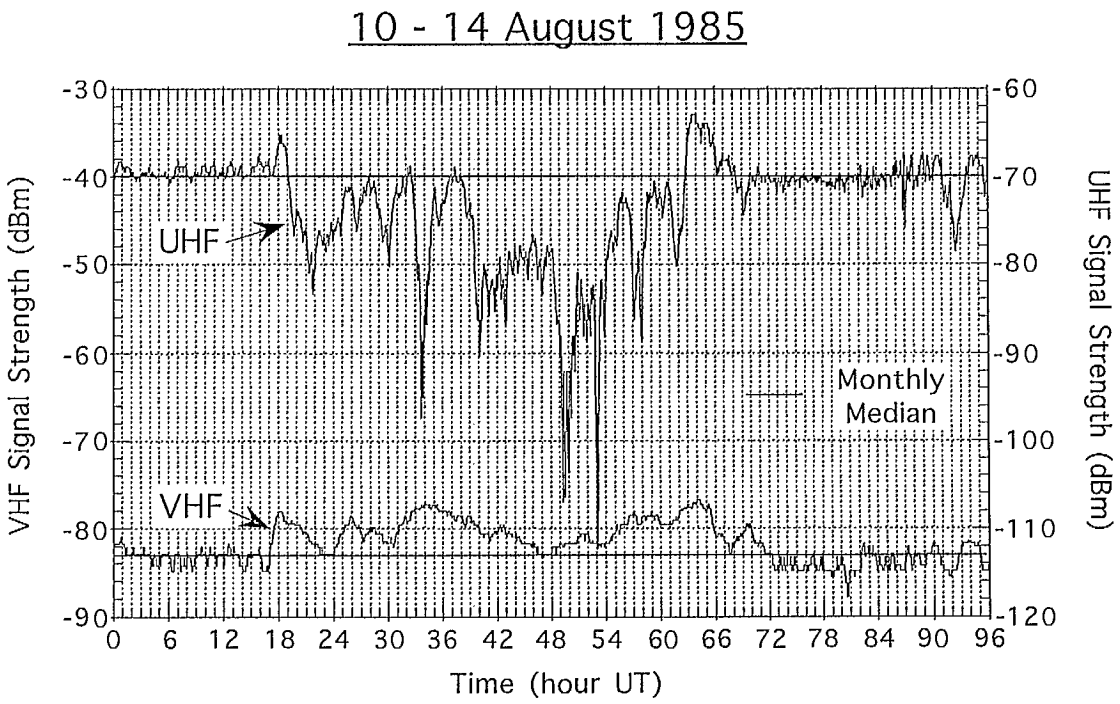

Figure 11: Comparison of median variations during a selected period on the path HURD-IRVINE.

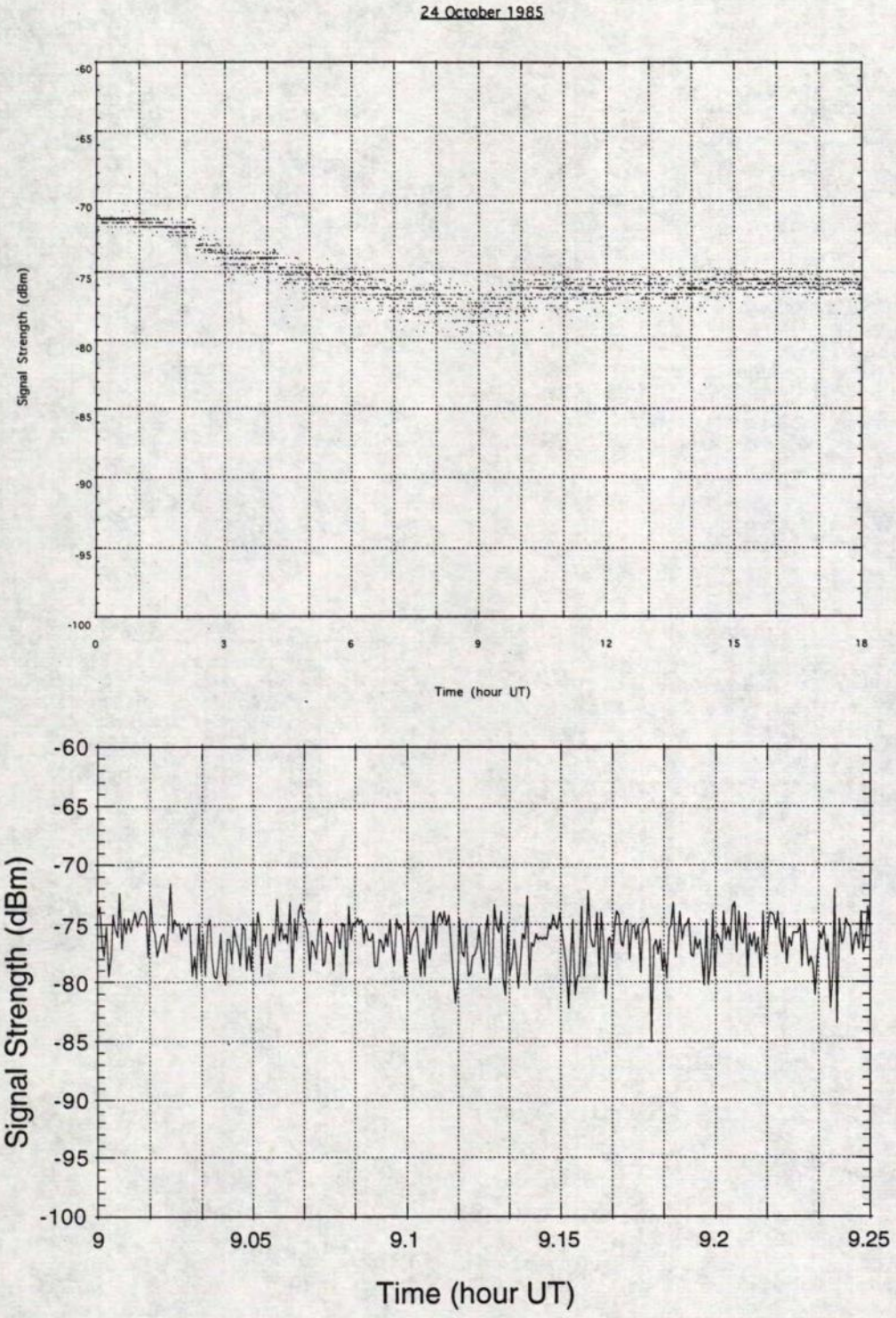

Figure 12: Example of scintillation noise observed during a selected period on the path HURD-IRVINE. Upper plot: 24-second medians, Lower plot: raw samples (2.5s).

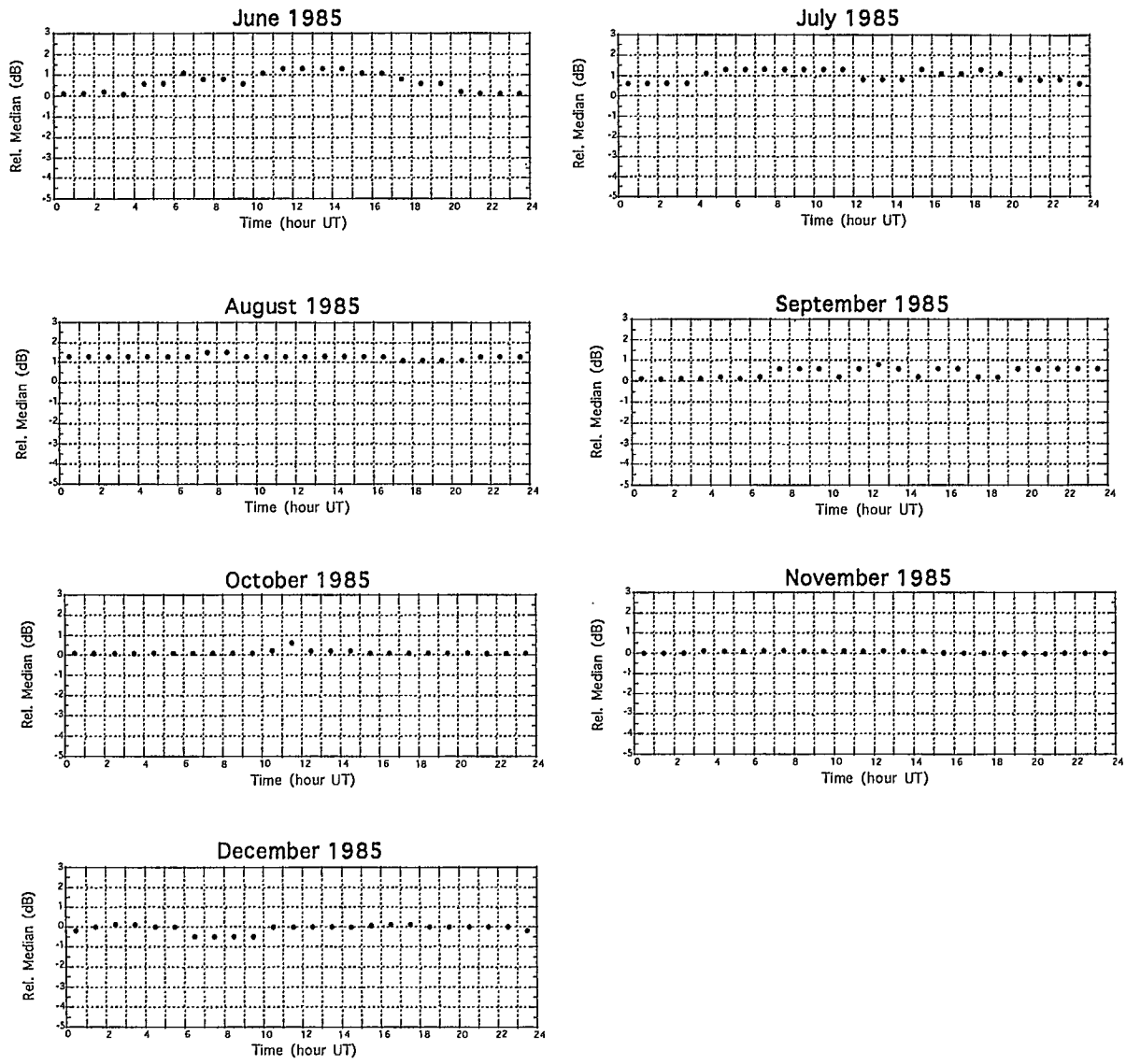

Figure 13: Diurnal variations of median signal level, relative to the long term median (-71.3 dBm), path HURD-IRVINE (UHF). (Page 1 of 2).

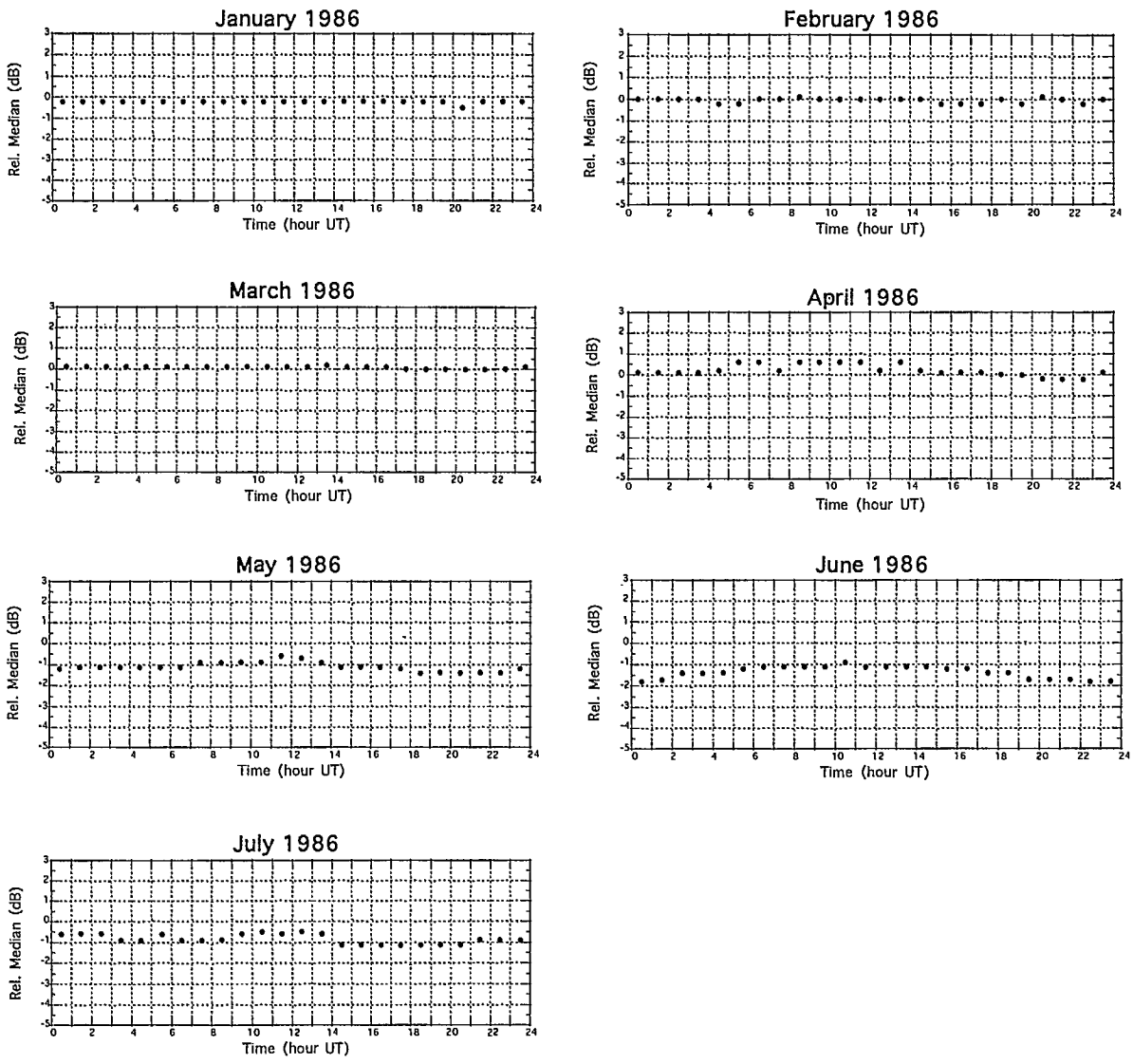

Figure 13: Diurnal variations of median signal level, relative to the long term median (-71.3 dBm), path HURD-IRVINE (UHF). (Page 2 of 2).

ANNEX "A"
MONTHLY CUMULATIVE DISTRIBUTIONS OF POWER RECEIVED

This annex is a graphical presentation of the monthly cumulative distributions of power received over each experimental path. The graphs cover the period June 1985 to July 1986. A Gaussian scale, expressed in percentage, is used as the abscissa. On the ordinate scale, the received power is expressed in decibels relative to 1 mW. The monthly cumulative distributions are presented in the following order:

FIGURE	PATH	
A1	SARGENT-HURD	UHF
A2	HURD-IRVINE	UHF
A3	IRVINE-MARTYR	UHF
A4	JOY-LEMIEUX	VHF
A5	LEMIEUX-SARGENT	VHF
A6	SARGENT-HURD	VHF
A7	HURD-IRVINE	VHF
A8	IRVINE-MARTYR	VHF
A9	STANLEY-MARTYR	VHF

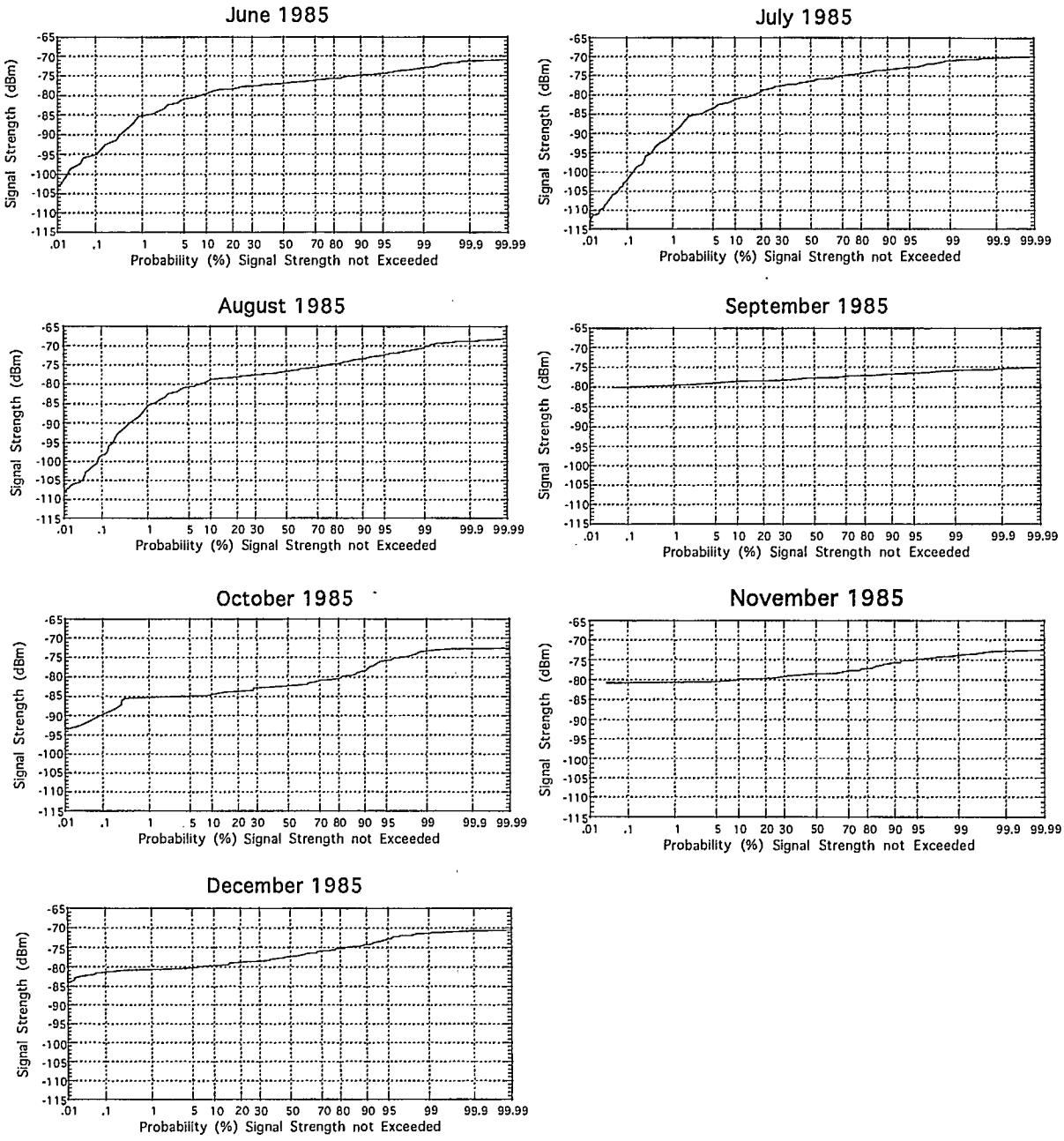

Figure A1: Monthly cumulative distributions of power received.
Sargent - Hurd (UHF).

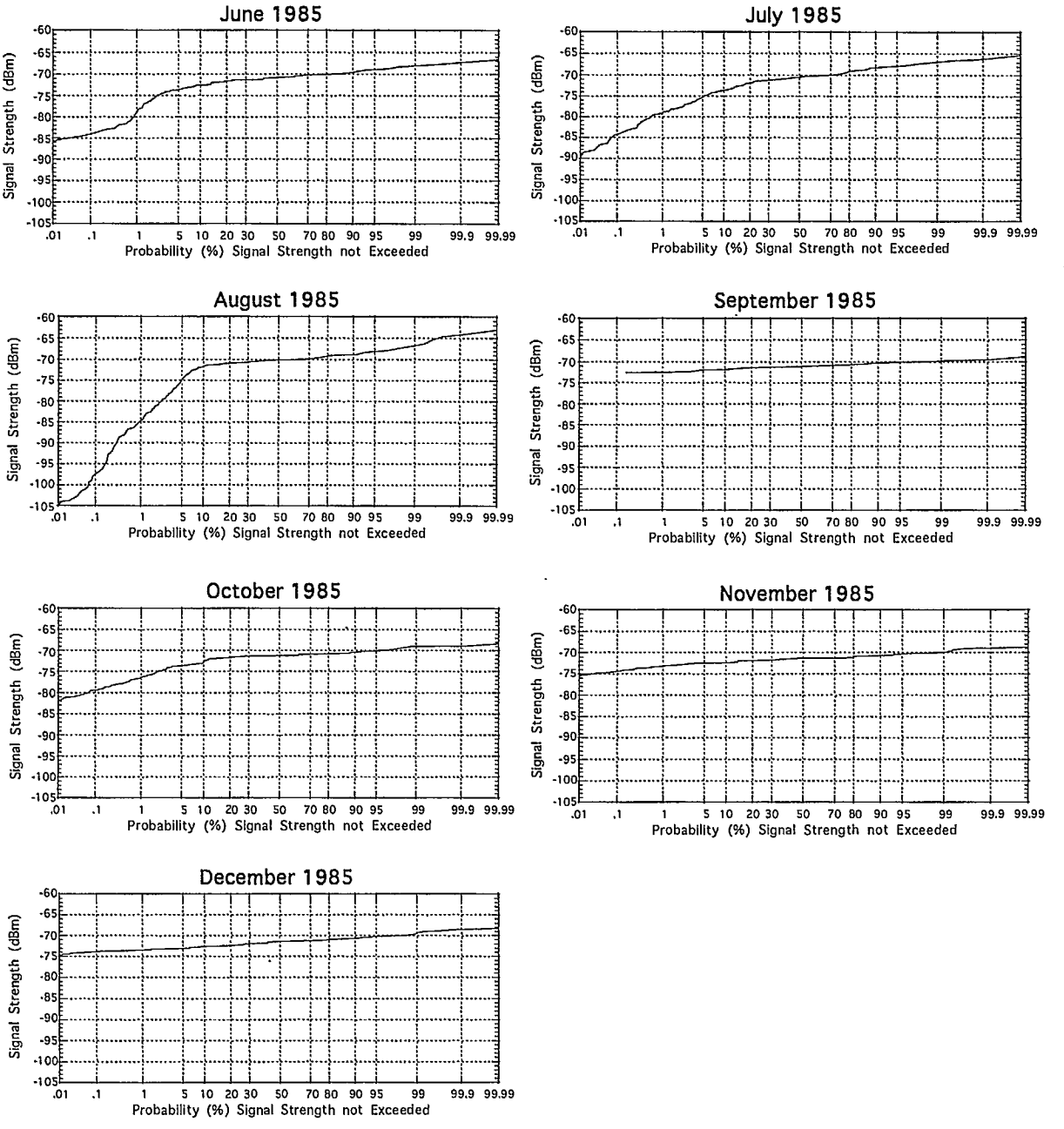

Figure A2: Monthly cumulative distributions of power received.
HURD - IRVINE (UHF) (Page 1 of 2).

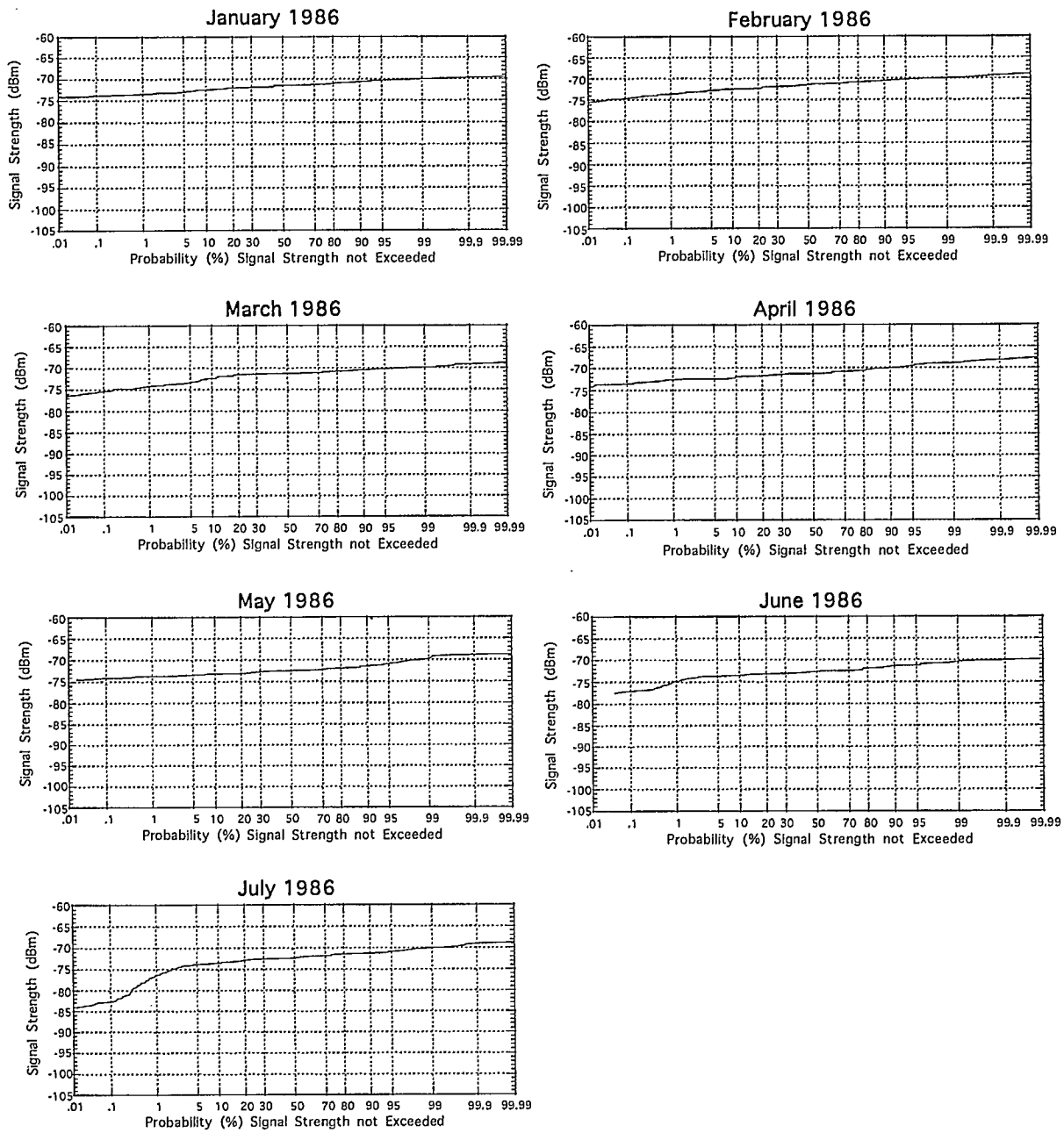

Figure A2: Monthly cumulative distributions of power received.
HURD - IRVINE (UHF) (Page 2 of 2).

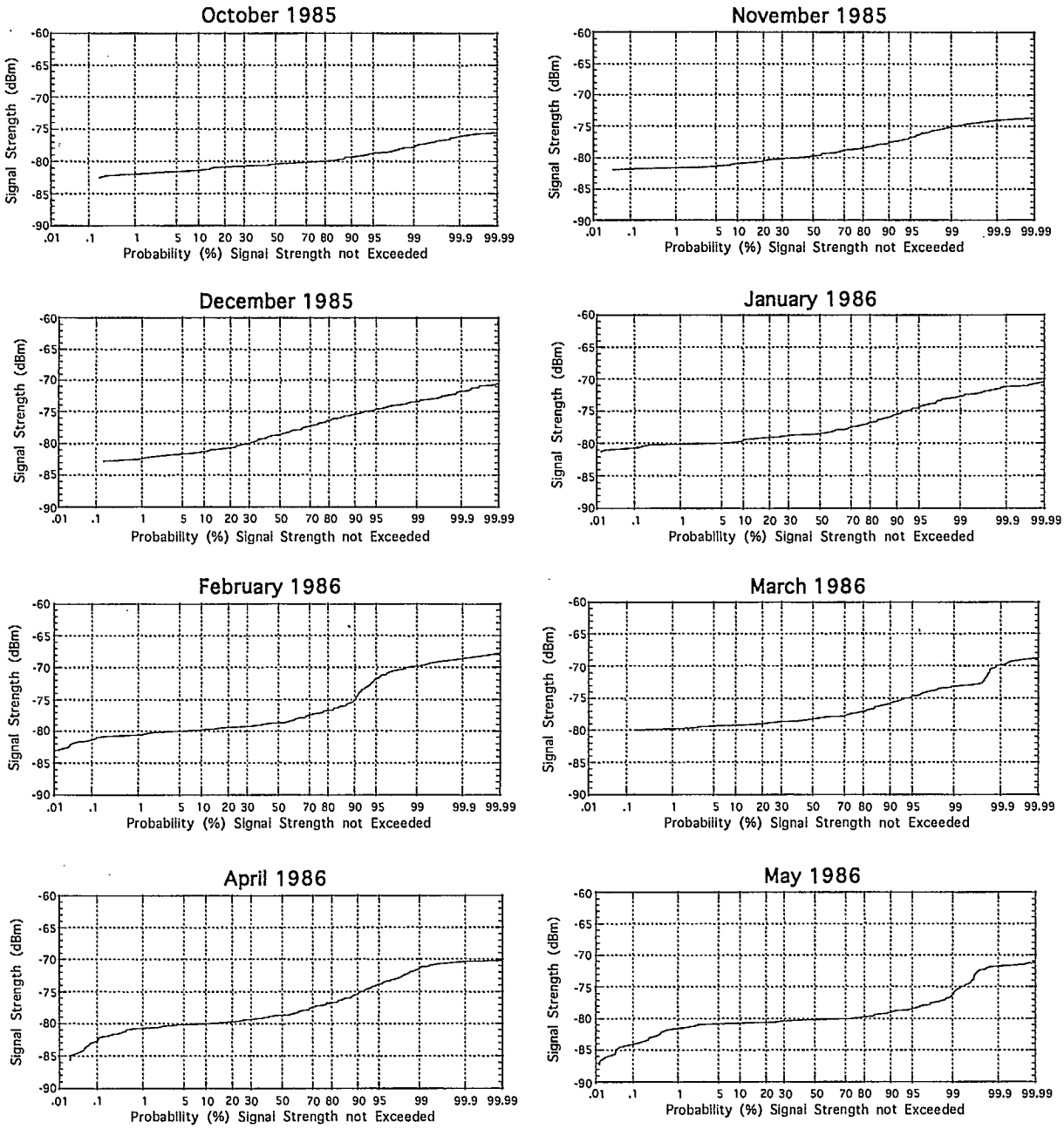

Figure A3: Monthly cumulative distributions of power received.
IRVINE - MARTYR (UHF).

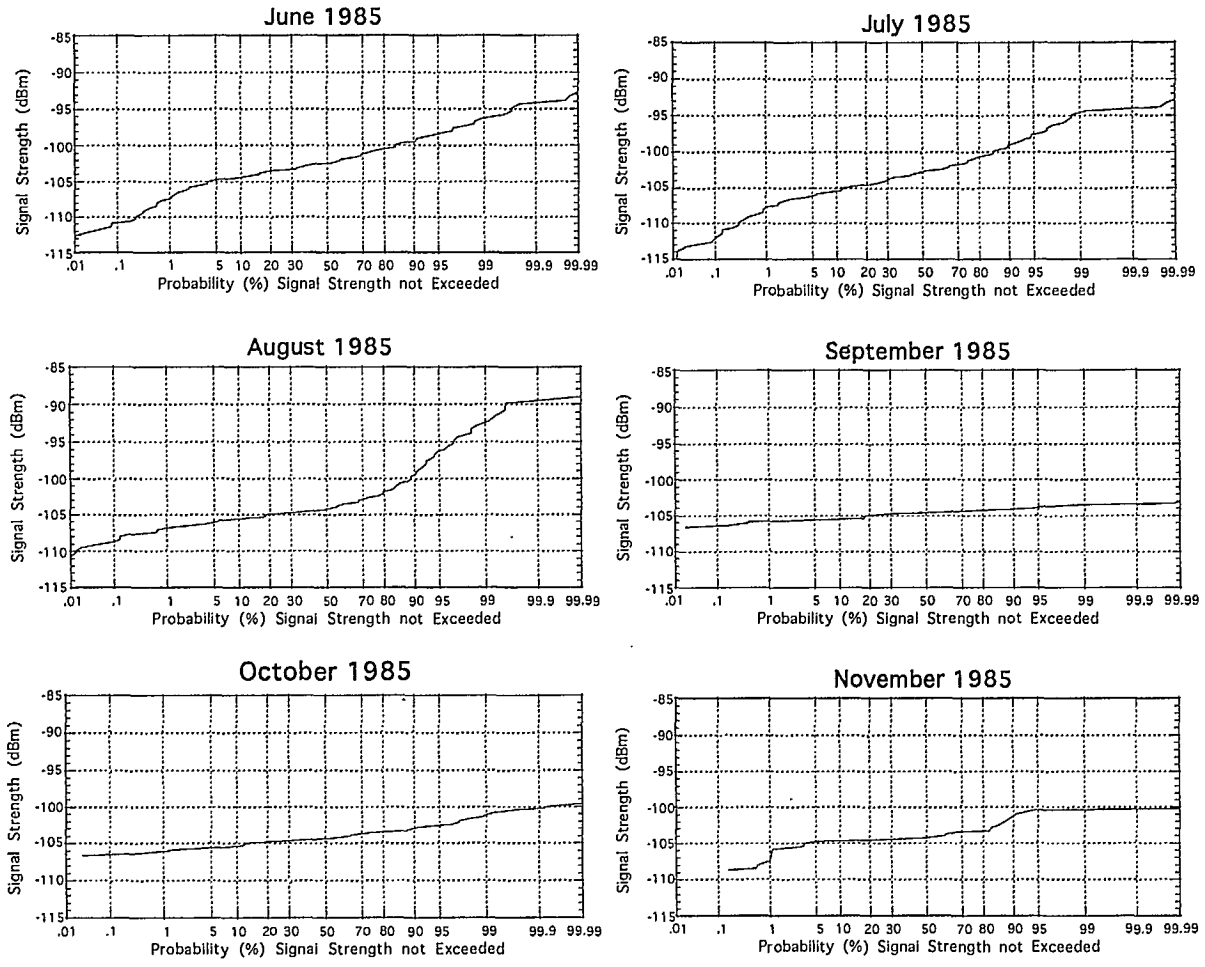

Figure A4: Monthly cumulative distributions of power received.
Cape Joy - Lemieux (VHF).

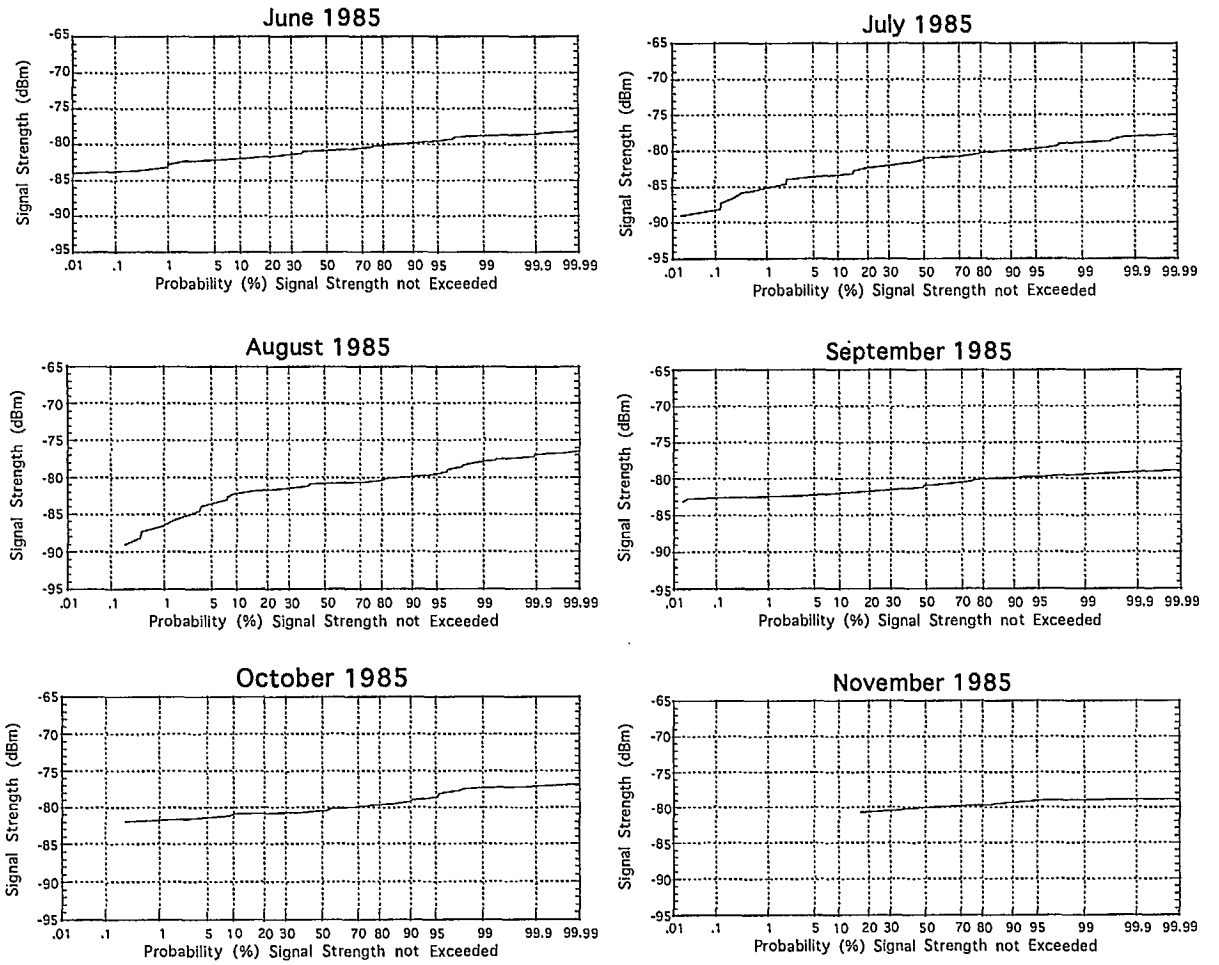

Figure A5: Monthly cumulative distributions of power received.
LEMIEUX - SARGENT (VHF)

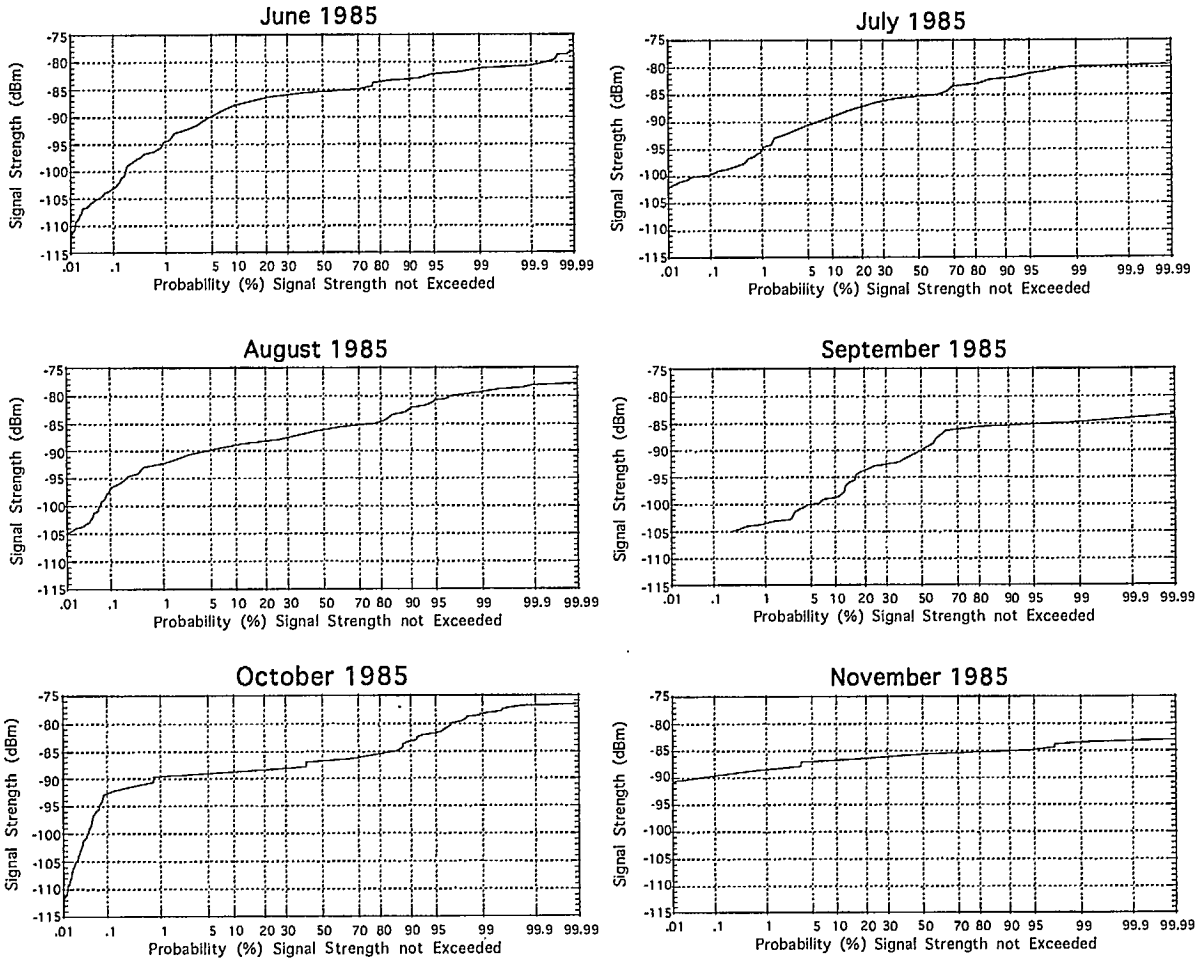

Figure A6: Monthly cumulative distributions of power received.
SARGENT - HURD (VHF).

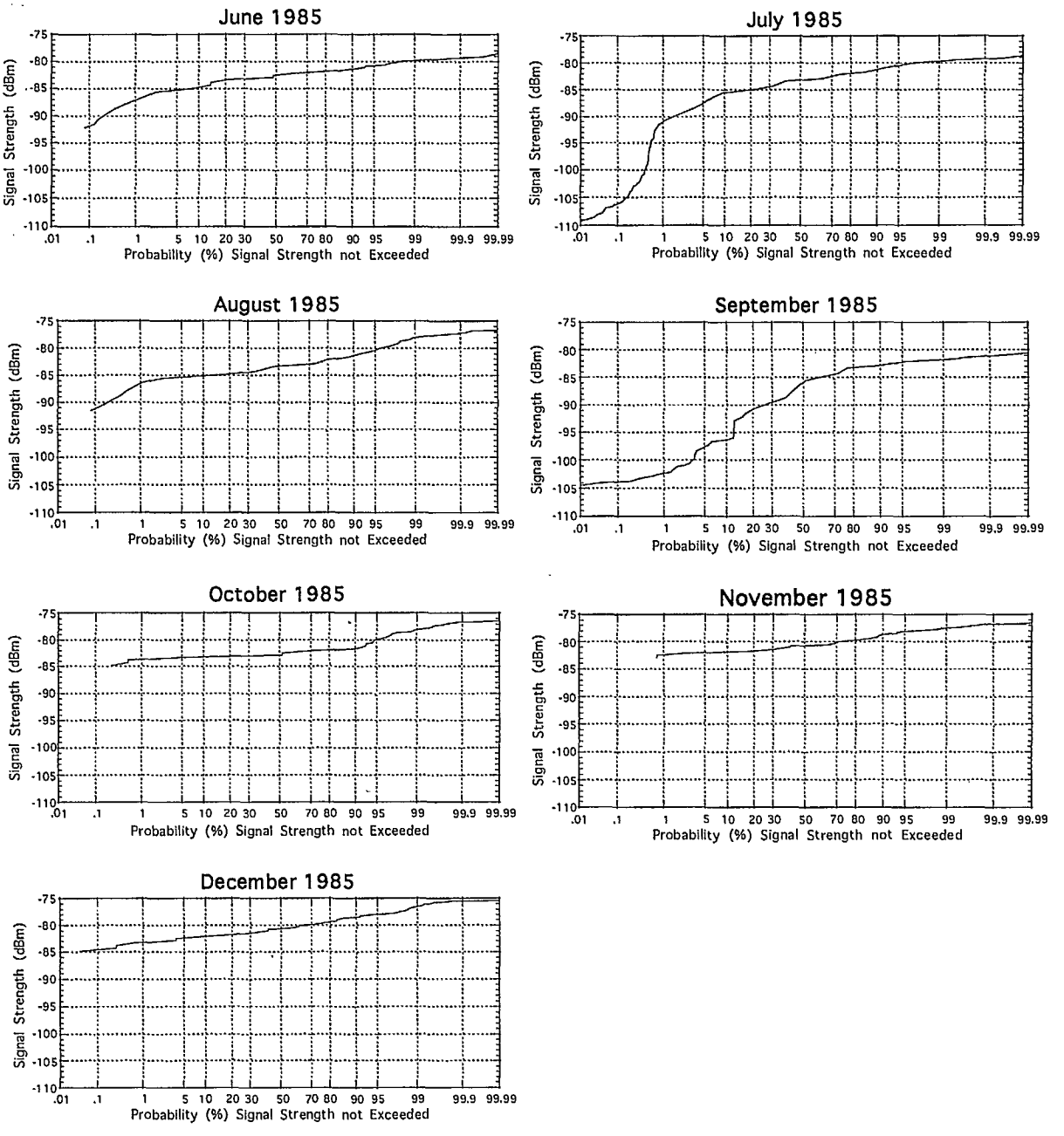

Figure A7: Monthly cumulative distributions of power received.
HURD - IRVINE (VHF) (Page 1 of 2).

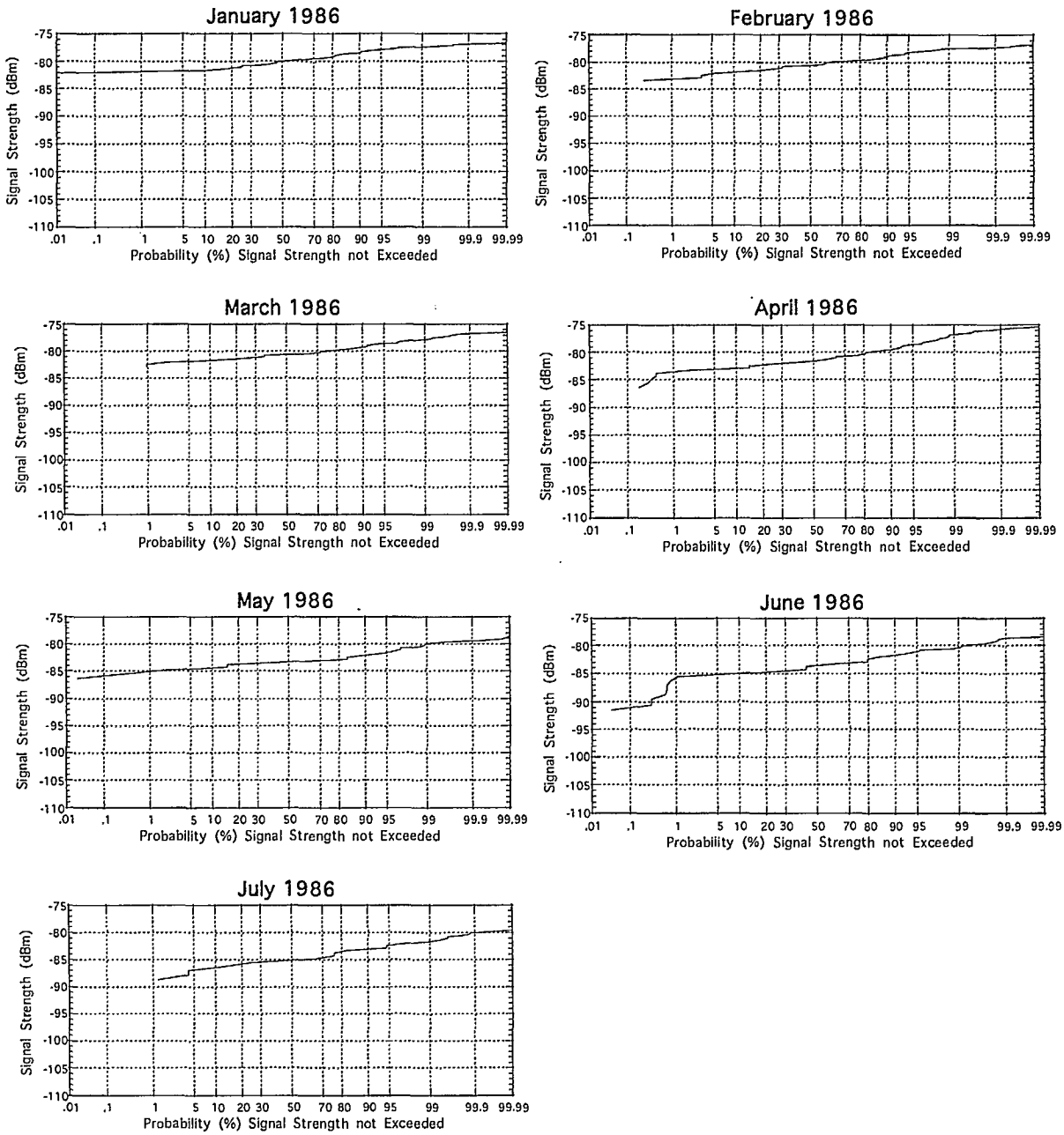

Figure A7: Monthly cumulative distributions of power received.
HURD - IRVINE (VHF) (Page 2 of 2).

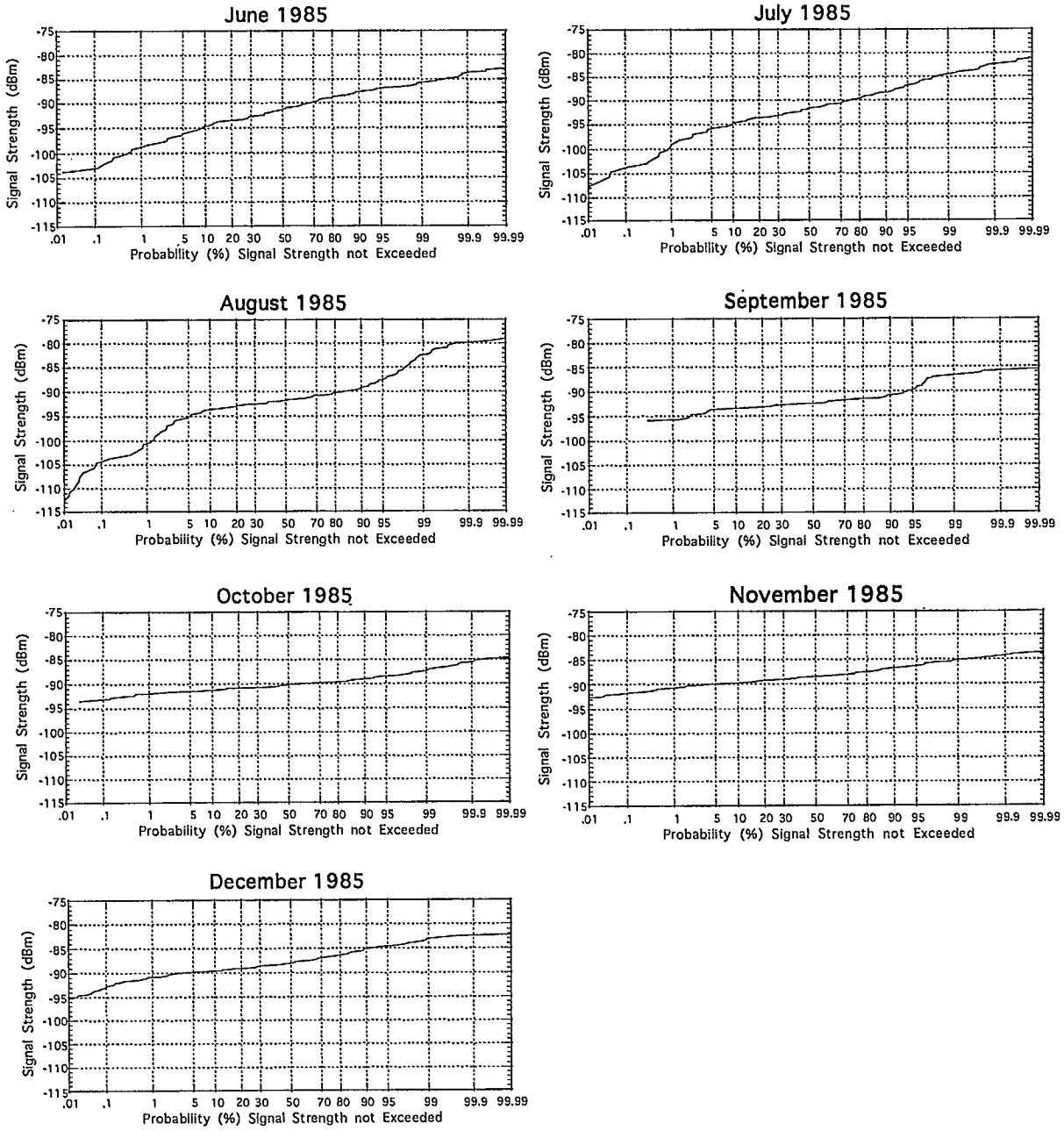

Figure A8: Monthly cumulative distributions of power received.
IRVINE à MARTYR (VHF) (Page 1 of 2).

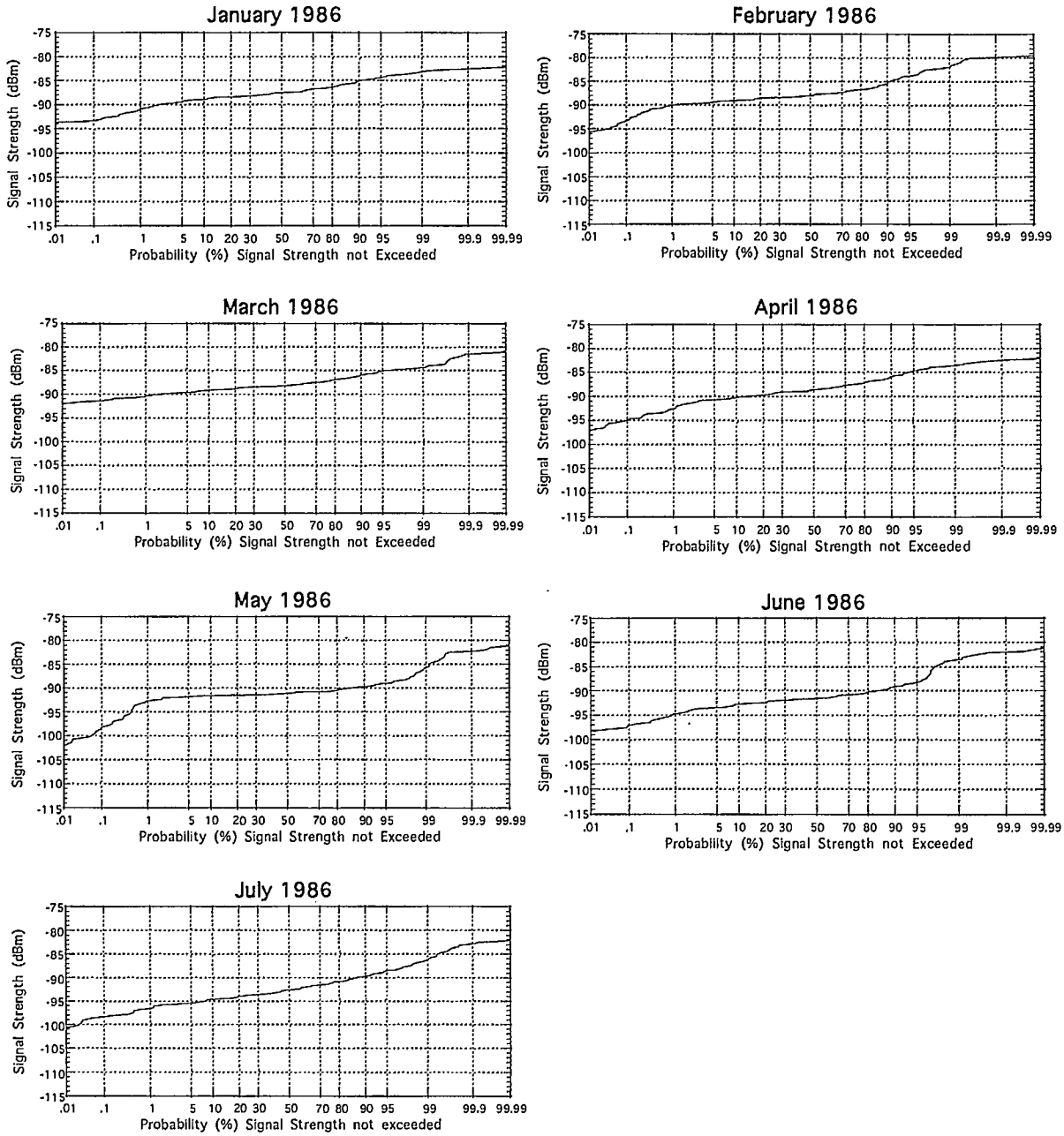

Figure A8: Monthly cumulative distributions of power received.
IRVINE à MARTYR (VHF) (Page 2 of 2).

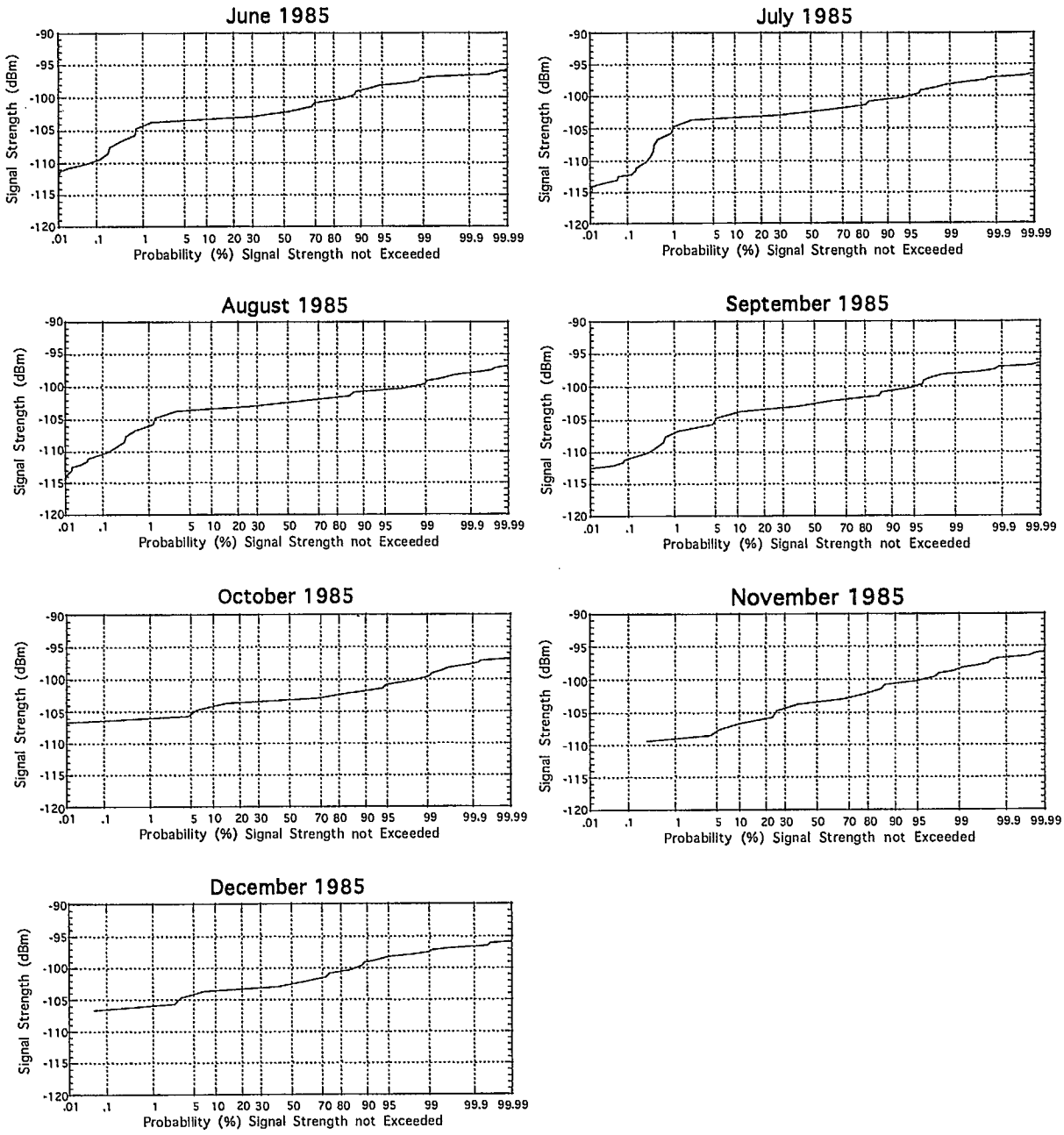

Figure A9: Monthly cumulative distributions of power received.
STANLEY - MARTYR (VHF) (Page 1 of 2).

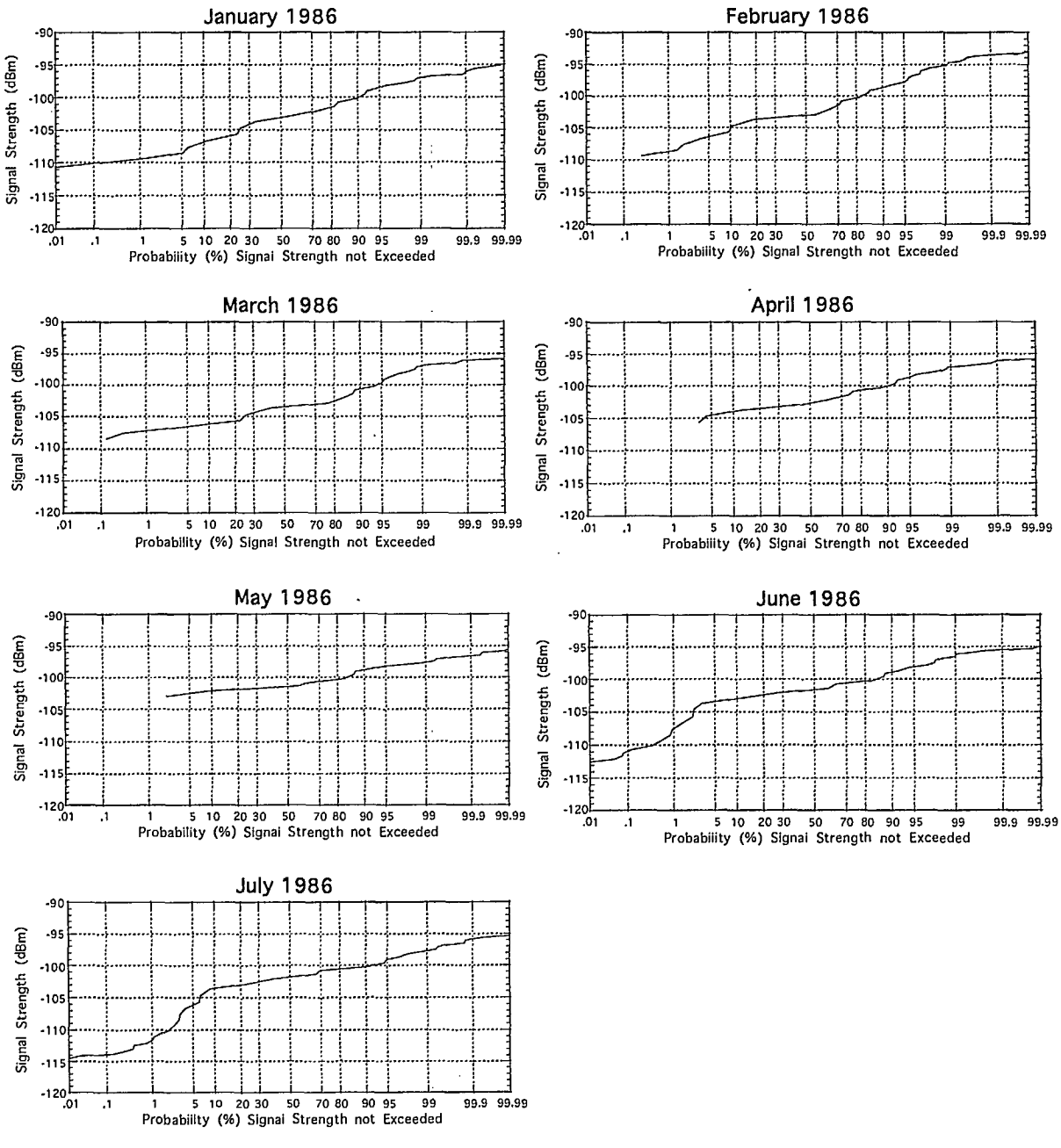

Figure A9: Monthly cumulative distributions of power received.
STANLEY - MARTYR (VHF) (Page 2 of 2).

ANNEX "B"
HOURLY MEDIAN VALUES OF POWER RECEIVED

This annex is a graphical presentation of the hourly median values of power received over each experimental path. The plots cover on a monthly basis the period June 1985 to July 1986. The hourly median values are presented in the following order:

FIGURE	PATH	
B1	SARGENT-HURD	UHF
B2	HURD-IRVINE	UHF
B3	IRVINE-MARTYR	UHF
B4	JOY-LEMIEUX	VHF
B5	LEMIEUX-SARGENT	VHF
B6	SARGENT-HURD	VHF
B7	HURD-IRVINE	VHF
B8	IRVINE-MARTYR	VHF
B9	STANLEY-MARTYR	VHF

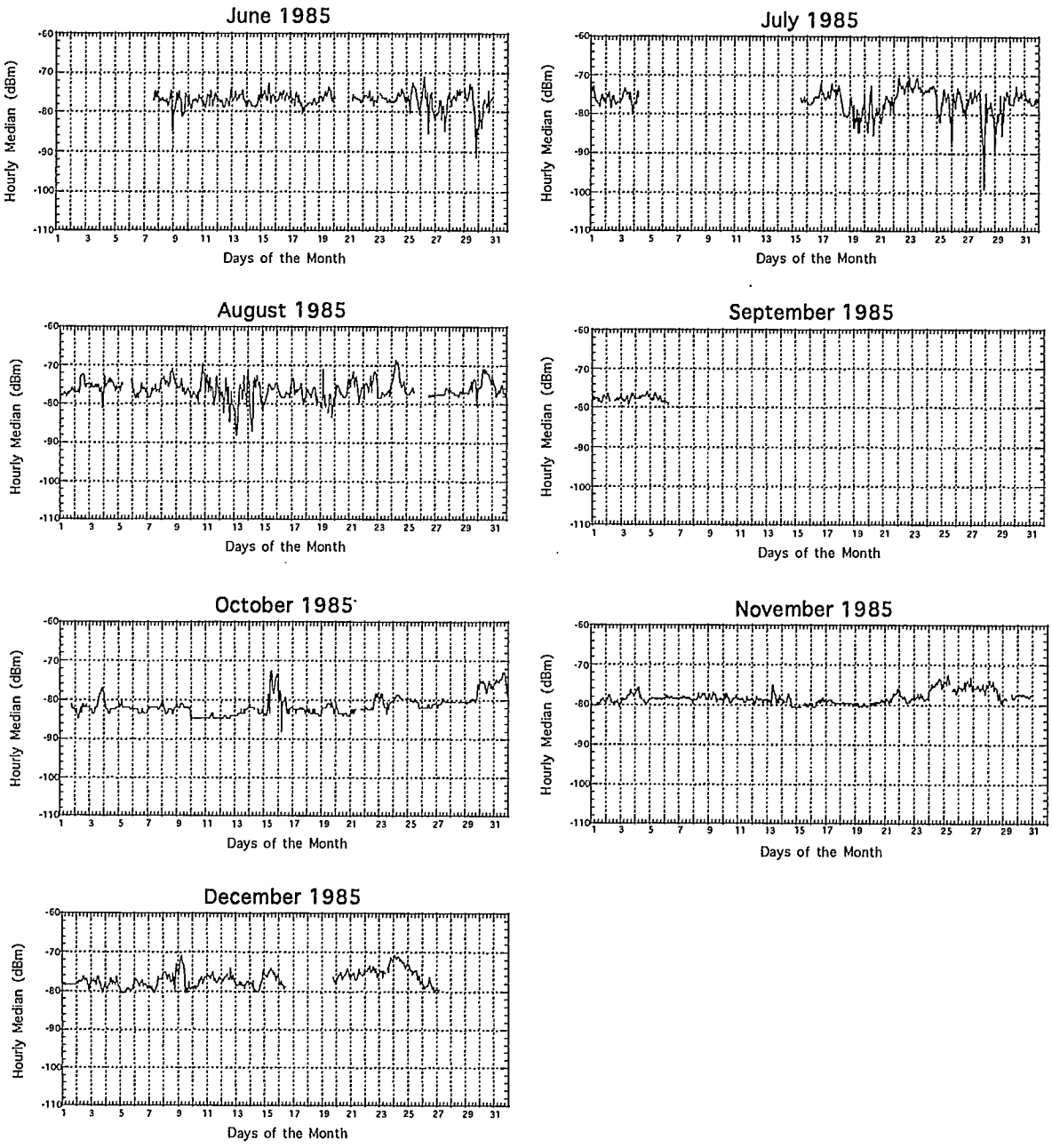

Figure B1: Hourly median values of power received.
SARGENT-HURD (UHF).

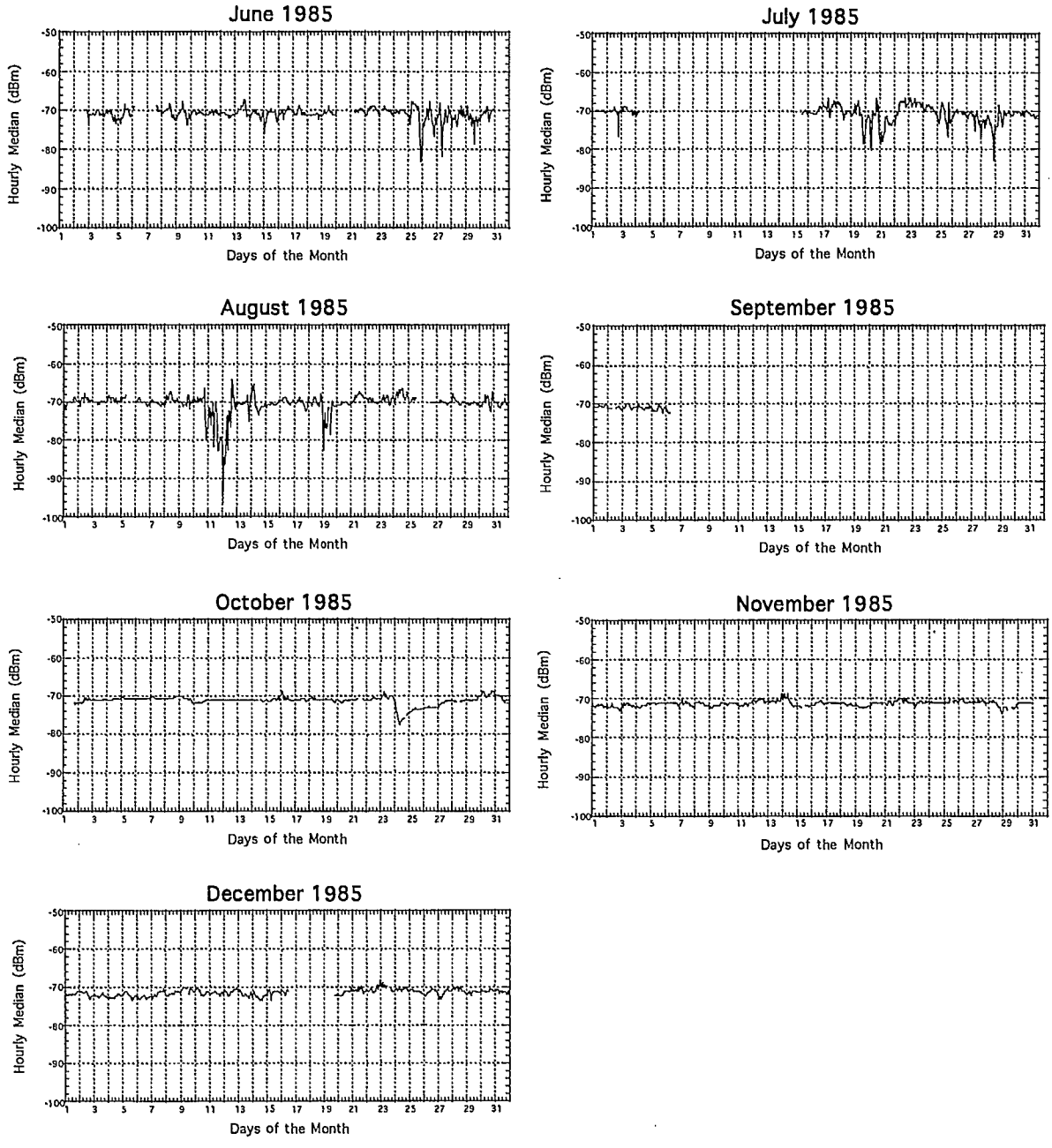

Figure B2: Hourly median values of power received.
HURD-IRVINE (UHF). (Page 1 of 2).

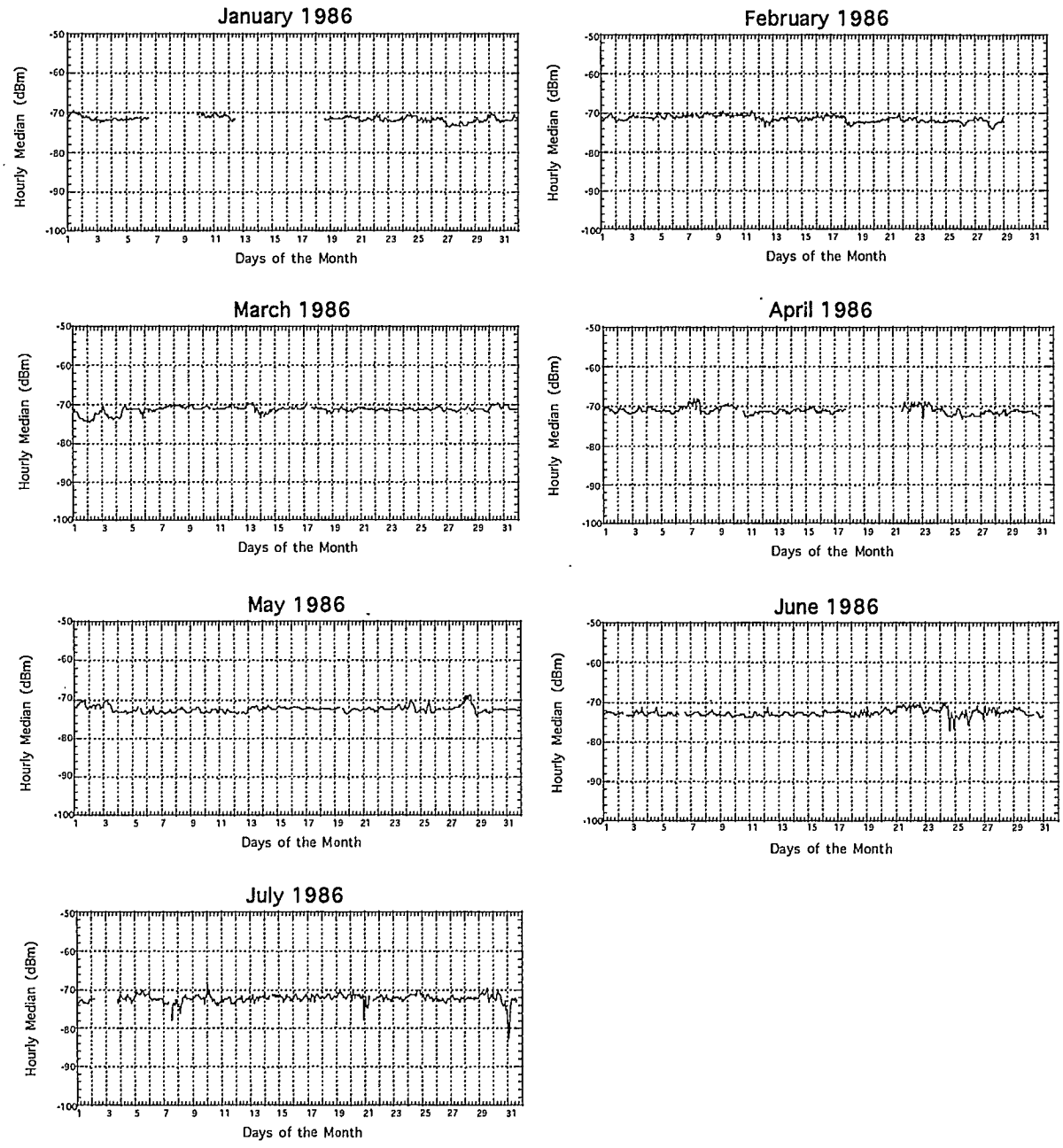

Figure B2: Hourly median values of power received.
HURD-IRVINE (UHF). (Page 2 of 2).

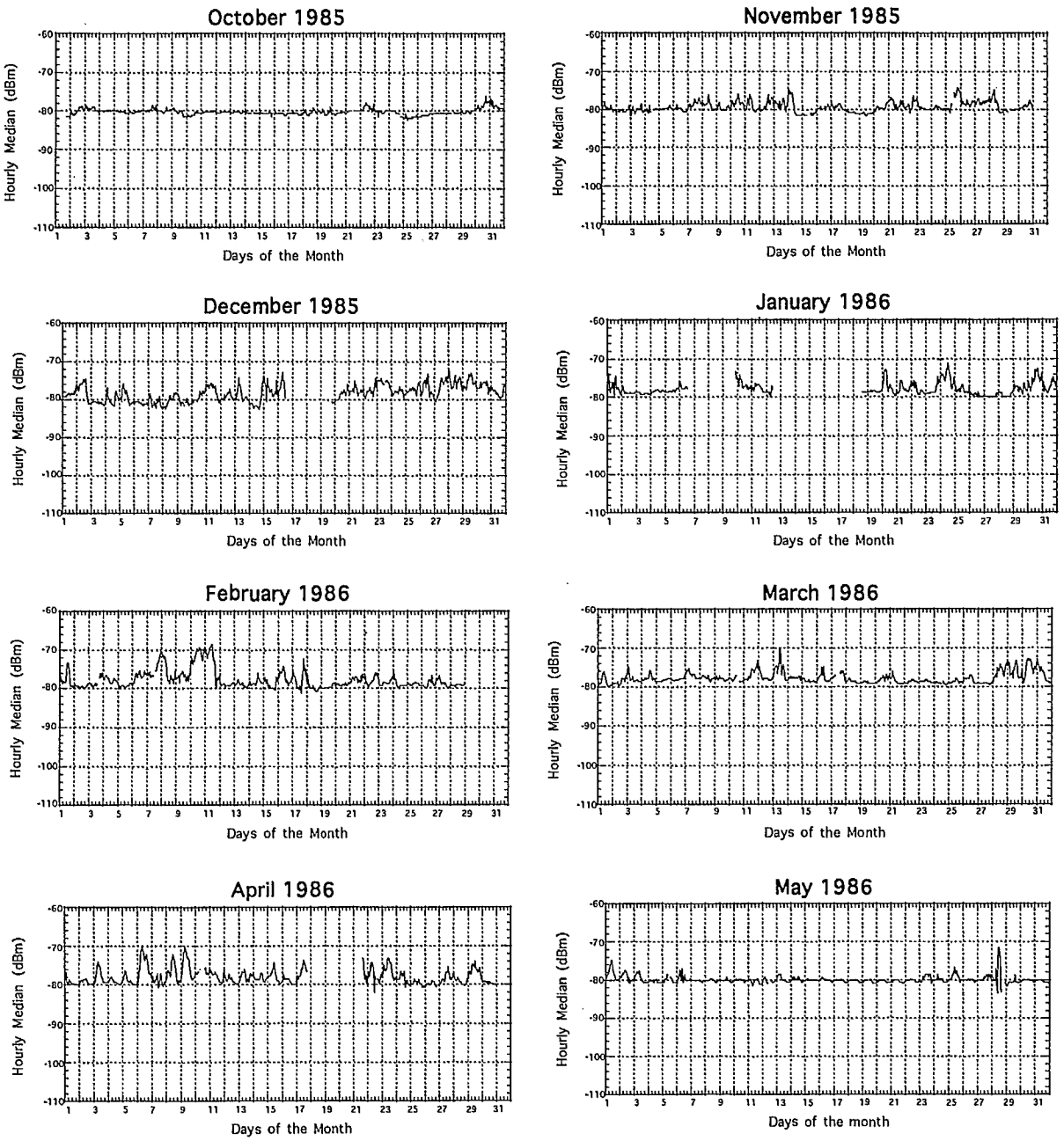

Figure B3: Hourly median values of power received.
IRVINE-MARTYR(UHF)

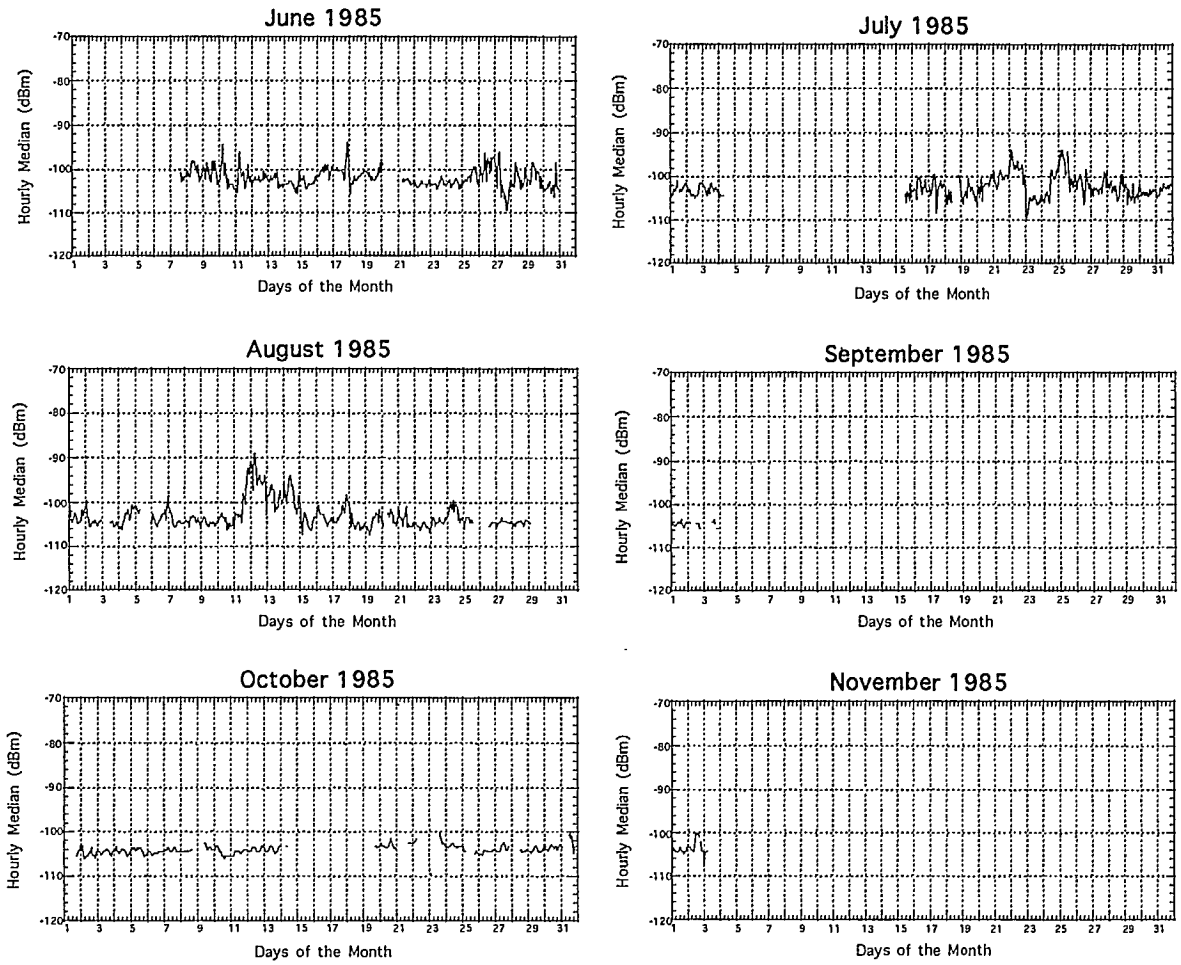

Figure B4: Hourly median values of power received.
JOY-LEMIEUX (VHF).

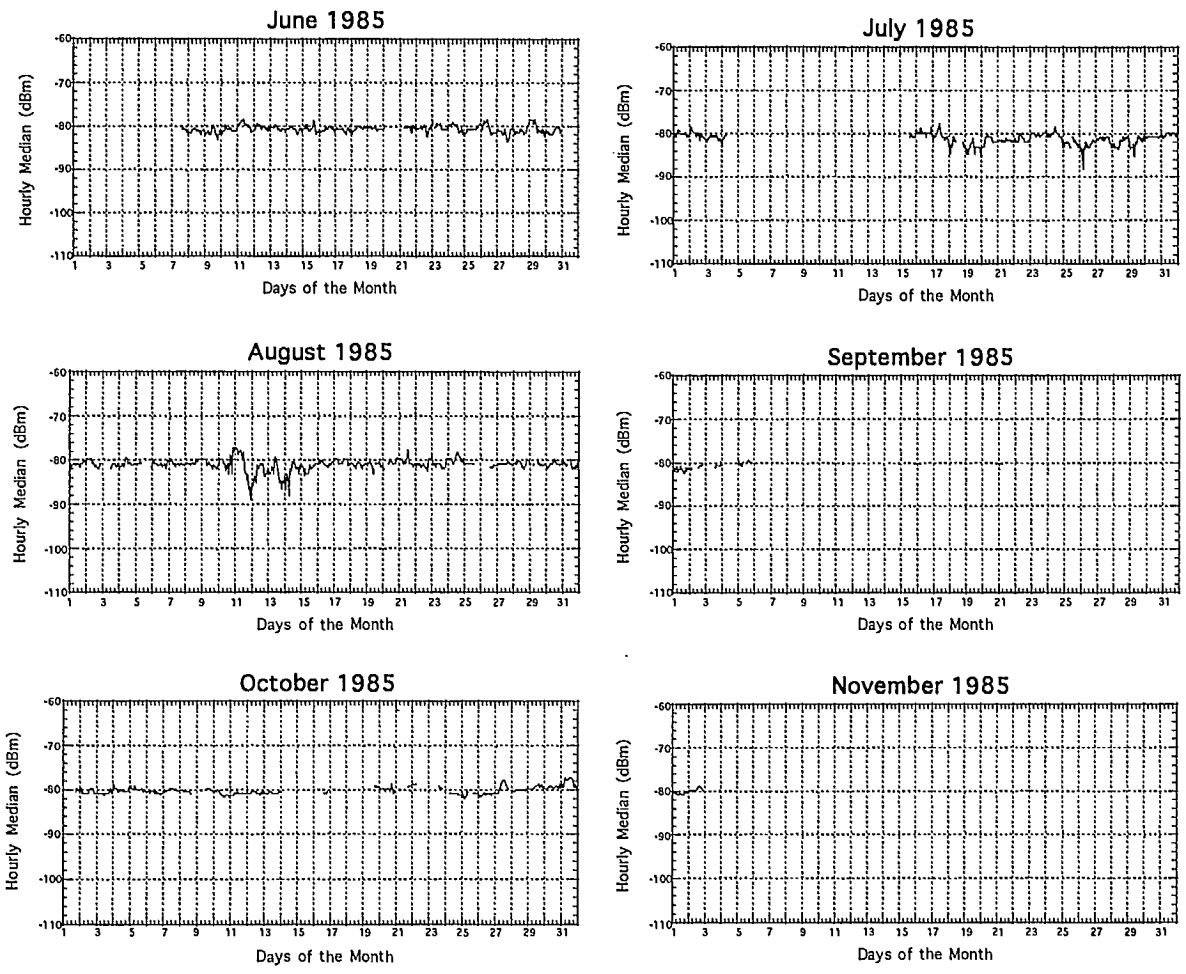

Figure B5: Hourly median values of power received.
LEMIEUX-SARGENT (VHF).

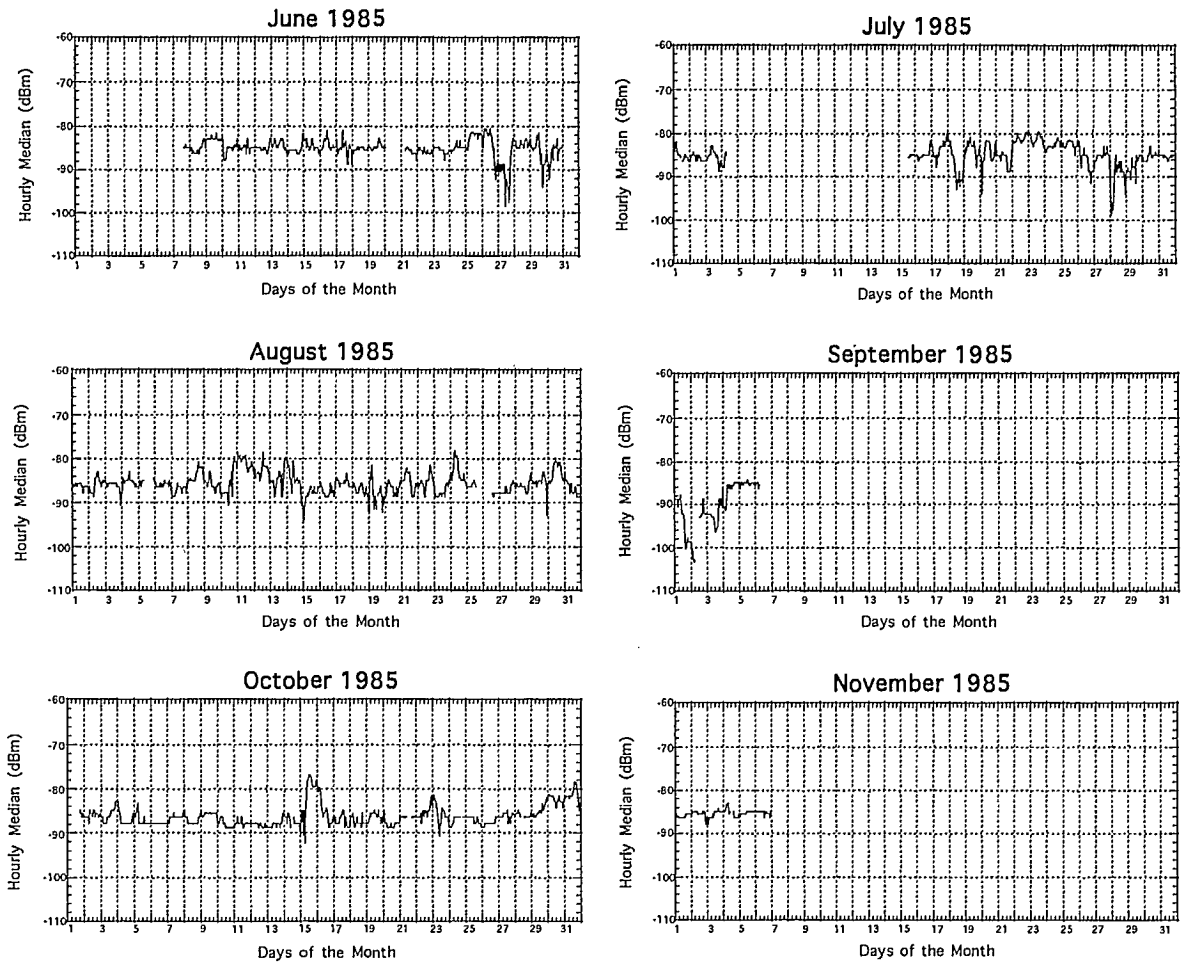

Figure B6: Hourly median values of power received.
SARGENT-HURD (VHF).

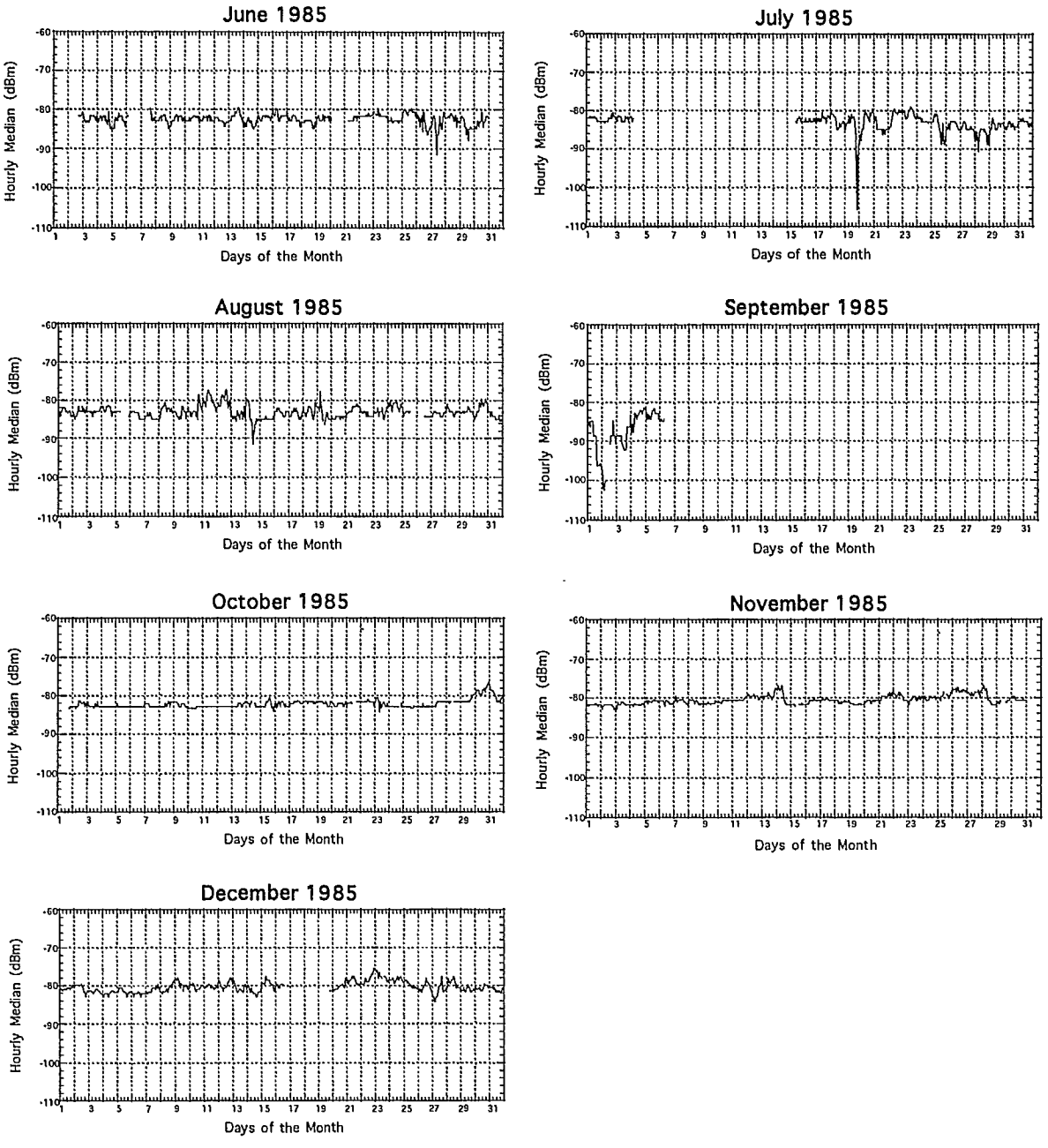

Figure B7: Hourly median values of power received.
HURD-IRVINE (VHF). (Page 1 of 2).

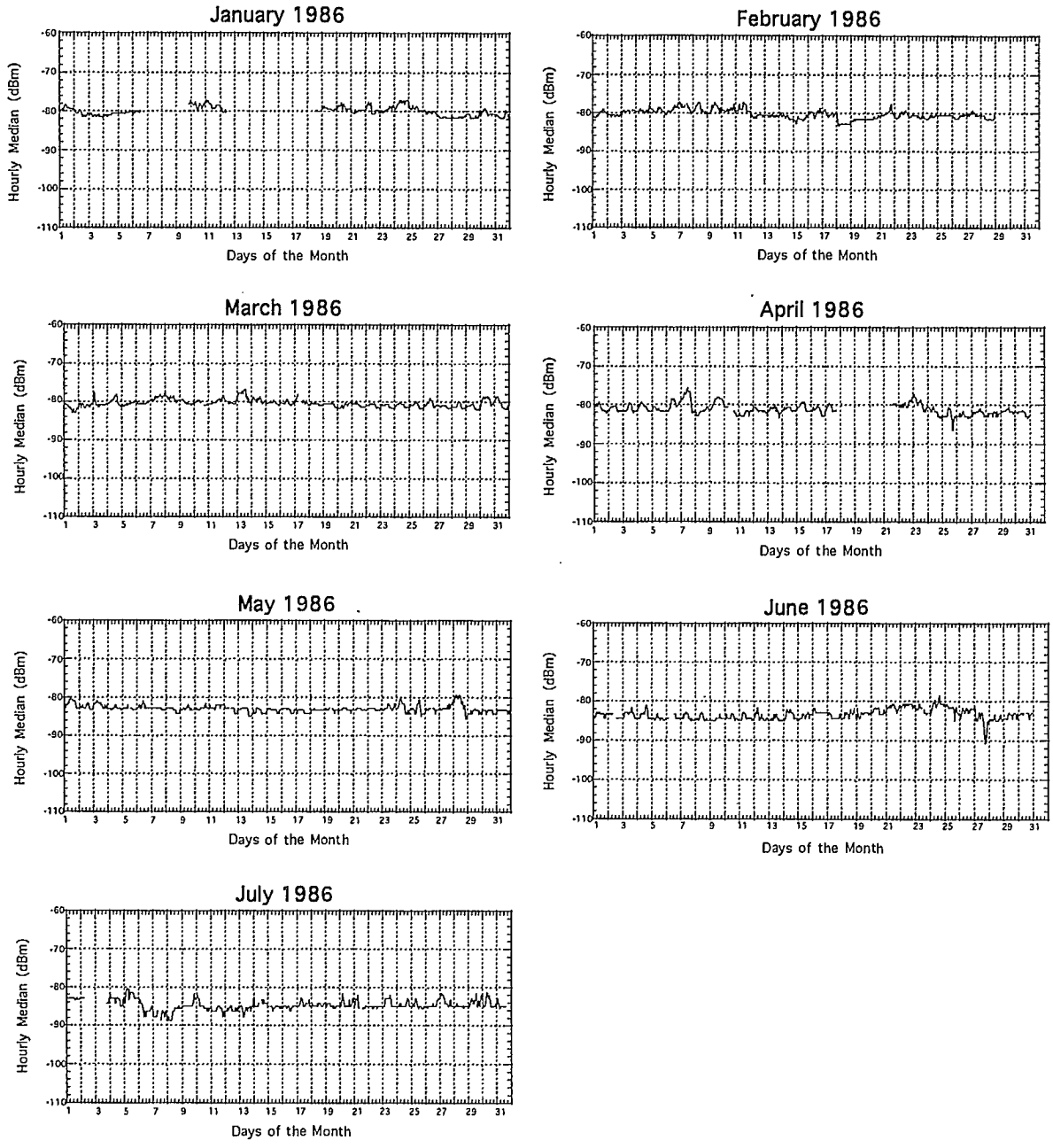

Figure B7: Hourly median values of power received.
HURD-IRVINE (VHF). (Page 2 of 2).

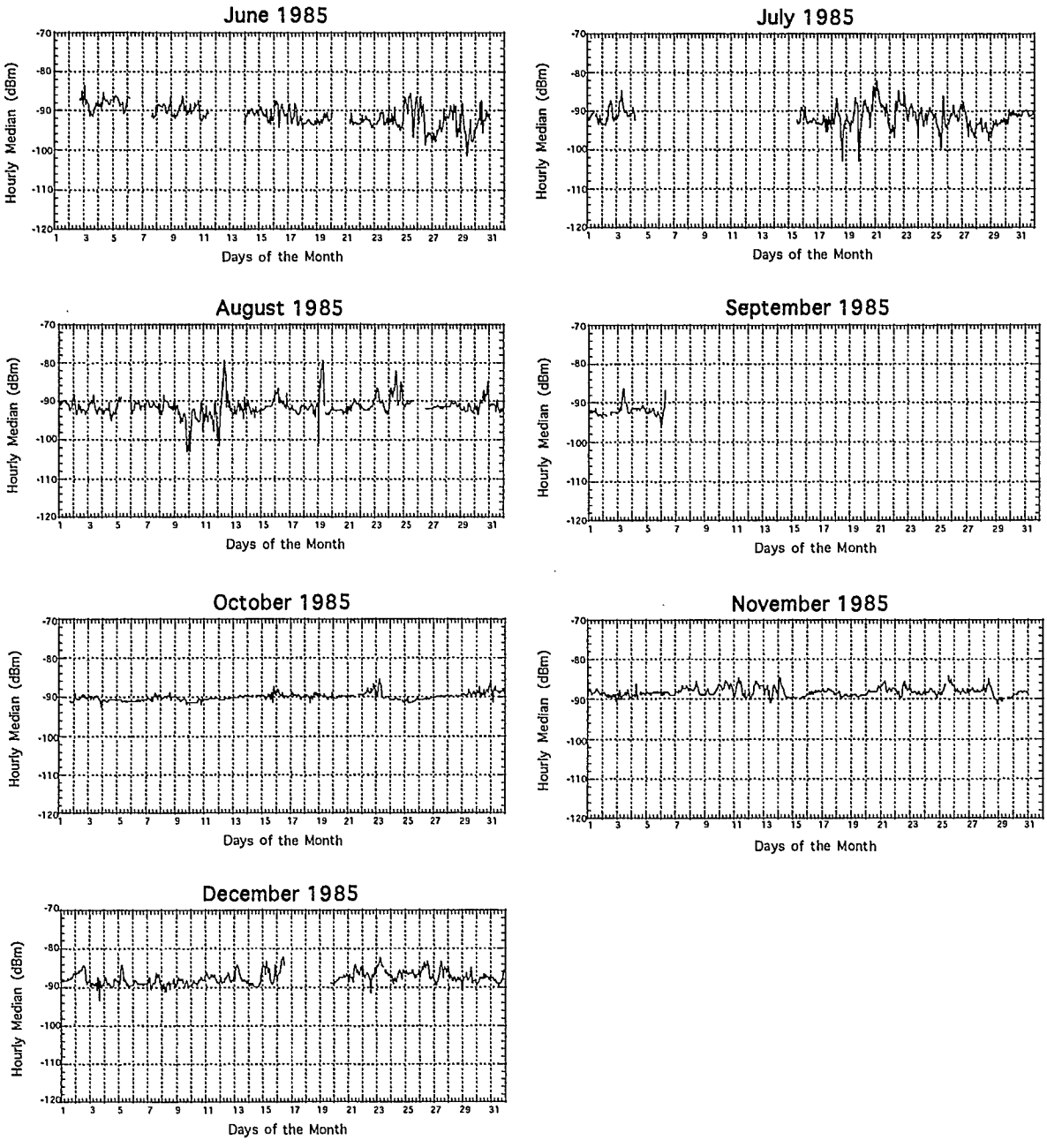

Figure B8: Hourly median values of power received.
IRVINE-MARTYR (VHF). (Page 1 of 2).

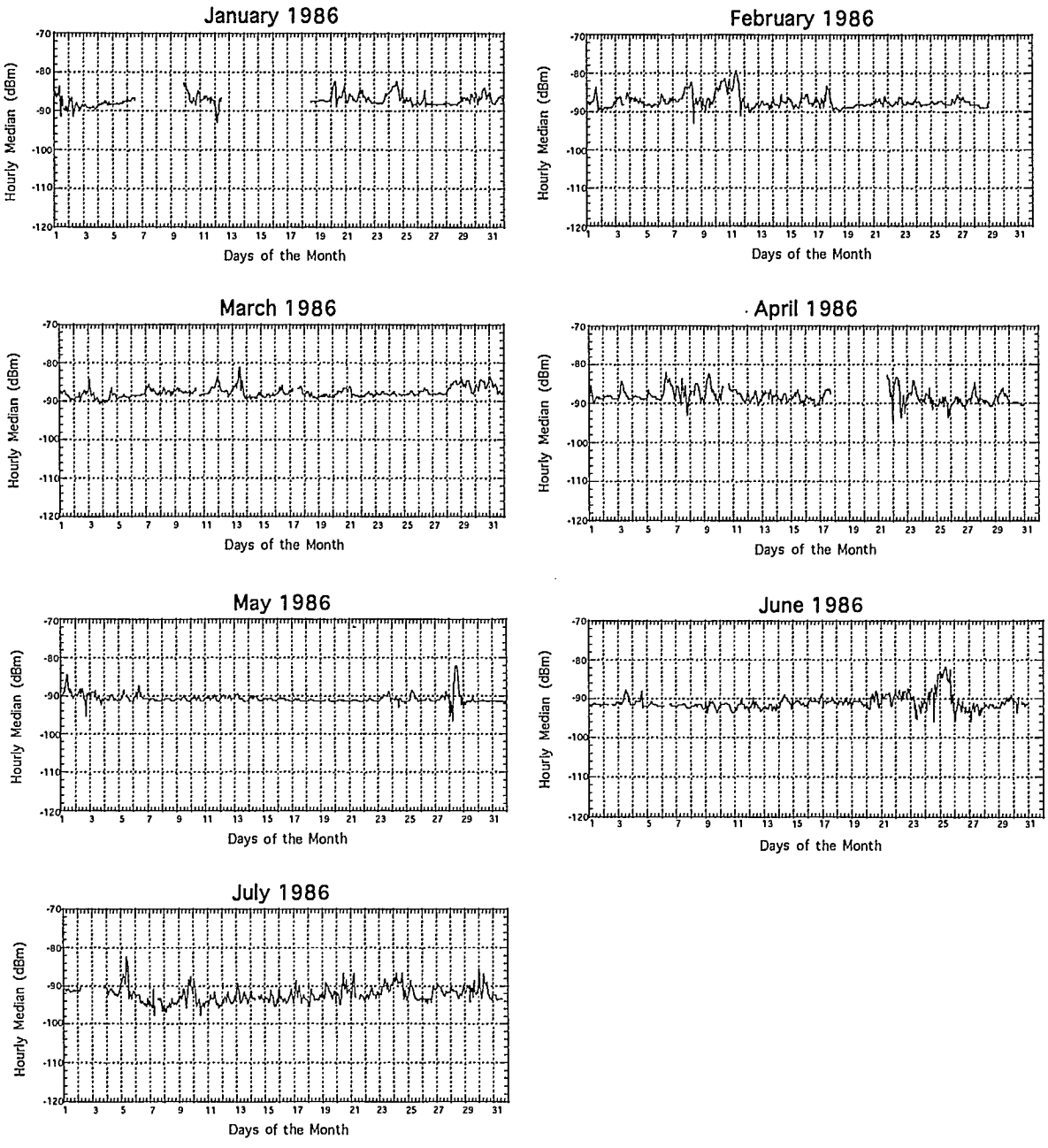

Figure B8: Hourly median values of power received.
IRVINE-MARTYR (VHF). (Page 2 of 2).

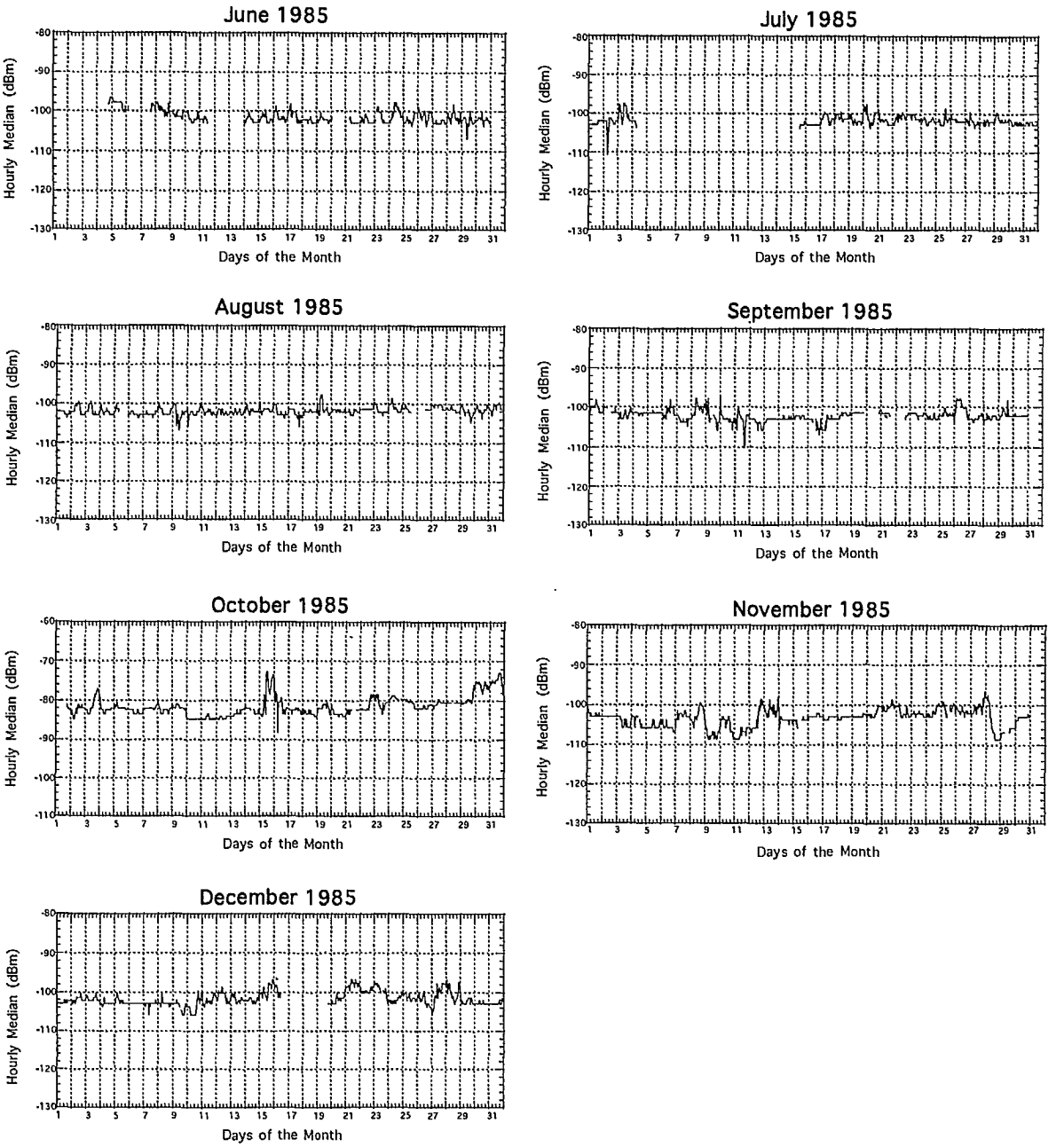

Figure B9: Hourly median values of power received.
STANLEY-MARTYR (VHF). (Page 1 of 2).

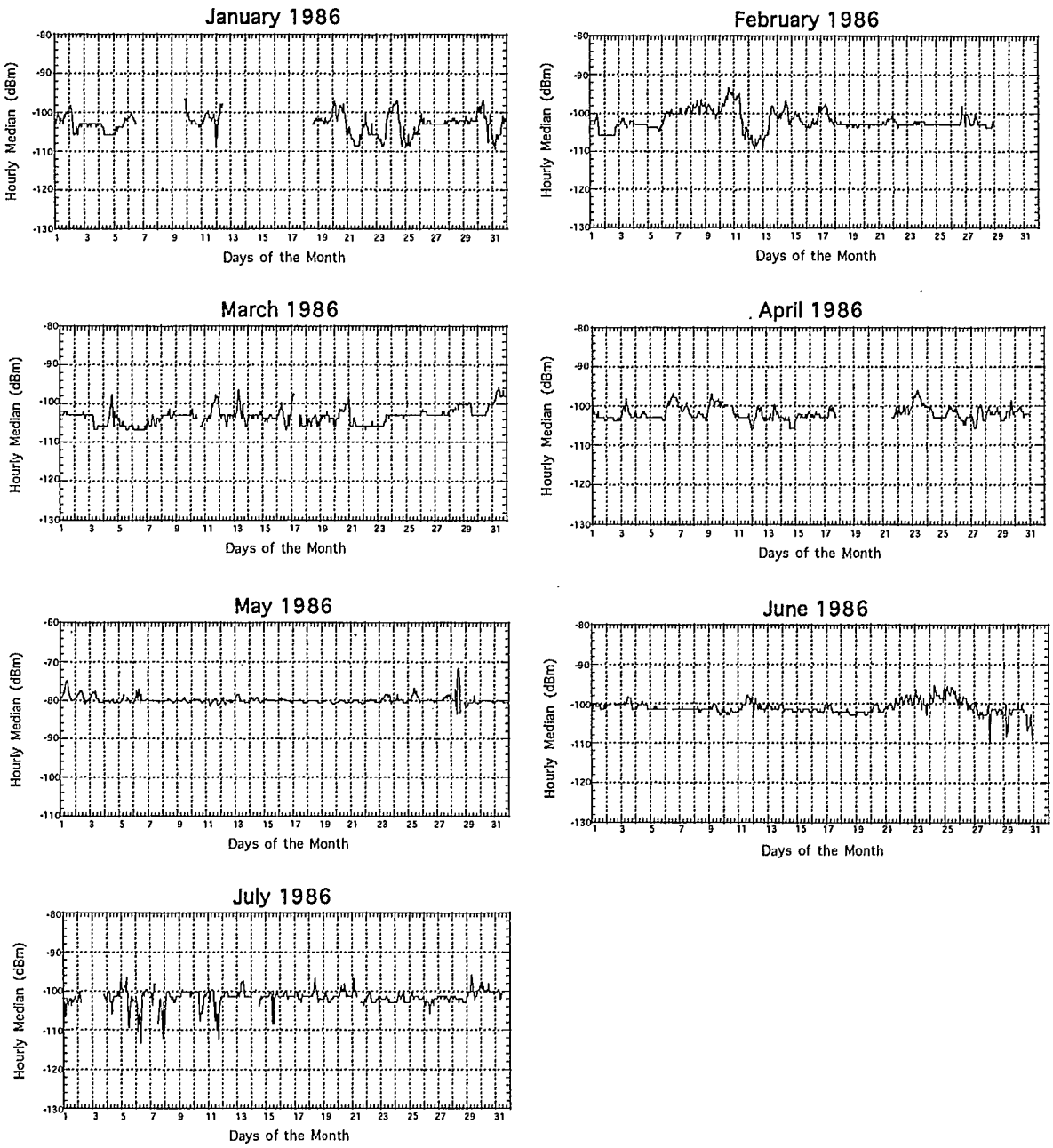

Figure B9: Hourly median values of power received.
STANLEY-MARTYR (VHF). (Page 2 of 2).

ANNEX "C"
MONTHLY FADE DEPTH AND ENHANCEMENT LEVEL STATISTICS

This annex is a graphical presentation of the monthly number of fades/enhancements measured over each experimental path. The plots covering selected periods of time are presented in this annex in the following order:

FIGURE	PATH	
C1	SARGENT-HURD	UHF
C2	HURD-IRVINE	UHF
C3	SARGENT-HURD	VHF
C4	HURD-IRVINE	VHF
C5	IRVINE-MARTYR	VHF
C6	STANLEY-MARTYR	VHF

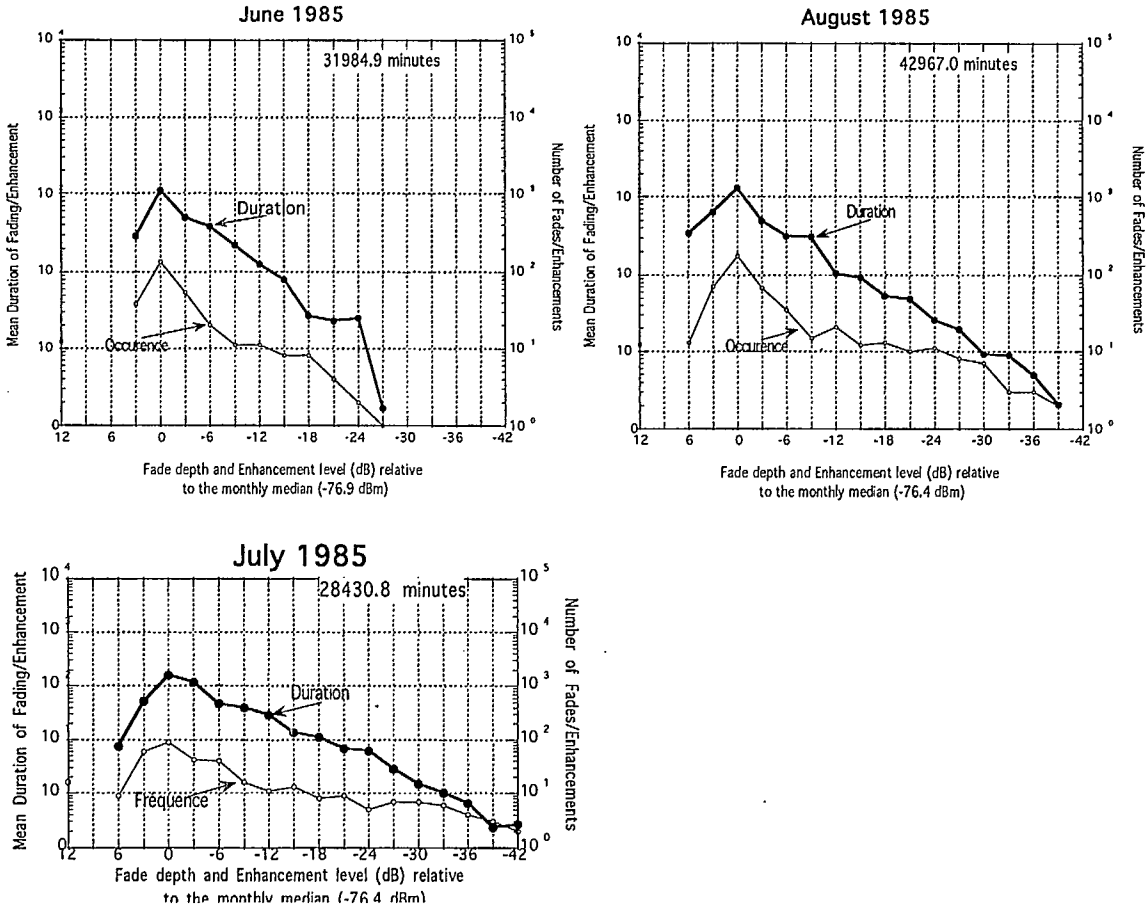

Figure C1: Number of fades/enhancements and their mean duration. Path: Sargent - Hurd (UHF).

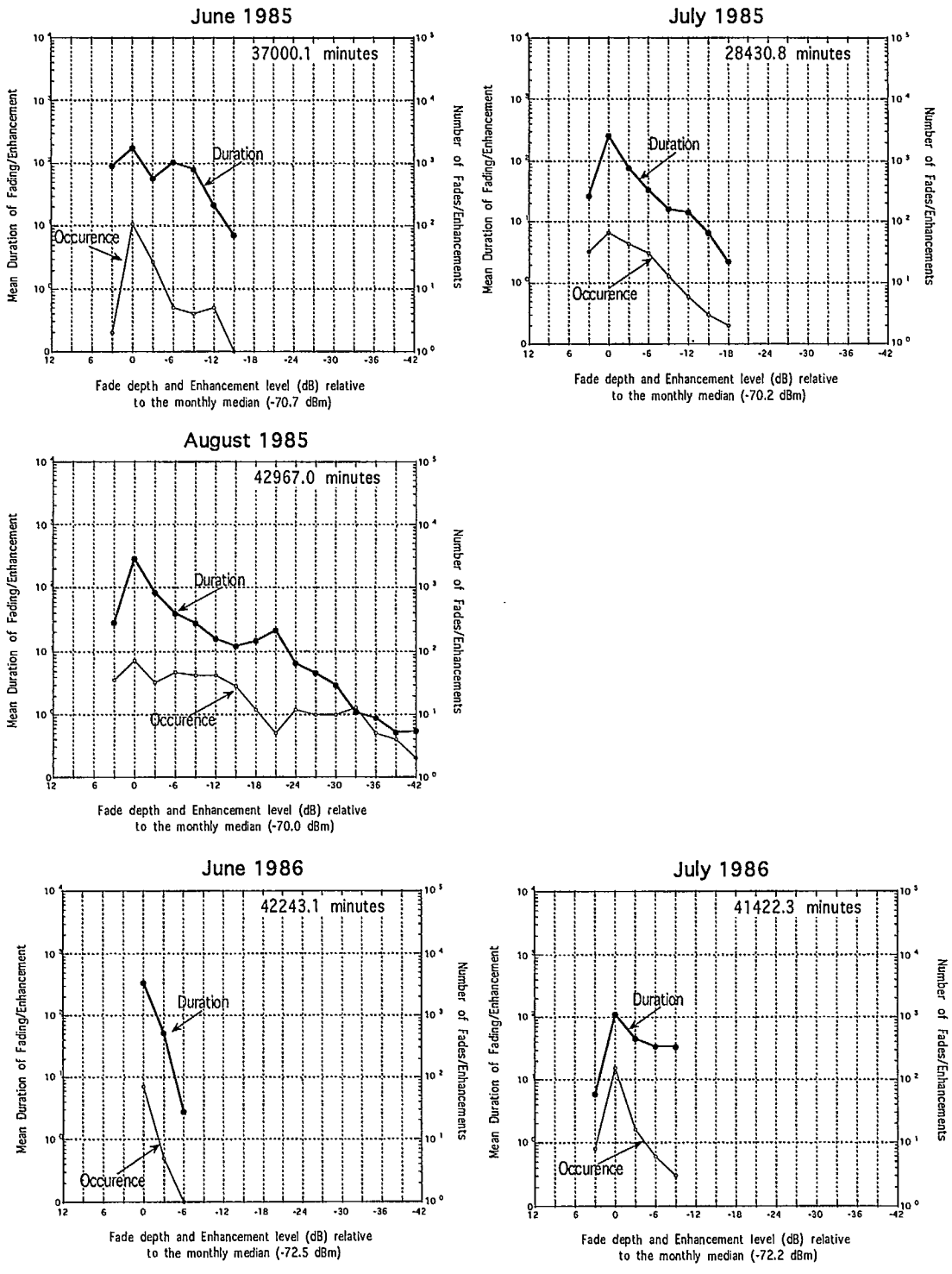

Figure C2: Number of fades/enhancements and their mean duration. Path: HURD - IRVINE (UHF).

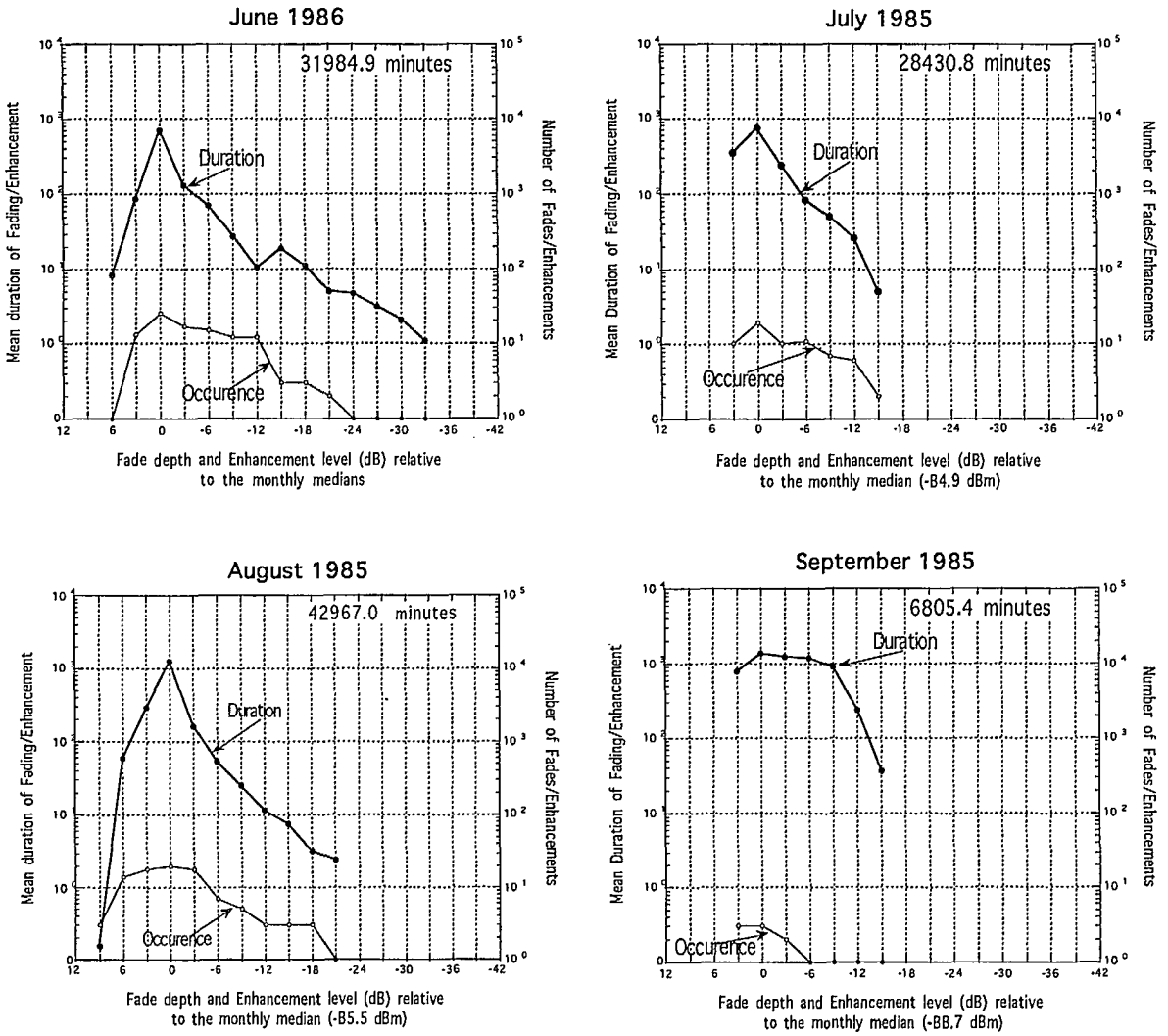

Figure C3: Number of fades/enhancements and their mean duration. Path: Sargent - Hurd (VHF).

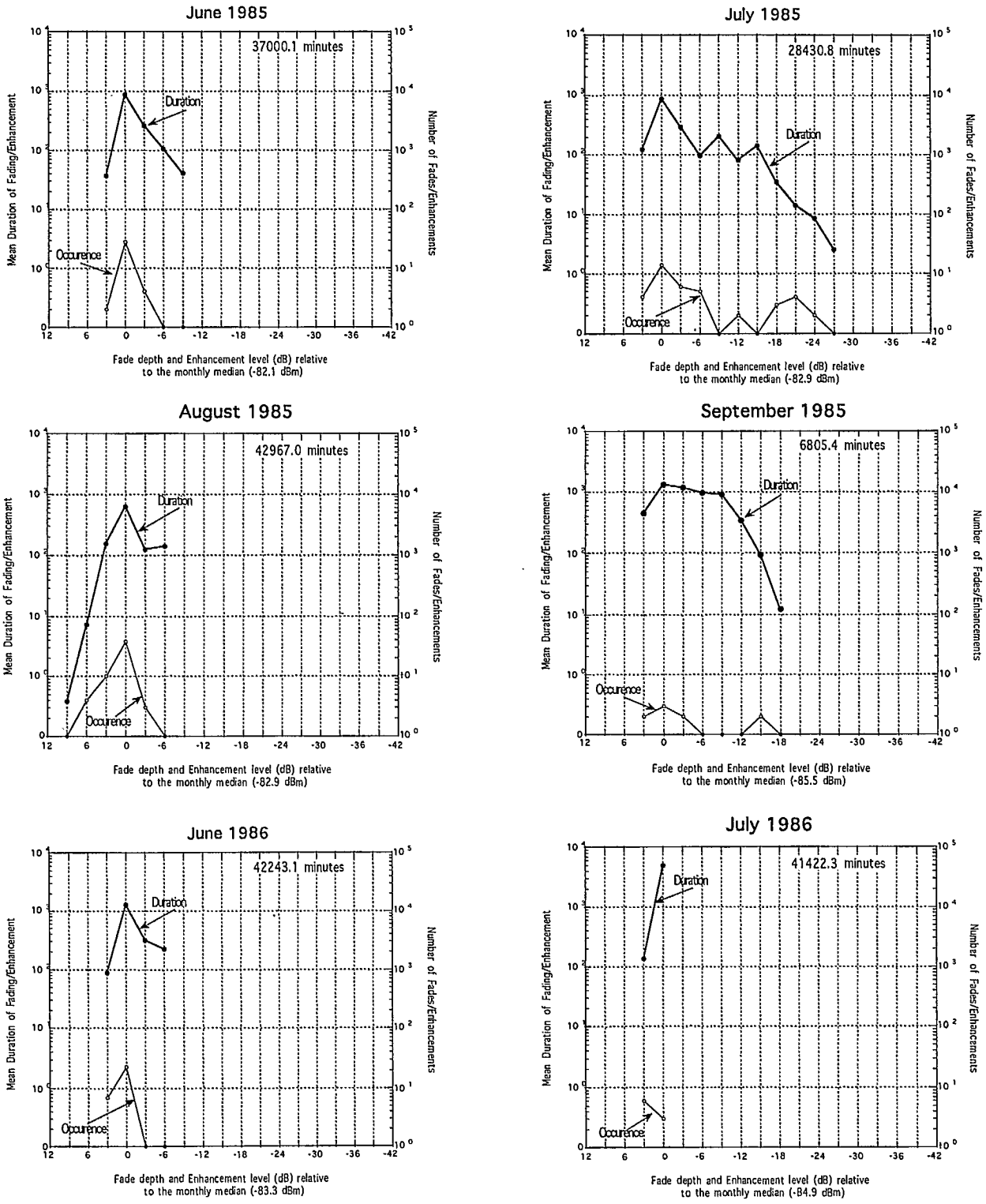

Figure C4: Number of fades/enhancements and their mean duration. Path: Hurd - Irvine (VHF).

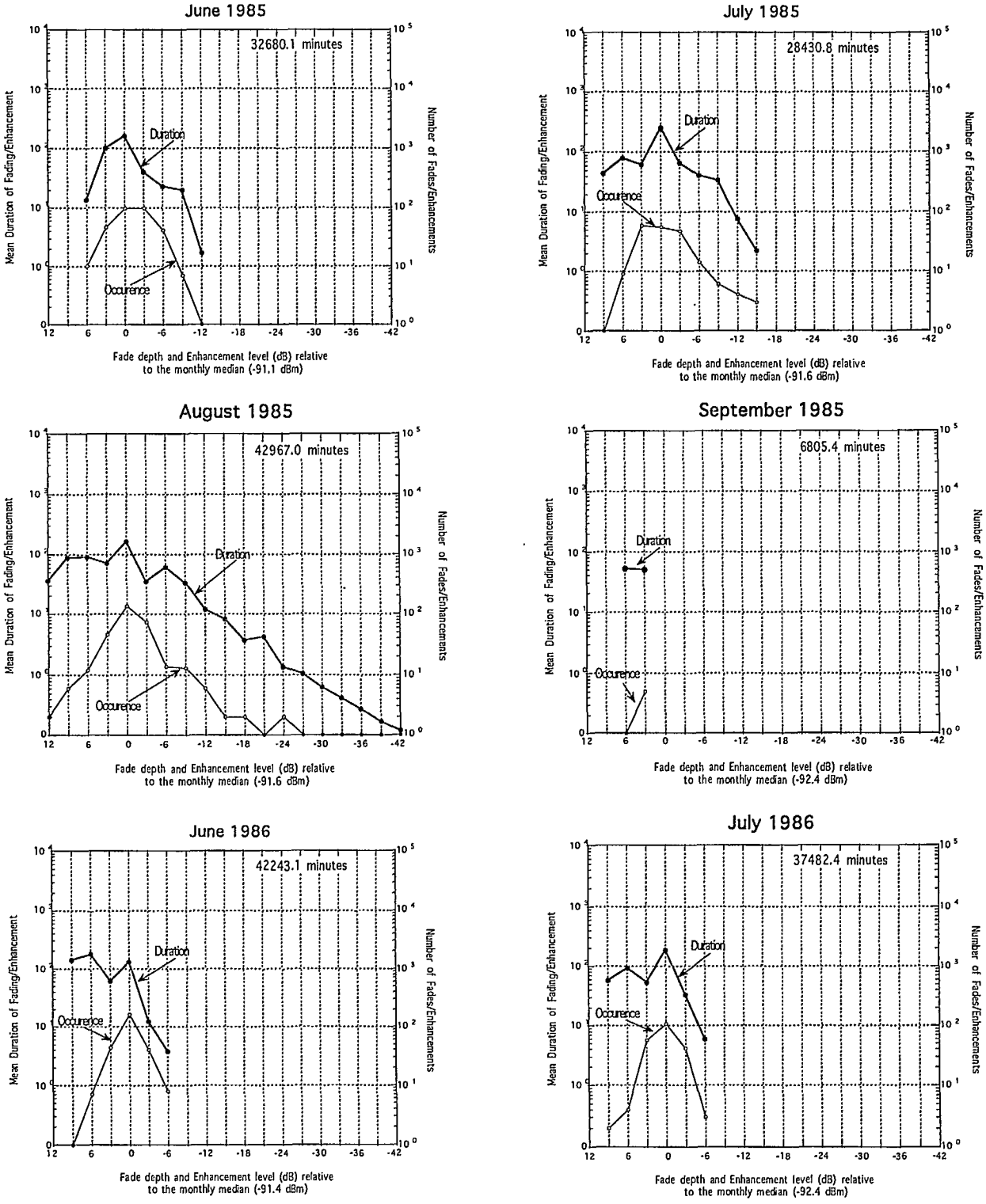

Figure C5: Number of fades/enhancements and their mean duration. Path: IRVINE - MARTYR (VHF).

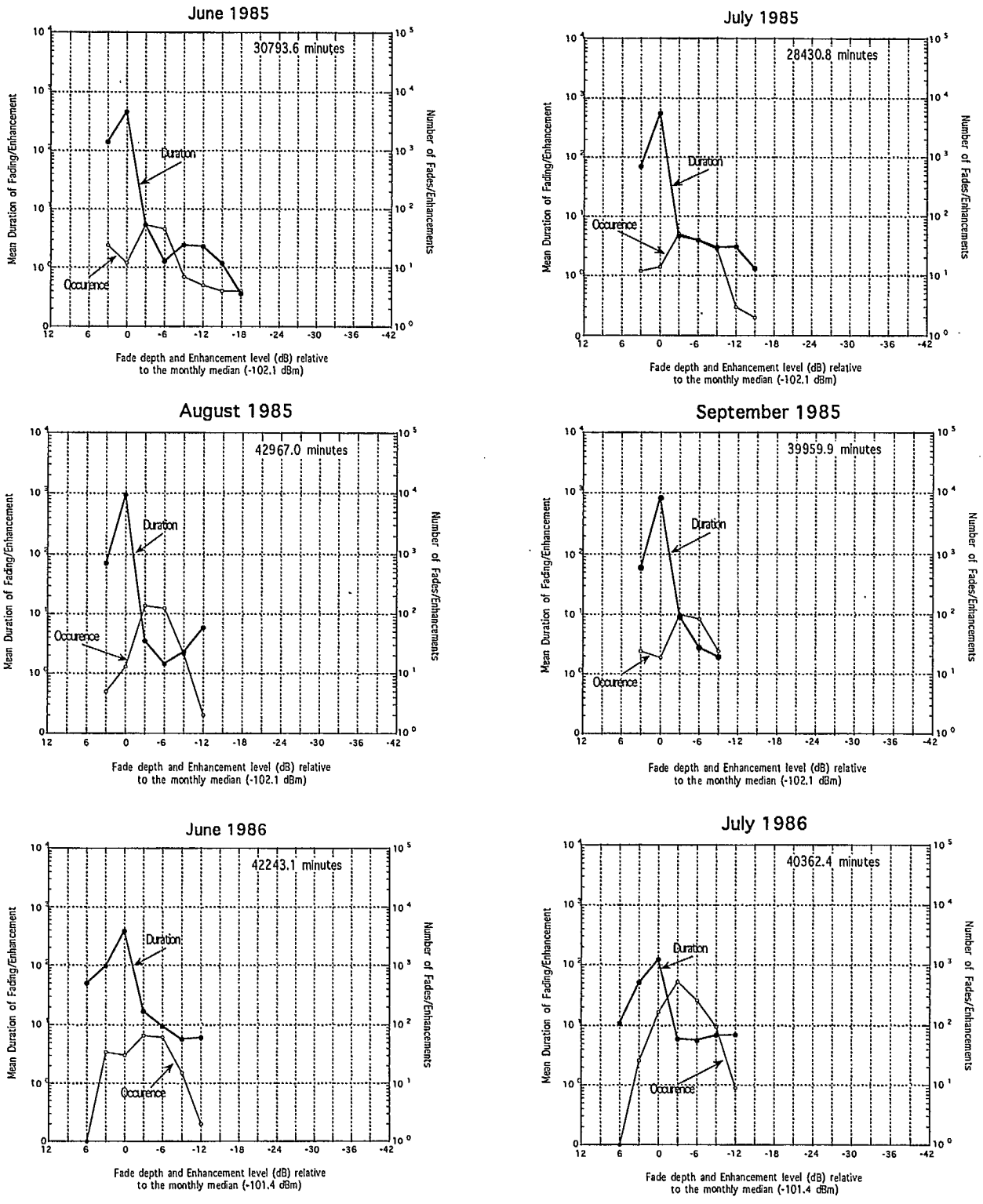

Figure C6: Number of fades/enhancements and their mean duration. Path: STANLEY - MARTYR (VHF).